Mitochondria in the life and death of mechanosensory hair cells

Sarah B. Pickett

A dissertation

submitted in partial fulfillment of the

requirements for the degree of

Doctor of Philosophy

University of Washington

2018

Reading Committee:

David Raible, Chair

David Perkel

Jennifer Stone

Program Authorized to Offer Degree:

Neuroscience

University of Washington

Abstract

Mitochondria in the life and death of mechanosensory hair cells

Sarah B. Pickett

Chair of the Supervisory Committee:
Professor David Raible
Department of Biological Structure

Hair cells are mechanosensory receptors found in the inner ear that mediate hearing and balance. In humans, damage and death of these cells is an underlying cause of hearing loss. Given the high prevalence of hearing loss, understanding the biology of these sensory cells continues to be an important endeavor to inform therapeutic strategies. The zebrafish has become a valuable model organism for advancing these efforts. In addition to hair cells of the inner ear, zebrafish also possess superficial hair cells of the lateral line sensory system, a sense devoted to detection of directional water flow. In combination with other advantages of the zebrafish model, the location of these hair cells has facilitated investigations of both normal hair cell function as well as mechanisms of hair cell death *in vivo.* In the following pages, I discuss the zebrafish as an auditory system model, highlighting structural and functional similarities between lateral line and cochlear hair cells, including selective susceptibility to environmental toxins. I then focus on a new investigation, relying on zebrafish to explore mitochondrial activity in lateral line hair cells. While this work is motivated by evidence demonstrating that mitochondria play a prominent role in hair cell damage and death, it begins to fill a gap in our understanding of how mitochondria function in response to normal cell activity. More specifically, I report on mitochondrial calcium

flux and oxidation, finding that both are regulated by mechanotransduction. I also examine whether variation in mitochondrial activity reflects differences in vulnerability of hair cells to the toxic drug neomycin. Overall, this study reveals a relationship between hair cell activity, mitochondrial activity, and susceptibility to damage.

TABLE OF CONTENTS

LIST OF FIGURES

LIST OF TABLES

LIST OF MOVIES

ACKNOWLEDGEMENTS

It has been a privilege to work alongside many exceptional scientists, outstanding teachers, and encouraging mentors who have guided me through my scientific career. I am honored to recognize these individuals and their crucial influence on my experience and training.

In beginning my acknowledgements, I would like to thank three scientists who provided my first opportunities for training in biological research: Drs. Murray Korc, Anthony Di Fiore, and Eric Schmidt. I am grateful for their mentorship and their encouragement to continue pursuing my love of science.

I believe that a thesis advisor has the single greatest influence on a student's graduate school experience; thus, I am especially grateful that Dr. David Raible was my advisor. I admire Dave as both a scientist and mentor. In particular, I admire Dave's investment in the success of his trainees – both personally and professionally – and his ability to foster collaboration among lab members and with the broader scientific community. These characteristics are increasingly important in today's research landscape and I hope that I, too, have taken on such qualities under Dave's tutelage.

Dave has expertly recruited a fabulous group of scientists to his lab. I have enjoyed working with the many members of the Raible Lab, because they are both excellent colleagues and excellent people. The group has changed a bit over time but has maintained a strong sense of comradery that I have come to truly value in a workplace. I will miss brainstorming, trouble shooting, and drinking boots with them. I am especially thankful for the enthusiastic encouragement and guidance provided by my post-doc mentors, Joy Sebe and Robert Esterberg, and for the moral support provided by my fellow graduate students and friends, Eric Thomas, Ivan Cruz, and Maddy Hewitt.

Thank you to the members of my thesis committee, Drs. Jennifer Stone, David Perkel, Rachel Wong, and David Kimelman, for providing valuable feedback and insight on numerous occasions. I have always felt that my committee had my best interests in mind and I am particularly grateful for their support in the last couple of years with regard to my career exploration.

I would also like acknowledge the influence of my extracurricular activities in graduate school. I am enormously appreciative of my experiences working with the Pacific Science Center Science Communication Fellows, UW ENGAGE, Dr. Scott Freeman and the meta-analysis coding team, and the Science Education Partnership and Assessment Laboratory at San Francisco State University. Working with these groups inspired me to reflect on how I teach and communicate about science and significantly changed the course of my career trajectory.

I am honored to have befriended a truly wonderful group of scientific peers during my tenure at UW. As my colleagues, I have so appreciated their input and critical feedback, their unique understanding in times of failure, and their eagerness to celebrate in times of victory. I am perhaps most grateful, though, for the times we spent catching up, venting, or laughing, often over a pitcher of beer. I would like to extend a special thanks to Drs. Leah Bakst, Steph Seeman, Florie D'Orazi, and Sweta Agrawal. Being the most junior graduate student among them, I had the pleasure of learning from their experiences and the displeasure of trailing behind them. I admire their generosity and tenacity and I am grateful for their friendship.

My successful completion of this thesis could not have been achieved without the overwhelming love and unending support of my family. They are hands down my biggest fans and cheerleaders. I want to specifically recognize my parents, Rob and Mindy Pickett. My parents have always worked extremely hard and they never let me give up on anything. In this way, I feel that they prepared me particularly well for the major commitment that is graduate school. Most of all, they have always believed in me and taught me to believe in myself.

Finally, I would like to thank my favorite neuroscientist, my husband Dr. Max Turner. Max directly and indirectly contributed to my scientific success in a number of ways, including reading numerous drafts of manuscripts and various applications, and – in honing his cooking skills – providing much needed sustenance after long days in lab. Scientific research can be grueling, but Max's enthusiasm, encouragement, and sense of humor helped me persevere. I continue to be inspired by his kindness and curiosity. Thank you for everything.

SP
Seattle, 2018

Chapter 1. INTRODUCTION

Hearing loss is a very common health issue, affecting over 30 million people in the US (Goman and Lin 2016). It can be caused by a number of factors including genetic disease, aging, loud noise exposure, and ototoxic compound exposure, each of which can lead to the dysfunction or loss of the sensory receptors that mediate hearing, the mechanosensory hair cells (Wong and Ryan 2015). The work presented in this thesis is motivated by understanding how normal hair cell functions are disrupted in damage and disease. My research identifies mitochondria as an essential factor in both hair cell life and death and relies on some particular advantages of using zebrafish as a model system to investigate hair cell biology. In the following chapter, I provide brief background on the sensory structures devoted to hearing in both mammals and fish. I then review a study of hair cell death that motivated my thesis work. In addition, I provide a roadmap of the subsequent chapters.

1.1 HEARING IN MAMMALS AND FISH

The sensory structures devoted to hearing vary across vertebrates and are housed within the bony labyrinth of the inner ear. In mammals, sound detection is mediated by cells in the organ of Corti within the spiraled, bony cochlea. In order for sound detection to take place, sound waves entering the ear are converted into mechanical movements. This occurs first via vibration of the eardrum coupled to the middle ear bones. Vibration of the middle ear bones is transmitted to the cochlea leading to displacement of cochlear fluid and the basilar membrane (Figure 1.1). Displacement causes the physical stimulation of the hair cells that reside atop the basilar membrane, which transduce the mechanical motion into electrical responses (Fettiplace and Hackney 2006; Ekdale 2016). Hair cells are arranged tonotopically along the cochlea: cells at the

base of the cochlea are tuned to higher frequency sounds and cells at the apex of the cochlea are tuned to lower frequency sounds. Hair cell frequency tuning is largely mediated by the structural properties (e.g., size and stiffness) of the basilar membrane. Cochlear hair cells can also be classified into two distinct types with different characteristics and innervation: inner and outer hair cells (Figure 1.1B). While inner hair cells are the primary sound sensors, outer hair cells serve as sound amplifiers (Fettiplace and Hackney 2006; Ekdale 2016). Mammalian vestibular sensory structures are also housed within the inner ear and, similarly, contain mechanosensory hair cells that mediate vestibular sensation. However, the focus of the work presented in this thesis is primarily devoted to modeling the auditory system.

Like mammals, fish also rely on inner ear structures for hearing. Fish hearing is mediated by the otolith organs, which include the utricle, saccule, and lagena. Mammalian otolith organs (utricle and saccule), by contrast, are devoted exclusively to vestibular function. The hair cell epithelia of these organs are situated beneath a calcium carbonate crystal, or otolith. Sound causes the body of the fish to move, but since otoliths are much denser than the body of the fish, they move more slowly. This difference in movement leads to mechanical stimulation of the hair cells (Popper and Fay 1993; Nicolson 2017). Some fish, including zebrafish, possess an additional specialization for hearing. The Weberian ossicles are small bones that transfer sound-induced vibrations from the swim bladder to the inner ear, serving to amplify sound (Fay and Popper 1974; Popper and Fay 1993).

In addition to the inner ear, fish (and amphibians) possess hair cells of another sensory system, the lateral line. Lateral line sensory organs, or neuromasts, are small clusters of hair cells and non-sensory support cells found along the surface of the animal (see Figure 2.1). In some fish species, neuromasts can also be found within open canals beneath the skin (Dijkgraaf 1963;

Webb 2013). Hair cells of both superficial and canal neuromasts are physically stimulated by external water flow. Fluid movement detection via the lateral line is required for fish orientation and navigation, as well as for predator avoidance and schooling behaviors (Bleckmann 2008; Webb 2013).

Auditory and lateral line hair cells share many structural and functional similarities, despite conveying information about distinct sensory modalities. Notably, due to the accessibility of the zebrafish superficial neuromasts, studies using the lateral line can more easily address questions of hair cell function and susceptibility, especially *in vivo*. In Chapter 2, I review conserved hair cell features and the contributions of zebrafish studies to our understanding of hair cell biology and human hearing disorders.

1.2 MECHANOSENSORY HAIR CELL DYSFUNCTION AND THE IMPORTANCE OF MITOCHONDRIA

One of the many similarities shared by zebrafish lateral line and mammalian inner ear hair cells is their response and susceptibility to aminoglycoside antibiotic exposure. Dying hair cells of both taxa generate reactive oxygen species (ROS) in response to aminoglycoside treatment (Clerici et al. 1996; Jiang et al. 2005; Choung et al. 2009; Esterberg et al. 2016) and are modestly protected by ROS reduction, either through antioxidant treatment or expression of ROS-neutralizing enzymes (e.g., catalase) (Sha and Schacht 2000; Sha et al. 2001a, b; McFadden et al. 2003; Kawamoto et al. 2004; Jiang et al. 2005; Ton and Parng 2005; Someya et al. 2009, 2010; Chen et al. 2013). My thesis was motivated in part by a recent study examining ROS in lateral line hair cells, in which we probed the origin of hair cell ROS and its role in aminoglycoside-induced hair cell death (Esterberg et al. 2016). The major findings of the study are described below (I was a contributing author to this work).

To monitor hair cell oxidation *in vivo,* two fluorescent indicators were used: the ROS indicator dye, CellROX (Figure 1.2), and hair cell specific expression of the dynamic reporter, HyPer (Belousov et al. 2006). Fluorescence was measured in living and dying cells following treatment with a low dose of the aminoglycoside antibiotic neomycin (Figure 1.3). Consistent with previous studies, neomycin treatment led to a significant increase in in the fluorescence of both indicators in dying cells, demonstrating an increase in cytoplasmic ROS. Some surviving cells also exhibited elevated ROS (Figure 1.3). Since mitochondria are considered to be one of the greatest producers of ROS in cells, mitochondrial oxidation was also monitored. To detect and visualize ROS in the organelles, hair cells were loaded with mitoSOX, a fluorescent indicator targeted to the mitochondria. An increase in MitoSOX fluorescence in dying cells revealed that mitochondrial ROS increases with neomycin-induced cell death. Evidence from subsequent experiments suggested that cytoplasmic ROS results from mitochondrial ROS production, which is driven by mitochondrial calcium uptake.

If mitochondria are the primary source of cytotoxic ROS increases during neomycin exposure, we predicted that specifically decreasing mitochondrial ROS would promote hair cell survival. We tested this through the use of an ROS scavenger targeted to the mitochondria (mitoTEMPO), compared to a general ROS scavenger (TEMPOL), in combination with neomycin treatment. Unlike TEMPOL, mitoTEMPO reduced both mitochondrial and cytoplasmic ROS and conferred significant hair cell protection against neomycin exposure. mitoTEMPO treatment also reduced ROS elevation and cell death caused by pharmacologically increasing mitochondrial calcium accumulation. These data suggest that oxidative changes in mitochondria play a key role in aminoglycoside-induced hair cell death.

Two questions arose from this study. First, what differentiates surviving cells from those that die? As observed in other studies, not all lateral line hair cells succumbed to low doses of neomycin (e.g., 50 μM); however, all cells are ultimately susceptible, as higher doses can be used to kill nearly 100% of the cells (Harris et al. 2003). Additionally, some surviving hair cells exhibited increased fluorescence of ROS indicators, indicating that elevation of ROS is not always cytotoxic. It is unclear why these cells are less susceptible. Second, beyond responding to hair cell damage, how do mitochondria respond to normal hair cell activity? While a growing body of literature has described mitochondrial stress and dysfunction during hair cell insult, research investigating mitochondrial activity and dynamics during normal hair cell function is remarkably sparse. As cells that constantly receive and filter sensory input, hair cells – like other neuronal cells – likely have a high metabolic demand (Niven and Laughlin 2008). Mitochondria, well known as the "power house of the cell," are crucial to sustain such demand through the generation of ATP; yet, as a byproduct of this process, mitochondria also produce ROS (Murphy 2009). If, as in damage conditions, mitochondria are major producers of ROS during normal hair cell function, perhaps differences in mitochondrial stress across cells contributes to hair cell susceptibility. The relationship between hair cell activity, mitochondrial activity, and cell death is explored in Chapter 3.

1.3 SUMMARY AND THESIS OVERVIEW

In subsequent chapters of this work, I describe and build on the history of zebrafish as a model organism with which to study hair cell activity and death. Chapter 2 provides an overview of hair cell function with a particular emphasis on the contributions of zebrafish studies to our understanding of hair cell functional development, activity, and hearing loss. In Chapter 3, I explore the influence of hair cell activity on mitochondrial activity and present evidence to suggest

that likelihood of hair cell death increases with cumulative mitochondrial stress. In the final chapter, I suggest future studies in which the zebrafish lateral line would continue to confer unique advantages for understanding the connection between sensory cell activity and mitochondrial behavior.

1.4 FIGURES

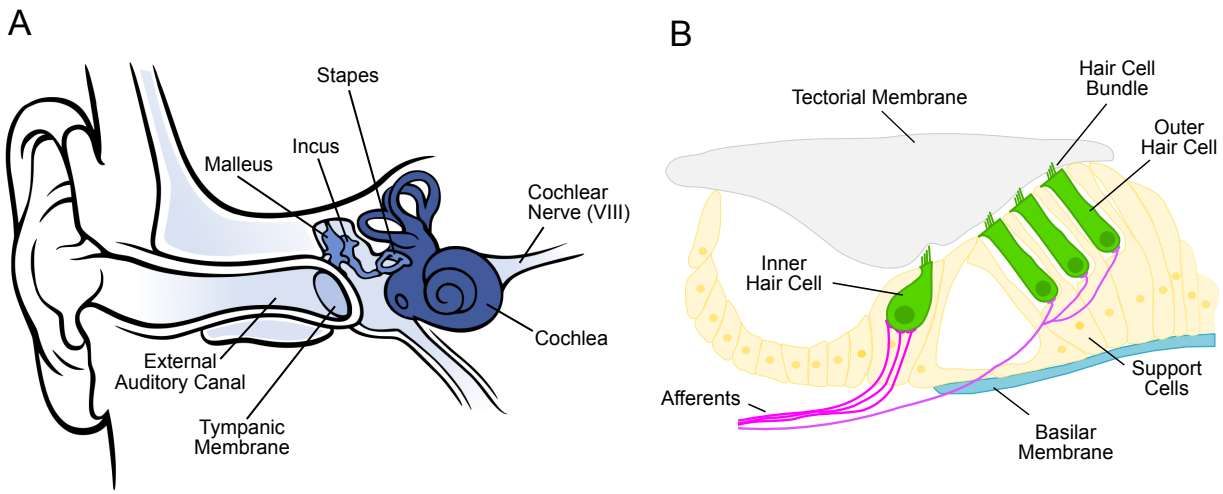

Figure 1.1. Anatomy and cellular structure of the inner ear.

(A) Schematic of the human ear. Sound waves cause vibration of the tympanic membrane (eardrum), which is conducted through three small bones (malleus, incus, and stapes) and transmitted to the cochlea. Adapted from Figure 1 in Chittka and Brockmann 2005. Creative Commons Copyright © 2005, Chittka and Brockmann. **(B)** Schematized cross-section through the organ of Corti within the cochlea. Sound-induced displacement of cochlear fluid and the basilar membrane causes deflection of the hair cell bundles, thus stimulating the cells. Hair cell sensory input is transmitted to the brain through afferent neurons of the VIIIth cranial nerve (also shown in A). Redrawn with permission from Figure 2 in Fettiplace and Hackney 2006. Copyright © 2006, Springer Nature.

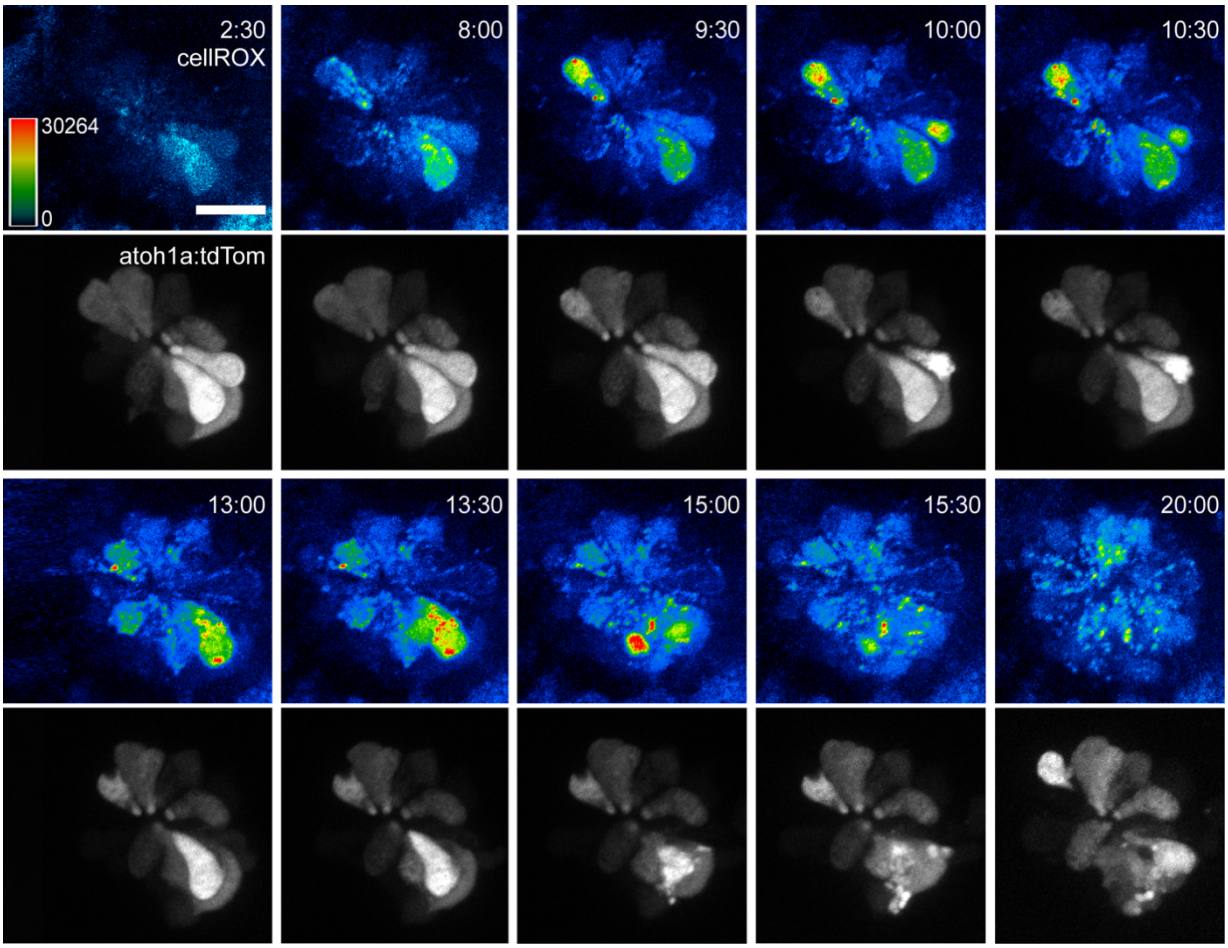

Figure 1.2. ROS increases in lateral line hair cells following neomycin treatment.

Frames from a time-lapse imaging video acquired from a transgenic [*Tg(atoh1a:tdTomato)*] fish labelled with CellROX and treated with 50 µM neomycin. CellROX fluorescence is shown as a heat map and tdTomato-positive cells are shown in gray scale. Time = minutes:seconds following neomycin addition. Scale bar = 20 µm. Figure adapted with permission from Esterberg et al. 2016. Copyright © 2016, American Society for Clinical Investigation.

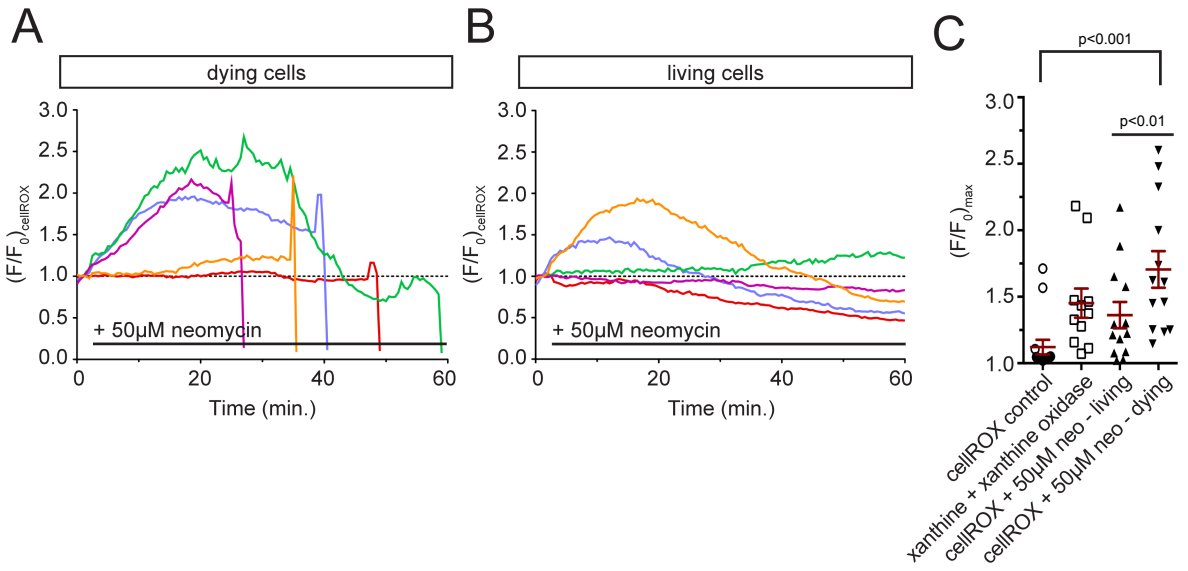

Figure 1.3. ROS increase in hair cells following neomycin exposure indicated by CellROX.

Normalized fluorescence intensity of individual cells labeled with CellROX that **(A)** die following 50 μM neomycin treatment, or **(B)** survive following treatment. Each colored line represents an individual cell and the dotted line corresponds with pre-treatment baseline fluorescence ($F/F_0 = 1$). **(C)** Plot of the maximum change in CellROX fluorescence in living or dying cells exposed to 50 μM neomycin. Maximum fluorescence is also shown for cells treated with xanthine oxidase and its substrate xanthine, which is known to generate ROS. Horizontal line and error bars = mean ± 1 SEM. Individual points represent mean neuromast fluorescence measured from fewer than 5 cells per neuromast and 1 to 3 neuromasts per animal. Figure adapted with permission from Esterberg et al. 2016.

Chapter 2. WATER WAVES TO SOUND WAVES: USING ZEBRAFISH TO EXPLORE HAIR CELL BIOLOGY

The contents of this chapter will be submitted for publication with the following authors:
Sarah B. Pickett and David W. Raible

2.1 ABSTRACT

Although perhaps best known for their use in developmental studies, over the last couple of decades zebrafish have become increasingly popular model organisms for investigating auditory system function and disease. Like mammals, zebrafish possess inner ear mechanosensory hair cells required for hearing, as well as superficial hair cells of the lateral line sensory system, which mediate detection of directional water flow. Complementing mammalian studies, zebrafish have been used to gain significant insights into many facets of hair cell biology, including mechanotransduction and synaptic physiology as well as mechanisms of both hereditary and acquired hair cell dysfunction. Here we provide an overview of this literature, highlighting some of the particular advantages of using zebrafish to investigate hearing and hearing loss.

2.2 INTRODUCTION

Hearing loss is extremely common in the United States, affecting nearly 1 in 4 individuals over the age of 12 (Goman and Lin 2016). Not only is it pervasive, hearing loss often occurs with a pattern that is particularly problematic for communication. For example, many individuals experience high frequency hearing loss before low frequency hearing loss. Since consonant speech sounds (e.g. “s”) have higher frequencies, with just mild or moderate hearing loss, the ability to perceive speech without amplification is dramatically reduced (Centers for Disease

Control and Prevention, 2015). The organ devoted to hearing is housed within a bony inner ear structure known as the cochlea. Despite being protected by this structure, cochlear cells are highly susceptible to genetic disease and environmental toxicity. Understanding the biology of auditory cells and the mechanisms of cell damage are critically important for considering new preventative and restorative treatments for hearing impairment.

Hair cells, the sensory cells that mediate hearing and balance, are mechanosensory receptors that transduce mechanical stimulation into electrical responses (Eatock et al. 2006). Hair cells synapse with afferent neurons that convey auditory information to the brain. Complementing mammalian studies, zebrafish have become an increasingly attractive and popular model system for investigating hair cell and neuronal function. Although zebrafish possess inner ear sensory epithelia, hair cells are also found as receptors of the lateral line sensory system. The lateral line allows fish and other aquatic organisms to detect directional water flow. The zebrafish model system offers many advantages for hair cell research, including: (1) zebrafish produce offspring in large numbers, providing the opportunity for quantitative analysis across many animals; (2) embryos and larvae are optically clear and lateral line hair cells are superficially located, making them amenable for *in vivo* imaging; (3) their small size allows them to be arrayed in multiwell plates for drug screening; and (4) genetic expression constructs can be easily introduced into embryos, and protocols are well established for both forward and reverse genetic manipulation, including CRISPR. Although not within the scope of this review, zebrafish have also been quite valuable in elucidating mechanisms of sensory development and hair cell regeneration (for recent reviews see Thomas et al. 2015 and Kniss et al. 2016). Here we address different aspects of hair cell function and the ways in which zebrafish

studies – including those focused on the lateral line system – have contributed to our understanding of auditory neuroscience.

2.3 THE ZEBRAFISH LATERAL LINE SYSTEM

Zebrafish are found throughout Southeast Asia in flowing streams and slow flowing or stagnant pools (reviewed in Parichy, 2015). Many of the predatory organisms that forage for zebrafish rely on suction feeding; thus, at relatively early developmental stages, zebrafish must be capable of detecting and responding to high velocity water flow (Engeszer et al. 2007; Arunachalam et al. 2013). The lateral line sensory system allows fish and other aquatic vertebrates to do just that. This mechanoreceptive sense, described as "touch at a distance," allows fish to orient in water currents and detect both predators and prey (Dijkgraaf 1963; Webb 2013). The lateral line organs, called neuromasts, contain clusters of mechanosensory hair cells and non-sensory support cells and are found on the surface of the zebrafish in a stereotyped arrangement (see Figure 2.1) (Metcalfe et al. 1985; Raible and Kruse 2000). Neuromasts found on the head comprise the anterior lateral line system (aLL), whereas those along the trunk form the posterior lateral line system (pLL). Lateral line hair cells are innervated by bipolar sensory neurons with central axonal projections terminating in the hindbrain and peripheral axons at the neuromasts. The afferents are organized into two ganglia near the ear based on the body positioning of the neuromasts they innervate. The axons of the aLL and pLL ganglia terminate in distinct locations within the hindbrain, leading to doubly somatotopic mapping of lateral line sensory input (Alexandre and Ghysen 1999). Zebrafish lateral line efferent neurons provide both excitatory and inhibitory input to hair cells and are also functionally segregated based on whether they innervate neuromasts of the aLL or pLL (Bricaud et al. 2001; Toro et al. 2015). Excitatory input is

mediated by dopamine signaling (Toro et al. 2015). Studies from Xenopus and other fish taxa suggest that cholinergic signaling likely decreases hair cell activity and may act as an adaptive filter during swimming activity (Flock and Russell 1973; Montgomery and Bodznick 1994; Dawkins et al. 2005).

Studies examining the behavioral relevance of the lateral line in zebrafish larvae have focused on the characteristic C-start escape response, in which the body curls and then quickly accelerates away from an impending threat while straightening (McHenry et al. 2009; Stewart and McHenry 2010; Stewart et al. 2013, 2014). In one of the earlier studies, zebrafish larvae were exposed to accelerated water flow, mimicking a predator strike, and the probability and latency of the response were measured. Upon ablation of lateral line hair cells, the response probability was significantly reduced. The response was recovered following hair cell regeneration, thus demonstrating a role for lateral-line hair cell input (McHenry et al. 2009). Hair cell stimulation may also be sufficient to drive this behavior or at least particular facets of it. Later work revealed that escape responses could be elicited through optogenetic stimulation of hair cell activity, however, this stimulation paradigm activated hair cells of both the lateral line and inner ear (Monesson-Olson et al. 2014). In goldfish, lateral line input specifically has been shown to contribute to the latency and directionality of the c-start response (Mirjany et al. 2011). Another behavior mediated by lateral line input (as well as visual input) is rheotaxis, or orientation to constant water flow (Suli et al. 2012). Similar to escape responses, chemically ablating hair cells or disrupting of hair cell transduction both significantly reduced the number of animals performing rheotaxis. Allowing for hair cell regeneration or recovery (both in number and function) restored the behavior.

The functional contributions of different neuromasts to behavioral responses may vary with position along the body. In an examination of lateral line function during swimming bursts relative to a suction source, ablation of just the most caudal neuromasts had a disproportionate behavioral affect that was not significantly different from depleting all pLL hair cells (Olszewski et al. 2012). Similar results were obtained in a study that combined behavioral experiments with mathematical modeling to study rheotaxis (Oteiza et al. 2017). As in previous work, significant reduction in rheotaxis was observed when the lateral line was ablated; however, while the pLL neuromasts were required for the behavior, the aLL neuromasts were not. In addition to hair cell location, larval fish seem to rely on the integration of bilateral hair cell input for rheotaxis, since laser ablation of hair cells on a single side led to a similar change in behavior compared to bilateral ablation. What about the contribution of a single neuromast? Although stimulation of a single neuromast was initially deemed insufficient to elicit motor behavior (based on electrophysiological recordings in the brainstem ventral motor root), a later study found that single neuromast stimulation was in fact sufficient drive fictive swimming and motor responses in anesthetized larvae (Liao 2010; Haehnel-Taguchi et al. 2014). The ability of a single neuromast to elicit behavior may stem from the fact that a given neuromast can be stably innervated by multiple neurons (Liao 2010; Haehnel-Taguchi et al. 2014; Pujol-Martí et al. 2014). Moreover, developmental differences in afferent innervation and electrophysiological properties could also contribute to behavioral output (Liao and Haehnel 2012).

2.4 ZEBRAFISH GENETIC MODELS OF HEARING LOSS

In addition to identifying important structures required for hair cell function (discussed below), zebrafish genetic studies have been used to investigate mutations and mechanisms underlying

human hereditary deafness. Although acquired human hearing loss is more common, congenital deafness is also quite prevalent, affecting 2-3 out of every 1000 newborn children (Morton and Nance 2006). Roughly 80% of congenital hearing loss is genetic, the forms of which can be categorized as: (1) non-syndromic, occurring in isolation; or (2) syndromic, occurring as part of a complex genetic disorder (Shearer et al. 2017). Although zebrafish cannot be used to study sensory deficits associated with dysfunction of cochlea-specific structures (e.g., the stria vascularis), they have been valuable models for uncovering aspects of both syndromic and non-syndromic deafness conditions (Whitfield 2002; Nicolson 2005, 2017). The many zebrafish models of human hereditary deafness genes (DFNs) are listed in Table 2.1.

One of the first zebrafish models of human genetic deafness disorders arose from the identification and characterization of mutations in the unconventional myosin gene, *myosin7a* (*myo7a*). Myo7a is motor molecule that serves as a scaffolding protein required for bundle integrity (Ernest et al. 2000; Blanco-Sánchez et al. 2014). The *myo7aa* zebrafish mutants, also known as *mariner*, were characterized by their lack of acoustic or vibrational sensitivity, absent microphonic potentials, and splayed bundle phenotype (Nicolson et al. 1998; Ernest et al. 2000). Paralleling mammalian discoveries, *Myo7A* was also one of the first genes identified as part of the mammalian cochlear hair cell mechanotransduction apparatus through characterization of the *shaker-1* mouse mutant (Gibson et al. 1995; Self et al. 1998). Mutations in human MYO7A are known to cause Usher Syndrome (clinical subtype 1) (USH1), a disorder characterized by progressive retinal degeneration and profound hearing and balance deficits (Reiners et al. 2006).

In addition to identifying mutations in genes required for hair cell function, understanding the trafficking, targeting, and assembly of these proteins has become a more active area of investigation. These studies provide additional insight into the mechanisms

underlying human hereditary deafness (Blanco-Sánchez et al. 2014; Maeda et al. 2014; Erickson et al. 2017). For example, following the identification of *myo7aa* mutations, additional zebrafish mutants were identified in genes homologous to the human USH1 genes, including *cdh23*, *pcdh15*, *harmonin* (*usch1c*), and *clarin1* (Söllner et al. 2004; Seiler et al. 2005; Phillips et al. 2011; Gopal et al. 2015). Subsequently, investigation of these zebrafish models provided unique insight into the causes of hair cell death associated with USH. Three of the USH1 proteins – Myo7aa, Cdh23, and Ush1c (and the intraflagellar transport protein, Ift88) – form complexes in the ER that are required for protein trafficking. Mutations in *cadherin23* or *ush1c* lead to defects in protein targeting, as well as induction of ER stress and apoptotic cell death. This may be linked to activation of the unfolded protein response in the ER, as components of the complex are missing and the complex is misassembled. Suppressing ER stress has been shown to reduce hair cell death in both zebrafish and mouse models of USH1 (Blanco-Sánchez et al. 2014; Hu et al. 2016).

Protein trafficking is also highlighted in the characterization of the zebrafish Transmembrane O-methyltransferase (*Tomt*) mutant, *mercury*, a model of non-syndromic deafness DFNB63. Although it was initially thought that hearing loss associated with DFNB63 was related to deficient catecholemine metabolism, Erickson et al., (2017) revealed that *mercury* mutants exhibit abolished mechanotransduction due to defects in TMC1/2 protein targeting, specifically (Erickson et al. 2017). Unlike other proteins required for mechanotransduction, Tomt is not expressed in the hair cell bundle, but rather in the Golgi apparatus. It remains unclear exactly how Tomt regulates TMC trafficking in the hair cells, but its role is conserved in mammalian hair cells (Cunningham et al. 2017).

2.5 MECHANOTRANSDUCTION ACTIVITY

The relationship between lateral line sensation and behavioral output is a clear benefit of using this system to study sensory and cell function. Many genes required for hair cell function were initially found through a large mutagenesis screen for animals with behavioral movement and balance deficits (Nicolson et al., 1998). The identified mutants, so-called "circler mutants," all responded to touch, but swam in a circular motion due to significant inner ear and lateral line hair cell dysfunction. As the individual genes underlying these phenotypes were identified, they were also found to share homology with mammalian genes, some of which are also known human hereditary deafness genes (discussed above, see Table 2.1). Notably, some of the first identified genes encode proteins required for mechanotransduction. The mechanism and components of hair cell mechanotransduction have been recently reviewed in Nicolson (2017) and will be described in brief.

Mechanotransduction is mediated by a specialized apical structure, the hair cell bundle, which is characterized by several stereocilia and an eccentric kinocilium. The stereocilia are composed primarily of actin filaments and have a staircase-like arrangement, such that they become progressively taller closer to the kinocilium, a true cilium. Stereocilia are connected by tip links, which gate mechanosensitive, non-selective cation channels at the tips of the stereocilia (Hudspeth and Corey 1977; Hudspeth and Jacobs 1979; Corey and Hudspeth 1979). Deflection of the stereocilia toward the kinocilium results in mechanotransduction channel opening and hair cell depolarization, while deflection away from the kinocilium leads to channel closing**.** Extracellular microphonic recordings were used to determine that stereocilia deflection promotes channel opening (Corey and Hudspeth 1980; Hudspeth 1982)

Although directional selectivity is a key element of hair cell mechanotransduction, this feature of mechanosensitivity develops with bundle maturation. Immature hair cells in both the cochlea and lateral line can be stimulated in the direction opposite their morphological polarity to elicit mechanotransduction currents (Waguespack et al. 2007; Kindt et al. 2012). While the immature cochlear hair cells lack directional sensitivity, immature lateral line hair cells in fact exhibit reverse directional sensitivity. This is followed by an intermediate stage of bi-directional sensitivity and finally mature directional sensitivity (which coincides with stereocilia tip link formation). The reversed mechanosensitivity of immature lateral line hair cells is mediated by the kinocilia and kinocilial links, as mutants lacking these structures (*ift88* mutants) do not exhibit early mechanosensory responsiveness or a reversal of functional polarity (Kindt et al. 2012). Although mammalian auditory hair cells lose their kinocilia following the onset of mechanotransduction, perhaps there is a role for the kinocilia in the early maturation of these cells as well (Lim and Anniko 1985).

The structure and components of the apical bundle are conserved between mammals and zebrafish. One of the proteins comprising the stereocilia tip links, for example, was identified in tandem in both zebrafish and mouse models. Both *waltzer* mice and *sputnik* circler mutants were found to have mutations in the gene encoding the calcium-dependent adhesion molecule cadherin23 (Cdh23) (Siemens et al. 2004; Söllner et al. 2004). Cdh23 interacts with protocadherin15 (Pcdh15) to form tip link filaments (Ahmed et al. 2006; Kazmierczak et al. 2007). The splayed bundle phenotype of the *waltzer* and *sputnik* mutants results in loss of mechanotransduction and corresponding auditory and balance defects, well recognized as circular ambulatory or swimming movement. Mutations in human CDH23 and PCDH15 also

lead to auditory and vestibular dysfunction, as well as visual loss, associated with the genetic disease Usher Syndrome (Reiners et al. 2006).

In addition to structural components of the hair cell bundle, proteins of the mechanotransduction channel complex are also conserved across taxa, including Tmie (Shen et al. 2008; Gleason et al. 2009; Zhao et al. 2014), Lhfpl5 (Longo-Guess et al. 2005; Maeda et al. 2017), the transmembrane channel-like proteins (Tmc1 and 2) (Pan et al. 2013; Maeda et al. 2014; Kurima et al. 2015; Erickson et al. 2017; Chou et al. 2017), and Tomt, a protein necessary for Tmc localization (Cunningham et al. 2017; Erickson et al. 2017). The exact pore-forming protein(s) of the mechanotransduction channel still remain unknown. Mirroring mammalian studies**,** zebrafish TRP channels were initially proposed, but with conflicting results. An early study of the unconventional TRP channel NompC (TRPN1) demonstrated a potential role in mechanotransduction, while mutation of TRP1A had no effect (Sidi et al. 2004; Prober et al. 2008). Primarily through study of mammalian hair cells, more recent evidence has pointed to TMC1/2 as the best candidates (Pan et al. 2013; Kurima et al. 2015). Support for this in the zebrafish literature stems from the interaction of Pcdh15 and Tmc2, as well as mechanotransduction deficits that result from improper Tmc1/2 trafficking (Maeda et al. 2014; Erickson et al. 2017).

2.6 Development of hair cell polarity

Given the importance of the hair bundle orientation for cell function and directional sensitivity, establishment and maintenance of hair cell planar cell polarity (PCP) is crucial. During development and regeneration in the lateral line system, sibling hair cells form apical bundles exhibiting mirror symmetrical orientation (López-Schier et al. 2004; López-Schier and Hudspeth 2006). Sibling pairs are born from a common progenitor that divides in a plane perpendicular to

the axis of polarity of the neuromast. The developing hair cells then undergo rearrangements ultimately leading to cells with oppositely oriented bundles (Wibowo et al. 2011). In this way, lateral line hair cells display PCP relative to each other as well as to the body axis.

The *vangl2* gene is known to be required for proper PCP in both mammalian inner ear and lateral line hair cells (Montcouquiol et al. 2003; Wang et al. 2005, 2006; López-Schier and Hudspeth 2006; Mirkovic et al. 2012). As in mammals, the Vangl2 protein is asymmetrically localized within lateral line hair cells, with protein accumulating in the apical side of the cells. *Vangl2*, or *trilobite*, mutants display misalignments in progenitor cell division and disrupted hair cell orientation, where hair cells are oriented randomly within the neuromast rather than in 180 degree-opposing directions (López-Schier and Hudspeth 2006; Mirkovic et al. 2012). *Vangl2* overexpression also disrupts orientation, as hair cells are observed with randomized orientation or uniform orientation bias within a neuromast.

Whereas Vangl2 is expressed, albeit asymmetrically, in all hair cells, another important regulator of PCP, the transcription factor Emx2, is only expressed in half of the hair cells within the neuromast (Jiang et al. 2017). *Emx2* CRISPR knockout leads to loss of mirror symmetry, as all hair cells become uniformly polarized in one direction (Jiang et al. 2017). Conversely, upon *emx2* overexpression, hair cells become uniformly polarized in the opposite orientation. These polarity changes have functional consequences, as calcium imaging demonstrates that hair cells ectopically expressing *emx2* maximally responded to stimulation in the same orientation (as opposed to only half of the hair cells responding in a wildtype neuromast). Asymmetric *Emx2* expression was also observed in mouse and chick utricles along the line of polarity reversal, a delineation of two regions of the organ with opposing hair cell polarities. As in the zebrafish experiments, *Emx2* knockout and overexpression in the mouse utricle also disrupted mirror

symmetry, together demonstrating a conserved role for Emx2 in PCP across vertebrates (Jiang et al. 2017).

In the lateral line, hair cell polarity is also important for innervation, as afferents demonstrate strict synaptic selectivity for hair cells of the same polarity (Nagiel et al. 2008, 2009; Faucherre et al. 2009; Dow et al. 2015). Illustrating this specificity, directional selectivity persists when contacts are formed with regenerating hair cells post-ablation, as well as during axonal regeneration (Nagiel et al. 2008; Faucherre et al. 2009). Curiously, although lack of mechanotransduction activity seems to alter the complexity of afferent peripheral arbors (Faucherre et al. 2010; Pujol-Martí et al. 2014), central and peripheral afferent innervation occurs normally in the absence of hair cell mechanotransduction activity or synaptic vesicle release (Nagiel et al. 2008, 2009; Faucherre et al. 2010; Pujol-Martí et al. 2012, 2014). In addition to regulating hair cell polarity, Emx2 regulates the recognition of directionally-selective neurons to hair cells (Ji et al. 2018).

In the mammalian cochlea, hair cell activity is certainly important for hair cell maturation and cochlear wiring, as spontaneous action potentials occur during development prior onset of auditory-induced stimulation (Johnson et al. 2011, 2013; Wang and Bergles 2015). However, like zebrafish, hair cells can be innervated even when neurotransmitter release is reduced or absent. Such innervation was observed in rodent *Vglut3* knockouts and *Cav1.3* knockouts, although these synapses do degenerate over time (Glueckert et al. 2003; Nemzou N. et al. 2006; Seal et al. 2008; Ruel et al. 2008). The role of these conserved genes in synaptic activity is discussed below.

2.7 SYNAPTIC ACTIVITY

Hair cells transduce mechanical stimulation into electrical signals through graded receptor potentials and neurotransmitter release to post-synaptic lateral line afferents. Patch clamp electrophysiology experiments reveal that lateral line hair cells exhibit K^+ and Ca^{2+} currents similar to those of other piscine, avian, and mammalian vestibular hair cells (Ricci et al. 2013; Olt et al. 2014, 2016). These include A-type and delayed-rectifier type K^+ currents. The details of the current profiles are distinct from those of the mammalian cochlea; however, hair cell conductances vary across the cochlea itself (Johnson 2015; Olt et al. 2016). Nevertheless, it is likely that the lateral line system will be most useful for studying general principles of hair cell physiology in an intact system.

Similar to the identification of proteins involved in mechanotransduction, circler mutants were critical in early studies of the lateral line hair cells and their afferent synapses. Identification of *slc17a8*, which encodes for the glutamate transporter Vglut3, as the gene underlying the *asteroid* mutation showed that lateral line hair cells – like cochlear hair cells – rely on glutamatergic synaptic transmission (Obholzer et al. 2008). Neurotransmitter release depends on calcium influx through L-type voltage-gated calcium channels, Cav1.3, localized to the basal membrane (Moser and Beutner 2000; Sidi et al. 2004; Sheets et al. 2012). As in *asteroid* mutants, lateral line afferents in *gemini* mutants (caused by a mutation in the *cacna1d* gene encoding for Cav1.3) do not respond to hair cell stimulation or exhibit any spontaneous activity due to abolished neurotransmitter release (Obholzer et al. 2008; Trapani and Nicolson 2011). The function of these genes is conserved in mammalian hair cells, as transmission is significantly impaired in both *Cav1.3* and *Vglut3* mouse mutants (Glueckert et al. 2003; Nemzou et al. 2006; Seal et al. 2008; Ruel et al. 2008).

Precise timing of hair cell neurotransmitter release allows afferent neurons to phase-lock their activity to hair cell stimulation, maintaining signal fidelity. The importance of proper vesicle release is illustrated by two mutants: the *comet* mutant and the *pinball wizard* mutant. The gene underlying the *comet* mutation is *synaptojanin1* (*synj1*), which is required for synaptic vesicle recycling. Although less severe than the other transmission mutants, *comet* mutants display delayed hair cell output relative to mechanical stimulation and disrupted afferent phase-locking (Trapani et al. 2009). In mice, synaptojanin dysfunction leads to more drastic phenotypes. *Synj1* mutants do not survive long after birth, although examination of cultured cortical neurons from mutant animals revealed reduced vesicle pools and reduced vesicle recycling with prolonged periods of stimulation (Kim et al. 2002). *Synj2* mutants, also known as *Mozart*, exhibit an auditory system-specific phenotype wherein cochlear hair cells degenerate (Manji et al. 2011). Timing of neurotransmitter release is also implicated in *Pinball wizard* mutants, affecting the *wrb* gene which encodes a small transmembrane protein required for membrane insertion of tail-anchored proteins. Mutants show reduced synaptic vesicle reserve pool and a reduction in proteins associated with synaptic vesicles, suggesting a lack of ability to replenish the vesicle pool. These animals display visual deficits in addition to balance deficits and diminishing auditory startle responses (Lin et al. 2016). Mutations in the mouse *Wrb* gene also cause reduced hearing as a result of synaptic disruption (Vogl et al. 2016). The WRB protein is targeted to the endoplasmic reticulum, where it regulates the membrane insertion of the hair cell synaptic regulator otoferlin.

Perhaps the most important structure allowing hair cells to transmit both the timing and intensity of mechanical stimulation is the synaptic ribbon. Synaptic ribbons are pre-synaptic electron densities that tether glutamate-filled vesicles near the active zone, thus permitting rapid

and sustained neurotransmitter release (Matthews and Fuchs 2010; Nicolson 2015). Hair cell synaptic ribbons are largely composed of the protein Ribeye, which is encoded by two paralogous genes in zebrafish: *ribeye a* and *b;* also known as *ctbp2a* and *ctbp2l* (Wan et al. 2005; Sheets et al. 2011). With the ability to easily induce genetic mutation and transgenesis, zebrafish have been useful models for investigating ribeye function in intact organisms.

Ribeye plays a critical role in directing ribbon organization and synaptic organization, particularly as related to appropriate localization and clustering of Cav1.3 channels (Sheets et al. 2011, 2017; Lv et al. 2016). In *ribeye* CRISPR knockouts, Lv et al. observed "ghost ribbons," or ribbons that lacked synaptic densities and did not appose any efferent or afferent neuronal connections (in addition to aberrant Cav1.3 channel clustering). Curiously, this did not correspond with any obvious deficits in postsynaptic activity. Overexpression of *ribeye* can lead to enlargement of hair cell ribbons; however, this did not increase Cav1.3 channel localization at the synapse (Sheets et al. 2017). Additionally, while these hair cells had more associated synaptic vesicles relative to wildtype and exhibited increased calcium signaling, ribbon enlargement corresponded with reduced afferent neuron spontaneous activity and increased response latency to the onset of hair cell stimulation. Investigating Ribeye activity has been complicated by the difficulty of completely disrupting gene and protein function. For example, in the CRISPR knockout study, Ribeye expression was dramatically reduced in double knockouts, but still detectable, albeit at low levels, at the presynapse by immunohistochemstiry (Lv et al. 2016). In mouse, *ctbp2* knockout is embryonic lethal (Hildebrand and Soriano 2002), however, RIBEYE disruption has been achieved through the generation of a Cre knockout mouse (Maxeiner et al. 2016). Cre-mediated excision removed the RIEBEYE A domain, but left the B domain, which is essentially identical to CtBP2. Truncation of the protein was found to interfere

with ribbon formation, however presynaptic active zones still formed, perhaps explaining the relatively small effect on synaptic transmission and mild hearing deficit observed (Becker et al. 2018; Jean et al. 2018). These results suggest that compensatory mechanisms may be masking the importance of RIBEYE function in both mammalian and zebrafish models.

While Ribeye is important for calcium channel localization and synaptic organization, ribbon size can in turn be influenced by calcium (Sheets et al. 2012). Additionally, although a postsynaptic target is not required for ribbon formation, the presence of a postsynapse does influence ribbon maintenance (Suli et al. 2016). Lack of innervation, as in *neurogenin* mutants or with lateral line nerve transection, corresponds with smaller ribbon size and improper ribbon localization. During hair cell regeneration, Ribeye clustering at the basal cell membrane corresponds with the timing of hair cell innervation (Suli et al. 2016). There also appears to be a dynamic aspect to the structure, as Ribeye protein is mobile within the ribbons and exchanged at a low rate, suggesting some level of turnover and renewal (Chen et al. 2017; Graydon et al. 2017). In addition to the importance of Ribeye, these studies highlight mechanisms that influence ribbon formation and maintenance.

In addition to genetic studies used to identify proteins important for synaptic transmission, the lateral line provides a means with which to understand the functional limits of the system. Although the formation of synaptic structures is relatively uniform across neuromast hair cells, some hair cells within individual neuromasts are synaptically silent upon mechanical stimulation despite robust depolarization (Zhang et al. 2018). Synaptically-inactive hair cells can become active within minutes after ablation of a neighboring active hair cell, suggesting the process is dynamically regulated. This regulation of presynaptic activity is independent of innervation and appears to depend on intact K^+ handling by surrounding supporting cells. It will

be interesting to see whether this tight regulation of synaptic activity extends to hair cells in other systems.

This model has also been used to identify mechanisms of damage that are quite difficult to address in the mammalian auditory system due to its inaccessible anatomical location. For example, neuronal damage following noise exposure was recently modeled in a study of glutamatergic transmission and excitotoxicity affecting lateral line afferents (Sebe et al. 2017). Hair cell stimulation leads to robust calcium influx into post-synaptic afferent terminals through calcium-permeable AMPA receptors. Prolonged receptor activation led to calcium accumulation, causing swelling and decreased afferent responsiveness, while blocking the calcium-permeable AMPA receptors prevented the excitotoxic effects. These results parallel mammalian studies of excitotoxicity in the cochlea following noise exposure (Puel et al. 1998). Calcium influx is followed by swelling of the spiral ganglia neuron terminals contacting inner hair cells, which can be caused or mitigated by activating or inhibiting AMPA receptors, respectively (Puel et al. 1998). As evidence from Sebe et al. (2017) supports functional conservation of calcium-permeable AMPA receptors across vertebrates, these channels are likely crucial players in the synaptic damage that occurs following noise overexposure leading to hearing loss. Beyond damage to terminals, glutamate excitotoxicity can lead to apoptotic lateral line hair cell death, even in the absence of afferent or efferent innervation (Sheets 2017). These findings suggest that glutamate accumulation following noise exposure may have a direct pathological effect on the hair cells as well as the afferents.

2.8 HAIR CELL DEATH

Hearing loss can occur due to aging, loud noise exposure, and ototoxic compound exposure. Of these, damage or death of the sensory hair cells is a common feature. In addition to their use as

genetic models of hearing loss, zebrafish have been extraordinary models for understanding mechanisms of hair cell death, particularly as a result of ototoxic drug exposure. In addition to their sensitivity to heavy metals (e.g., copper), lateral line hair cells are susceptible to the otherwise therapeutic aminoglycoside antibiotics (e.g., neomycin and gentamicin) and chemotherapeutic agents such as cisplatin (Harris et al. 2003; Ton and Parng 2005; Linbo et al. 2006; Hernández et al. 2006; Ou et al. 2007; Olivari et al. 2008; Van Trump et al. 2010). Despite their importance for treating disease, the unwanted side effect of these compounds has led to an effort to understand their specific off-target toxicity as well as the development of means to protect hair cells from the ensuing damage. Larval zebrafish are particularly well suited to this line of inquiry. Ototoxic compounds can be added to the media of free swimming larvae and hair cell loss can be easily monitored via vital dye staining or transgenic animals with fluorescently labeled hair cells. Moreover, the accessibility of lateral line hair cells allows for live-imaging studies of drug entry and the post-exposure events that lead to cell death. Importantly, these compounds also kill hair cells in a reliably dose-dependent fashion (Harris et al. 2003; Ou et al. 2007). In combination with the ability to obtain many zebrafish larvae at once, the ability to generate a reliable dose-response curve has provided a valuable tool for evaluating means of hair cell protection and sensitization in both genetic and small molecule screens (Figure 2.2). The zebrafish model also has the potential to identify new ototoxic compounds, previously identified by anecdotal patient reports. Systematic screening of drugs alone or in combinations has revealed ototoxic drugs that should be studied further in mammalian systems (Chiu et al. 2008; Hirose et al. 2011).

2.8.1 *Mitochondrial dysfunction leading to hair cell death*

Zebrafish have been quite useful for understanding subcellular events leading to hair cell death, with a particular focus on mitochondria. Mitochondrial dysfunction is a universal feature of multiple modes of hair cell damage and death, including noise damage, age-related hearing loss, and aminoglycoside-exposure (Kopke et al. 1999; Pickles 2004; Böttger and Schacht 2013). Following aminoglycoside antibiotic treatment, dying hair cells across vertebrate taxa exhibit a suite of cellular and morphological changes, including dilated and swollen mitochondria (Duvall and Wersäll 1964; Bagger-Sjöbäck and Wersäll 1978; Lang and Liu 1997; Hirose et al. 2004; Owens et al. 2007). Additional evidence of mitochondrial distress stems from the production of reactive oxygen species (ROS) and the modest protective effects of treatment with antioxidants or expression of ROS-reducing enzymes (Clerici et al. 1996; Sha and Schacht 2000; Sha et al. 2001a, b; McFadden et al. 2003; Kawamoto et al. 2004; Jiang et al. 2005; Ton and Parng 2005; Choung et al. 2009; Someya et al. 2009, 2010; Jensen-Smith et al. 2012; Chen et al. 2013; Quan et al. 2015; Takumida et al. 2016). Incidentally, ROS production is not limited to aminoglycoside treatment, as similar results have been observed with copper treatment in larval zebrafish (Olivari et al. 2008).

Mitochondrial ROS production in response to treatment with neomycin occurs due to toxic calcium elevation and transfer between intracellular compartments. Through live-imaging studies during neomycin exposure, Esterberg et al. (2013,14) determined that calcium flows from the ER to the mitochondria, causing depolarization of the organelles and production of ROS (Esterberg et al. 2013, 2014). As mitochondrial membrane potential is lost, calcium is then released into the cytoplasm, and cells ultimately lose membrane integrity. Manipulation of calcium flow can either protect or sensitize cells to neomycin treatment. Specifically reducing

mitochondrial ROS production using a targeted ROS sink also conferred hair cell protection (Esterberg et al. 2016).

Given the importance of mitochondria for both hair cell function and death, research devoted to understanding the role of mitochondrial networks, biogenesis, and dynamics will likely be an important area of exploration. In support of this avenue, a recent study found that application of mdivi-1 – a mitochondrial fission inhibitor – protected hair cells from cisplatin-induced hair cell toxicity (Vargo et al. 2017). This suggests that mitochondrial dynamics may play a role in hair cell viability. Beyond understanding ototoxic-induced hair cell dysfunction, mitochondria-focused studies would provide additional insight into the hearing impairment caused by mutations in mitochondrial genes that lead to syndromic and non-syndromic hearing loss (Kokotas et al. 2007; Luo et al. 2013; Ding et al. 2013).

2.8.2 *Genetic screening for modulators of hair cell death*

A major facet of drug-induced ototoxicity is entry into hair cells (Olivari et al. 2008; Coffin et al. 2009; Thomas et al. 2013; Hailey et al. 2017). Across taxa, active mechanotransduction is required for drug entry, presumably through the large mechanotransduction channels (Gale et al. 2001; Marcotti et al. 2005; Alharazneh et al. 2011). As a result, blocking mechanotransduction, and thus drug uptake, remains one of the most potent means of protecting hair cells. This is evidenced in part by the fact that the MET-incapable mutants in both mouse and zebrafish are resistant to neomycin (Richardson et al. 1997; Seiler and Nicolson 1999; Vu et al. 2013; Thomas et al. 2013). In order to investigate other genetic modulators of hair cell death, Owens and colleagues conducted a forward genetic screen identifying mutations that conferred hair cell protection (Owens et al. 2008). Although the genes identified had quite disparate functions,

many of them influence hair cell mechanotransduction to some extent (Owens et al. 2008; Hailey et al. 2012; Stawicki et al. 2014, 2016).

Two of the mutants, *persephone* and *merovingian*, were found to have mutations in genes that relate to ionic balance homeostasis. *Persephone* possesses a mutation in the *slc4a1b* gene encoding a chloride/bicarbonate exchanger, which fails to properly target to the cell membrane. *Persephone* mutants are resistant to multiple aminoglycosides and partially resistant to cisplatin. Recapitulating the mutant phenotype, pharmacological blockade of the exchanger and elevated extracellular bicarbonate concentration can be used to protect wildtype hair cells (Hailey et al. 2012). A mutation in the *gmc2* gene was found to underlie the *merovingian* mutant. Gmc2 is a transcription factor involved in the production of a particular type of ionocyte (H+-ATPase-rich)**,** which maintains and regulates whole body pH in fish. Like *persephone*, *merovingian* mutants displayed strong neomycin resistance and moderate resistance to cisplatin, in addition to an acidified extracellular environment surrounding lateral line hair cells (Stawicki et al. 2014). Both *persephone* and *merovingian* mutants exhibit decreased mechanotransduction and drug uptake, highlighting the importance of ionic balance for both proper hair cell function and protection. This is further bolstered by the finding that elevated extracellular calcium or magnesium concentration have a similar effect (Coffin et al. 2009).

Identification of another mutant from the screen led to the investigation of a completely different group of genes: cilia genes related to intraflagellar transport (IFT) and the ciliary transition zone (Stawicki et al. 2016). Mutations in cilia-related genes typically lead to a variety of diseases known as ciliopathies. Unlike auditory hair cells, lateral line and vestibular hair cells maintain a single true cilium, the kinocilium (discussed above). Mutations in the IFT genes have different effects on hair cells compared to the transition zone mutants. Unlike the transition zone

mutants, IFT mutants show defects in kinocilia formation and aminoglycoside uptake in addition to protection. For both groups, the stereocilia of the hair cells appear normal.

2.8.3 *Small molecule screening for modulators of hair cell death*

In addition to genetic screening, zebrafish larvae are ideal model organisms for small molecule screening. This is due in part to their small size and the ability to obtain many hundreds of animals for a given experiment. Moreover, the surface location of lateral line hair cells means that hair cell survival or death can be determined based on relative fluorescence with animals in a 96-well plate. A number of small molecule screens have been conducted to identify ototoxins as well as compounds that confer hair cell protection (Ton and Parng 2005; Owens et al. 2008; Ou et al. 2009; Coffin et al. 2010, 2013b; Kruger et al. 2016). In screening protective compounds, ideal candidate molecules must show protection 1) at low doses; 2) without interfering with the therapeutic function of the drugs; and 3) without inhibiting mechanotransduction or drug uptake.

Depending on the design, one downside of the broad screens is that the mechanistic action of the compounds is unknown. In a screen conducted by Coffin *et al.*, a more focused approach was taken in selecting compounds with known intracellular targets that might confer protection against neomycin, gentamicin, or cisplatin exposure (Coffin et al. 2013b). Some compounds were protective against multiple insults; however, most of the hits were protective against only one or two of the toxins. For example, autophagy inhibitor 3-MA protected hair cells from both aminoglycosides and cisplatin, while an antioxidant, D-methionine, protected hair cells from gentamicin and cisplatin. Interestingly, caspase inhibition was not found to protect zebrafish hair cells, contrasting studies of inner ear hair cells in rodent and chick (Cheng et al. 2005), suggesting that some mechanisms of cell death may not be conserved across taxa.

The genetic and small molecule screens highlight the multitude of mechanisms that contribute to hair cell susceptibility or protection, likely reflecting the multiple cell death pathways activated during drug-induced hair cell death. Recent exploration of aminoglycoside drug entry and trafficking has provided some additional insight into how different cell death mechanisms may be activated. Hailey *et al.* observed that entry was mediated both by mechanotransduction and endocytosis, consistent with many studies finding that toxicity is mechanotransduction dependent (as discussed above), and with a prior documentation of apical vesicle pools in hair cells that could mediate entry (Seiler and Nicolson 1999; Hailey et al. 2017). Upon entering hair cells, aminoglycosides accumulate diffusely in the cytoplasm and in discrete lysosomes. Interestingly, intracellular accumulation differs depending on the aminoglycoside used. While neomycin remains largely diffuse and more slowly accumulates into lysosomes, the opposite is true for gentamicin. Inhibition of endocytosis and vesicle budding reduces lysosomal accumulation for both compounds and increased gentamicin-induced cell death, but not neomycin-induced cell death. Alternatively, increasing lysosomal accumulation relative to the cytoplasmic accumulation reduced cell death. Together, these data suggest that lysosomal compartmentalization has a protective effect. Overall they also support the idea that different aminoglycosides activate different cell death pathways (Owens et al. 2009; Coffin et al. 2013a).

The ultimate goal of studying the mechanisms of hair cell death and protection is to develop therapeutic strategies for preventing human hearing loss. In progressing toward this goal, recent small molecule screens have been used to identify protective compounds that were also validated in mammalian systems. Using a zebrafish screen, Kenyon *et al.* identified 13 compounds that also protected hair cells in mammalian cochlear cultures from the

aminoglycoside antibiotic gentamicin (Kenyon et al. 2017). This study focused on compounds that block mechanotransduction, preventing aminoglycoside entry. Another recent screen built on previous identification of the protective compound PROTO-1, this time conducting a new search with analogs synthesized to develop a structure-activity relationship (Owens et al. 2008; Chowdhury et al. 2018). Use of a new compound, ORC-13661, was validated in rats *in vivo* during co-administration with the aminoglycoside antibiotic amikacin. With oral administration, ORC-13661 treatment provided significant hearing protection compared to rats treated with amikacin only, as determined via ABR testing. While taking different approaches, both studies highlight using zebrafish in progressing the development of otoprotectants that will alleviate hearing loss associated with therapeutic drug treatment.

2.9 CONCLUSION

The zebrafish is a unique and convenient model for investigating the biology of genes, cells, and structures that share homology with the mammalian auditory system. Among other advantages, the surface location of the lateral line as well as the ease of genetic manipulation in zebrafish have facilitated important studies contributing to our understanding of human hereditary deafness as well as acquired hearing loss due to hair cell or neuronal toxicity. Moreover, the use of zebrafish in small molecule screens constitutes the first steps in developing therapeutic compounds to prevent cochlear damage in the first place. With the emergence of CRISPR and other technologies, zebrafish studies have the potential to significantly advance understanding of subcellular structures and events that contribute to hair cell function and disease.

2.10 ACKNOWLEDGEMENTS

The authors thank Eric Thomas for his thoughtful comments and Lavinia Sheets for her insights and expertise in improving this manuscript.

2.11 FIGURES

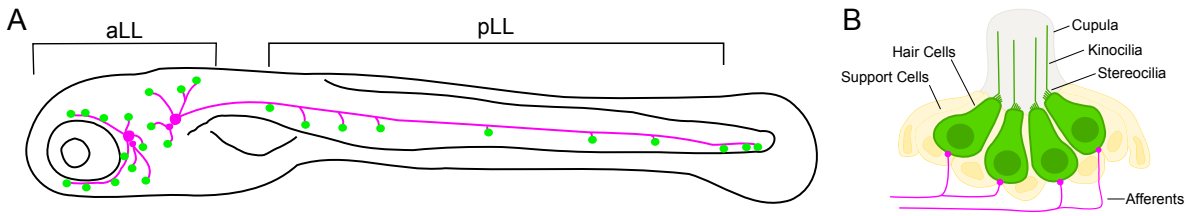

Figure 2.1. Anatomy of the zebrafish lateral line.

(A) Schematized visualization of the anterior (aLL) and posterior (pLL) lateral line of a larval zebrafish. Neuromasts are represented by the green dots and innervation is represented by the magenta lines. **(B)** Schematized cross section of a lateral line neuromast, including structures and cell types.

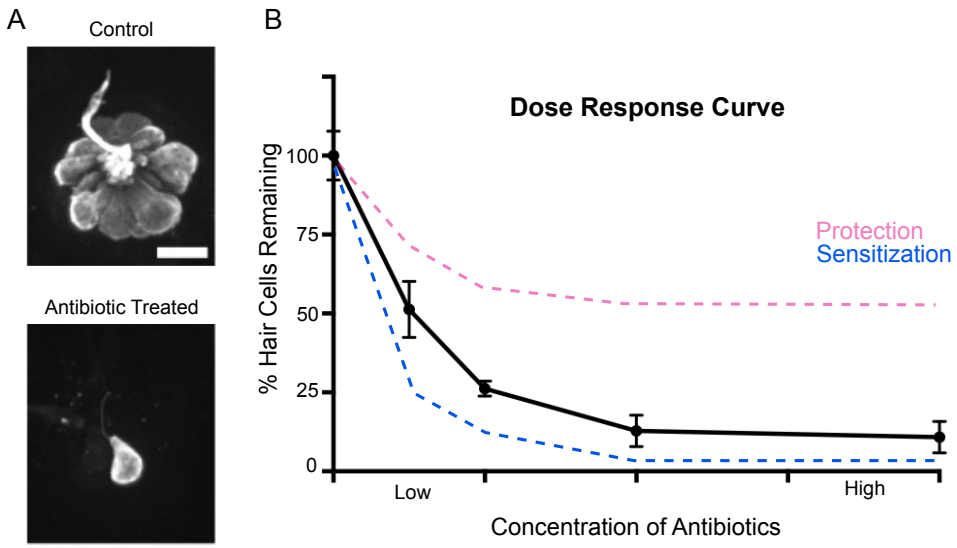

Figure 2.2. Using a dose response curve to assay hair cell death modulators.

(A) Lateral line hair cells labelled with parvalbumin in control or antibiotic treated conditions. Scale bar = 10 μm. **(B)** Hair cells can be counted following treatment with different concentrations of toxic aminoglycoside antibiotics. As antibiotic concentrations increase, the number of hair cells remaining decreases. The resulting dose-response curve can be reliably reproduced across experiments. As a result, mutations or compounds can easily be assayed for effects on hair cell death. Hair cell protection or sensitization would be indicated by shifts in the curve (pink and blue lines, respectively). Data points represent the mean percentage of hair cells remaining. Error bars = SD. Figure adapted from Stawicki et al. (2014). CC BY 3.0.

2.12 TABLES

Table 2.1. Zebrafish models of human hereditary hearing loss

DFNA/B	Human Gene	Zebrafish Gene	Zebrafish Reference
DFNA2A	KCNQ4	*kcnq4*	(Wu et al. 2014)[1]
DFNA3A,B DFNB1A,B	GJB2, GJB6	*cx30.3**	(Chang-Chien et al. 2014)[2]
DFNA5	GSDME	*gsdmeb*	(Busch-Nentwich et al. 2004)[2]
DFNA8,12 DFNB21	TECTA	*tecta*	(Stooke-Vaughan et al. 2015)[2]
DFNA10	EYA4	*eya4*	(Wang et al. 2008)[2,3]
DFNA11 DFNB2	MYO7A	*myo7aa*	(Nicolson et al. 1998; Ernest et al. 2000)[2,3]
DFNA22 DFNB37	MYO6	*myo6b*	(Seiler et al. 2004; Kappler et al. 2004)[2,3]
DFNA23	SIX1	*six1a*	(Bricaud and Collazo 2006, 2011)[2]
DFNA25	SLC17A8	*slc17a8*	(Obholzer et al. 2008)[3]
DFNA28	GRHL2B	*grhl2b*	(Han et al. 2011)[2,3]
DFNA36 DFNB7,11	TMC1	*tmc2**	(Chou et al. 2017)[3]
DFNA50	MIRN96	*mir96*	(Li et al. 2010)[2]
DFNA68	HOMER2	*homer2*	(Azaiez et al. 2015)[2]
DFNA71	DMXL2	*rbc3α*	(Einhorn et al. 2012)[3]
DFNB4	SLC26A4	*slc26a3**	(Bayaa et al. 2009)[1]
DFNB6	TMIE	*tmie*	(Shen et al. 2008; Gleason et al. 2009)[2,3]
DFNB9	OTOF	*otofa/b*	(Chatterjee et al. 2015)[3]
DFNB12	CDH23	*cdh23*	(Nicolson et al. 1998; Söllner et al. 2004; Blanco-Sánchez et al. 2014)[2,3]
DFNB18	USH1C	*ush1c*	(Phillips et al. 2011; Blanco-Sánchez et al. 2014)[2,3]
DFNB18B	OTOG	*otog*	(Stooke-Vaughan et al. 2015)[2]
DFNB23	PCDH15	*pcdh15a*	(Seiler et al. 2005; Maeda et al. 2014, 2017)[2,3]
DFNB24	RDX	*msna*	(Pataky et al. 2004)[1]
DFNB31	WHRN	*whrnb*	(Blanco-Sánchez et al. 2014)[1]
DFNB32,105	CDC14A	*cdc14aa*	(Delmaghani et al. 2016; Imtiaz et al. 2018)[2,4]

DFNB42	ILDR1	*ildr1b*	(Sang et al. 2014)[2,3]
DFNB44	ADCY1	*adcy1b*	(Santos-Cortez et al. 2014)[3]
DFNB49	CIB2	*cib2*	(Riazuddin et al. 2012)[2,3]
DFNB57	PDZD7	*pdzd7a*	(Ebermann et al. 2010)[2,3]
DFNB61	SLC26A5	*slc26a5*	(Weber et al. 2003; Albert et al. 2007; Schaechinger and Oliver 2007; Tan et al. 2011)[1§]
DFNB63	LRTOMT/COMT2	*tompt*	(Nicolson et al. 1998; Erickson et al. 2017)[3]
DFNB66	DCDC2	*dcdc2b*	(Grati et al. 2015)[2,3]
DFNB66,67	LHFPL5	*lhfpl5a*	(Maeda et al. 2017)
DFNB68	S1PR2	*mil**	(Hu et al. 2013)[2]
DFNB74	MSRB3	*msrb3*	(Shen et al. 2015)[2,3]
DFNB84	OTOGL	*otogl*	(Yariz et al. 2012)[2,3]
DFN89	KARS	*kars*	(Santos-Cortez et al. 2013)[1]
DFNB93	CABP2	*cabp2*	(Di Donato et al. 2013)[1]
DFNB99	TMEM132E	*tmem132e*	(Li et al. 2015)[2,3]

DFN genes were identified using the Hereditary Hearing Loss website (http://hereditaryhearingloss.org/) and cross referenced using the Zebrafish Information Network (ZFIN) online database (https://zfin.org/).
[1]Denotes studies with expression data only.
[2]Denotes studies in which a morphological and/or developmental mutant phenotype was observed.
[3]Denotes studies in which a physiological and/or behavioral mutant phenotype was observed.
[4]Note: Phenotypic inconsistency observed between CRISPR knock-out (Imtiaz et al. 2018) and morpholino knock-down (Delmaghani et al. 2016) methodologies.
*Homologous gene.
[§]Characterization of protein function.

Chapter 3. CUMULATIVE MITOCHONDRIAL ACTIVITY CONFERS SELECTIVE SUSCEPTIBILITY IN LATERAL LINE MECHANOSENSORY HAIR CELLS

The contents of this chapter have been submitted for publication with the following authors:
Sarah B. Pickett, Joy Y. Sebe, Robert Esterberg, Tor Linbo, Dale W. Hailey, David W. Raible

3.1 ABSTRACT

Mitochondria play a prominent role in mechanosensory hair cell damage and death. Although hair cells are thought to be energetically demanding cells, how mitochondria respond to these demands and how this might relate to cell death is largely unexplored. Using genetically encoded indicators, we found mitochondrial calcium flux and oxidation are regulated by mechanotransduction and demonstrate that hair cell activity has both acute and long-term consequences on mitochondrial function. We tested whether variation in mitochondrial activity reflected differences in vulnerability of hair cells to the toxic drug neomycin. We observed that susceptibility did not correspond to the acute level of mitochondrial activity but rather to the cumulative history of hair cell and mitochondrial activity.

3.2 INTRODUCTION

Neurons are some of the most energy demanding cells in the body (Ames 2000). Because of this, they are particularly vulnerable to disruptions in mitochondrial and metabolic function. Despite the importance of proper mitochondrial function for all neuronal cell types, some subpopulations are more vulnerable than others, such as those affected by Parkinson's Disease, ALS, and other neurodegenerative diseases (Saxena and Caroni 2011; Jové et al. 2014). This selective

susceptibility of affected subpopulations has been attributed in part to their high physiological activity and altered response to oxidative stress. In addition to high activity levels, advanced age is also a major risk factor for neurodegenerative diseases, suggesting a connection between aging and selective cell death. Increased selective susceptibility over time could be attributed, at least in part, to the accumulation of oxidative damage caused by reactive oxygen species (ROS), as hypothesized by the free radical theory of aging (Harman 1956; Beckman and Ames 1998; Finkel and Holbrook 2000). Mitochondria have been identified as a major source of ROS and ROS production increases with age (Beckman and Ames 1998; Wallace 2005). If accumulation of mitochondrial oxidation and stress are related to cellular activity, highly active or older cells that have experienced more accumulated activity over time may be more vulnerable to acute damage.

Selective susceptibility is not limited to the central nervous system. Peripheral sensory cells are also highly active as they constantly receive and filter sensory input. Among the peripheral receptors, selective cell death has been well documented for hair cells, the mechanosensory cells of the mammalian inner ear that mediate hearing and balance. Auditory hair cell loss is a common cause of hearing impairment and can occur as a result of exposure to loud noise or clinical therapeutic compounds, and with aging (Yang et al. 2015). Hair cell loss occurs in a characteristic pattern relative to both the frequency tuning of the cells and the cell type (inner vs. outer hair cells). After exposure to aminoglycoside antibiotics or with advancing age, for example, hair cells tuned to higher sound frequencies are lost before those tuned to lower frequencies. Similarly, outer hair cells are more susceptible to damage than inner hair cells (Richardson and Russell 1991; Forge and Richardson 1993; Kamimura et al. 1999; Kopke et al. 1999; Forge and Schacht 2000; Alharazneh et al. 2011; Mahendrasingam et al. 2011). The cause

of differential susceptibility for hair cells remains unclear, although some evidence suggests that differences in hair cell metabolism, free radical damage, or calcium (Ca^{2+}) handling may be contributors, thus implicating mitochondrial involvement (Sha et al. 2001a; Engel et al. 2006; Jensen-Smith et al. 2012). A role for mitochondria is further supported by evidence of mitochondrial dysfunction during hair cell damage. Across species, dying hair cells exhibit swollen mitochondrial morphology and generate ROS in response to ototoxic agents, including aminoglycoside antibiotics and copper (Fermin and Igarashi; Lundquist and Wersäll 1966; Bagger-Sjöbäck and Wersäll 1978; Hirose et al. 1999; Mangiardi et al. 2004; Owens et al. 2007; Olivari et al. 2008; Choung et al. 2009; Esterberg et al. 2013, 2014, 2016).

In this study, we investigate the relationship between mitochondrial activity and selective toxicity of aminoglycosides using the zebrafish lateral line system. Sensory input from the lateral line is mediated by externally located clusters of mechanosensitive hair cells, called neuromasts. These cells allow fish to detect changes in water flow and to navigate their environment. They also share many similarities with hair cells of the inner ear (see Nicolson 2017 for review). This includes conservation with human deafness genes as well as susceptibility to compounds that are ototoxic (Whitfield 2002; Harris et al. 2003; Nicolson 2005; Ton and Parng 2005; Ou et al. 2007). Moreover, the surface location of the lateral line system provides a unique advantage in that we can monitor cellular changes that occur *in vivo* during physical or chemical manipulation with subcellular resolution. Like auditory hair cells, lateral line hair cells of older zebrafish are more susceptible to aminoglycoside-induced cell death (Santos et al. 2006). Unlike cochlear hair cells, lateral line hair cells do not exhibit intrinsic frequency selectivity and, although lateral line hair cells can be classified based on their polarity, they are not otherwise functionally sub-classified by type as are mammalian auditory and vestibular hair cells (Kroese and Van Netten

1989; Jiang et al. 2017). For this reason, it has been particularly puzzling why some lateral line hair cells are more susceptible than others. Here we have imaged cumulative mitochondrial responses to hair cell stimulation or application of toxic aminoglycosides. We demonstrate that hair cell mechanotransduction (MET) activity has both acute and long-term effects on mitochondrial activity. Moreover, we demonstrate that cumulative changes in mitochondrial activity correspond with hair cell susceptibility to damage.

3.3 RESULTS

3.3.1 *Acute mitochondrial activity depends on hair cell mechanotransduction*

To examine mitochondrial responses to hair cell MET activity, we conducted *in vivo* time-lapse imaging studies of lateral line hair cells expressing genetically encoded Ca^{2+} indicators. To visualize hair cell responses to stereocilia deflection, we used the *Tg[myo6b:RGECO]*^{vo10Tg} line in which the red Ca^{2+} indicator RGECO is cytoplasmically expressed in hair cells (referred to as cytoRGECO) (Maeda et al. 2014). We simultaneously monitored mitochondrial Ca^{2+} in the same cells using a mitochondrially targeted GCaMP3 also expressed in hair cells (*Tg[myo6b:mitoGCaMP3]*^{w119}] (referred to as mitoGCaMP) (Esterberg et al. 2014, 2016). Hair cells were imaged at a single plane and mechanically stimulated at two frequencies, 1 or 10 Hz, using a pressure wave applied via a waterjet pipette. In many cases, both cytoRGECO and mitoGCaMP fluorescence intensity increased, indicating that hair cell stimulation causes an influx of Ca^{2+} into both the cytoplasm and mitochondria of the activated cells. Sample frames from four different videos are shown in Figure 3.1 for cytoRGECO (panels A,B) and mitoGCaMP (panels C,D). These data demonstrate that mitochondria respond directly to hair cell MET. The two signals differ, however, in their kinetics. While cytoplasmic Ca^{2+} levels increase and decrease rapidly with the onset and offset of waterjet stimulation, mitochondrial Ca^{2+} levels

exhibit a delayed rise and decay more slowly (Figure 3.1E). This is shown in traces of Ca^{2+} responses (Figure 3.1E, 1I-L) and in summary plots of rise times (Figure 3.1H; 1 vs 10 Hz: cyto 9.1 ± 0.6s vs 8.9 ± 0.7s; mito 26 ± 3.8s vs 13 ± 0.9s; mean ± SE; n = 21 cells). The integrated area (Figure 1.1F; 1 vs 10 Hz: cyto 3.0 ± 0.4 vs 5.6 ± 0.7; mito 2.0 ± 0.6 vs 11 ± 1.3; mean ± SE; n = 19 cells) and peak change in the response (Figure 3.1G; 1 vs 10 Hz: cyto 1.2 ± 0.03 vs 1.3 ± 0.04; mito 1.1 ± 0.03 vs 1.5 ± 0.06; mean ± SE; n = 21 cells) were significantly greater for both the cytoplasm and mitochondria at the higher frequency.

Our time-lapse studies revealed stimulation-dependent variability in mitochondrial Ca^{2+} responses. With a low frequency (1Hz) pressure wave, we observed either no change, a decrease, or an increase in mitochondrial response. With a high frequency (10Hz) pressure wave, however, we saw a shift in the polarity of all mitochondrial responses to an increase in fluorescence. At 1Hz stimulation, cells exhibiting an increase in cytoRGECO fluorescence (reflecting MET activity) exhibited either no change (48%), a decrease (19%), or an increase (33%) in mitoGCaMP fluorescence. When 10 Hz stimulation was applied, mitoGCaMP fluorescence increased in all cells, regardless of the response to 1 Hz. For example, figures Figure **3.1**J and L show mitoGCaMP fluorescence from cells in which increased stimulation frequency increased the peak Ca^{2+} response (Figure 3.1J) or reversed the polarity (Figure 3.1L). In both cases, 10 Hz stimulation also increases the amplitude of the cytoplasmic Ca^{2+} signal (Figure 3.1I and K), indicating that increased hair stimulation causes increased Ca^{2+} influx. For all cells, 10 Hz stimulation increased the integrated area and peak fluorescence for both mitochondrial and cytoplasmic Ca^{2+} signals (Figure 3.1F, G), while rise time was reduced only for mitochondrial Ca^{2+} (Figure 3.1H). Together, these data suggest that the degree of mitochondrial response to hair cell activation corresponds with the intensity of activation.

To assay acute mitochondrial activity another way, we used the cationic dye JC1, a marker of mitochondrial membrane potential. JC1 fluorescence shifts from green to red upon aggregation in energized mitochondria. As a result, JC1 provides a readout of relative mitochondrial membrane potential as an indicator of mitochondrial activity. To assess whether MET activity altered mitochondrial activity, we examined JC1 in wildtype or heterozygous larvae (WT/Het) and in *cadherin23* mutant larvae, also referred to as *sputnik* mutants (Nicolson et al. 1998). As in mammalian hair cells, Cadherin23 is a critical component of the tip links necessary for function of the MET apparatus; thus *sputnik* mutant hair cells are MET inactive (Söllner et al. 2004). Example images of JC1-labelled hair cells are shown in Figure 3.2A and B. JC1 was analyzed as a ratio of red to green fluorescence intensity. Compared to age-matched WT/Het siblings, *sputnik* mutants exhibited significantly lower JC1 fluorescence ratios, indicating that the mitochondria are depolarized (Figure 3.2C) (WT/Het: 0.25 ± 0.24 n = 8 fish, Mutant: 0.05 ± 0.07 n = 8 fish, Mann-Whitney U test, $p < 0.01$, mean ratio ± SD). These results suggest that mitochondrial activity is reduced in the absence of MET.

3.3.2 *Mechanotransduction has long-term effects on mitochondria*

The waterjet studies reveal that mitochondria respond directly to hair cell MET activity. Ca^{2+} flux can have multiple effects on mitochondrial function, including regulation of electron transport during oxidative phosphorylation (OXPHOS) and generation of ROS (Brookes 2004). We next wanted to examine whether acute MET activity causes persistent effects on the state of mitochondria. To look at cumulative mitochondrial activity over time, we used a transgenic zebrafish expressing the reporter mitoTimer in all hair cells (Tg[*myo6b:mitoTimer*]^{w208}; here referred to as mitoTimer). mitoTimer encodes a DsRed mutant (DsRed1-E5) with a COXVIII mitochondrial targeting sequence (Terskikh 2000). While newly synthesized mitoTimer

fluoresces green, the fluorescence shifts irreversibly to red over time due to dehydrogenization of the Tyr-67 residue (Yarbrough et al. 2001; Verkhusha et al. 2004). The change in fluorescence spectra and the means by which it occurs has made mitoTimer a useful tool to examine mitochondrial turnover and transport, as well as reporting cumulative redox history (Ferree et al. 2013; Hernandez et al. 2013; Laker et al. 2014, 2017; Stotland and Gottlieb 2015; Wilson et al. 2017). We used mitoTimer to first examine changes in the state of mitochondria during neuromast maturation. mitoTimer signal was measured from 2 days post-fertilization (dpf), when lateral line hair cells are first observed in development, through 5dpf, the point at which the neuromast is considered functionally mature. Example images of mitoTimer-expressing hair cells are shown in Figure 3.3A and B. mitoTimer fluorescence, reported as a ratio of red to green, increases significantly between 3 and 5dpf (Figure 3.3C) (2dpf: 0.28 ± 0.22, 3dpf: 0.17 ± 0.12, 5dpf: 1.11 ± 0.62; Kruskal-Wallis test, Dunn's post-test, $p < 0.001$; mean ratio ± SD; n = 7-11 fish). The ratio shift corresponds with the timing of functional maturation of the neuromast, including increased hair cell MET activity. These observations suggest that cumulative mitochondrial activity increases with hair cell activity.

mitoTimer is a multifaceted indicator that can reflect multiple aspects of mitochondrial activity and metabolism, including oxidation, over time. During hair cell maturation, two factors could contribute to changes in mitoTimer fluorescence: the age of the cell and rate of oxidation in the organelle. Because some hair cells are added to the neuromast during development from 2-5dpf, differences in mitoTimer ratio may reflect the relative age of hair cells in the cluster. To test this idea, we incubated free-swimming larvae in the nuclear dye Hoechst for 30 minutes at 3dpf. This is an intermediate developmental time point relative to neuromast functional maturity, where only some hair cells have active mechanotransduction and additional hair cells are still

being added to the cluster. At 4dpf, we measured the ratio of mitoTimer fluorescence in individual cells, comparing older (Hoechst labeled) to younger (unlabeled) hair cells. Figure 3.4A shows an example image of Hoechst staining in mitoTimer-expressing hair cells 24 hours after labeling. To directly compare hair cells within the same neuromast, we normalized the mitoTimer ratio for each individual cell to the median ratio of the neuromast as a whole. We found that younger hair cells lacking Hoechst labeling have a mitoTimer ratio near or below the median (Figure 3.4B). The opposite is true for older hair cells that are positive for Hoechst labeling after 24 hours (Hoechst positive: 1.71 ± 0.52, n = 45 cells; Hoechst negative: 0.80 ± 0.45, n = 80 cells; Mann-Whitney U test, $p < 0.001$; mean ratio (normalized) ± SD; 5 fish per group). We confirmed that Hoechst labeling itself does not increase the mitoTimer fluorescence ratio by comparing the distribution of single cell red:green fluorescence from zebrafish treated with Hoechst to an untreated group (Figure 3.4C). Together, these experiments suggest that cells with increased mitoTimer ratios are older and, as a result, have also been capable of MET activity for a longer period of time.

We next tested whether long-term changes in MET activity resulted in alterations in mitochondrial activity, reflected by changes in mitoTimer fluorescence. We first assayed this in the absence of hair cell stimulation by measuring mitoTimer fluorescence in *sputnik* mutants. Compared to age-matched WT/Het siblings, the mitoTimer fluorescence ratio is significantly decreased in *sputnik* mutants, with a difference of 66.3% (Figure 3.5A-C) (Mann-Whitney U test, $p < 0.001$; n = 14 WT/Het fish and 15 mutant fish). Similar results were obtained when embryos were incubated in the MET-blocking drug benzamil (200 μM) for 48 hours (3-5dpf) (Figure 3.5D-F) (Hailey et al. 2017). We observed a reduction of 43.4% relative to 0.5 % DMSO control (Mann-Whitney U test, $p < 0.001$; n = 17 fish per group). We next asked if sustained hair

cell stimulation increases mitoTimer fluorescence. To increase hair cell stimulation, water currents were generated around the larvae by placing them on an orbital shaker at 60 RPM for 24 hours at room temperature. While orbital shaking significantly increased the mitoTimer fluorescence ratio in WT/Het fish, a significant shift was not observed in age-matched *sputnik* mutant siblings (Figure 3.6A) (WT/Het Control: 100 ± 34 n = 47 fish, WT/Het Orbital shaker: 128 ± 47 n = 48 fish, Mutant Control: 58 ± 24 n = 27 fish, Mutant Orbital shaker: 70 ± 21 n = 28 fish; Kruskal-Wallis test, Dunn's post-test, $p < 0.05$; mean ratio reported as a percent of WT/Het Control ± SD).

Changes in mitoTimer fluorescence caused by increased MET activity may reflect changes in mitochondrial oxidation (Laker et al. 2014; Wilson et al. 2017). We therefore examined hair cells labeled with the ROS-indicator dye CellROX green in combination with orbital rotation. CellROX is a cumulative fluorescent dye that localizes to nuclei, exhibiting weak fluorescence that increases in brightness upon oxidation. With longer incubation times, CellROX labels both hair cell and support cell nuclei (Supplemental Figure 3.10). Hair cell fluorescence was measured in a single image plane selected to maximize the hair cell nuclei visualized and avoid signal from support cells. Hair cells were distinguished based on their nuclear shape and apical position within the neuromast (Supplemental Figure 3.10). Similar to the mitoTimer fluorescent shift, orbital shaking significantly increased CellROX fluorescence in WT/Het fish (Figure 3.6B) (WT/Het Control: 100 ± 23 n = 20 fish, WT/Het Orbital shaker: 217 ± 124 n = 20 fish, Mutant Control: 105 ± 55 n = 21 fish, Mutant Orbital shaker: 138 ± 58 n = 20 fish; Kruskal-Wallis test, Dunn's post-test, $p < 0.001$; mean ratio reported as a percent of WT/Het Control ± SD). These results demonstrate that cumulative mitochondrial activity and hair cell oxidation are influenced by long-term changes in MET activity.

While changes in mitoTimer fluorescence reflect mitochondrial oxidation, they might also reflect rates of mitochondrial protein import or turnover. To investigate the effect of hair cell activity on mitochondrial turnover, we conducted photoactivation experiments with mitochondrially-localized, photo-convertible Eos, Tg[*myo6b:mitoEos*]^{w207}, in WT/Het and *sputnik* mutants. Under normal conditions, Eos protein fluoresces green, but undergoes an irreversible conformational change following UV light exposure, which converts its emitted fluorescence to red. Mitochondria-localized Eos in hair cells was photoconverted at 5dpf and then monitored over time to measure loss of red fluorescence as an estimate of mitochondrial or mitochondrial protein turnover. WT/Het and *sputnik* fish taken at 5dpf were imaged at 8 and 16 hours post-photoconversion. Figure 3.7 shows the change in fluorescence at these time points. While green fluorescence remained consistent (data not shown), the percent decrease in red fluorescence was 38.9% and 75.5% for wildtype and mutants, respectively (Mann-Whitney U test, $p < 0.001$; $n = 9$ fish per group). The change in red fluorescence over time indicates that mitochondrial or protein turnover increases with reduced hair cell activity.

3.3.3 *History of hair cell activity predicts likelihood of hair cell susceptibility to damage*

Like mammalian auditory and vestibular hair cells, zebrafish lateral line hair cells are highly susceptible to damage caused by aminoglycoside antibiotics and become oxidized following drug exposure. Mitochondria play a key role, as a recent zebrafish study identified mitochondria as the source of ROS during neomycin-induced hair cell death following mitochondrial Ca^{2+} elevation (Esterberg et al. 2016). Moreover, mitigating mitochondrial ROS generation and Ca^{2+} uptake confers enhanced hair cell protection. Previous studies have also noted selective and asynchronous hair cell death as a result of aminoglycoside exposure, as well as variation in levels of ROS and Ca^{2+} in individual cells. The underlying causes of this differential vulnerability

remain puzzling, particularly because aminoglycoside exposure is comparable for all hair cells in a neuromast (Hailey et al. 2017).

Since mitochondrial Ca^{2+} influx and oxidation also occur in response to hair cell stimulation, we sought to determine whether acute hair cell activity corresponds with selective susceptibility to damage. To do so, time-lapse imaging was conducted with fish co-expressing hair cell-specific mitoGCaMP3 and cytoRGECO. Since mitochondrial and cytoplasmic Ca^{2+} levels increase with hair cell stimulation, measuring the baseline fluorescence of these indicators provides an estimate of hair cell activity just prior to neomycin exposure. Baseline fluorescence was recorded prior to treatment, with values across cells reflecting an 8-fold range for mitoGCaMP and an 11-fold range for cytoRGECO. Animals were then treated with 50 μM neomycin, a concentration that leads to approximately 40% hair cell death (Harris et al. 2003). Cells were subsequently categorized as alive or dead based on observed fragmentation and clearance from the neuromast (Esterberg et al. 2013). Consistent with previous studies, we found no difference in the baseline fluorescence values of living and dying cells for both mitoGCaMP3 and cytoRGECO (Figure 3.8A) (n = 78 living cells, 28 dying cells from 5 fish) (Esterberg et al. 2013). We also examined whether differences in mitochondrial polarity measured with JC1 correspond with differences in neomycin susceptibility. Again, we observed no difference in the mean fluorescence ratios of living and dying cells using this measure (n = 46 living cells, 35 dying cells from 6 fish) (Figure 3.8B). Together these results demonstrate that acute differences in hair cell or mitochondrial activity just prior to neomycin exposure do not correspond with likelihood of subsequent hair cell death.

We next examined whether differences in mitoTimer fluorescence, reflecting cumulative changes in mitochondrial activity, would correlate with susceptibility to damage. Figure 3.9A

shows a time series of mitoTimer-expressing hair cells following neomycin treatment. Baseline ratios of mitoTimer for individual cells were normalized to the median ratio of all cells in the corresponding neuromast. We observed that the average mitoTimer ratio for surviving hair cells was below the median ratio at baseline, while the average ratio for cells that die following treatment was above the median (Figure 3.9B) (Live: 0.77 ± 0.37, Die: 1.30 ± 0.34; Mann-Whitney U test, $p < 0.001$; mean ratio (normalized) ± SD; n = 142 living cells, 74 dying cells from 6 fish). We also calculated the degree to which classifying cells as red (red:green above median) or green (red:green below median) was effective in prospectively identifying those that would live or die. Using this classification, 58 of 74 dying cells were redder, while only 42 of 142 living cells were so ($p<0.0001$, Fisher Exact Test). This distribution shows that the red-green classification scheme provides a sensitivity of 0.78, specificity of 0.70, and a diagnostic odds ratio of 8.63, reflecting strong predictive value. In this case, the diagnostic odds ratio indicates that red cells are over eight-fold more likely to die than live after neomycin exposure. Together with our previous results, this suggests that the most susceptible cells are the older and historically more MET active cells in the cluster. In this way, the cumulative history of mitochondrial activity in hair cells predicts their vulnerability to neomycin exposure.

3.4 Discussion

By monitoring lateral line hair cells using live-imaging techniques, we were able to uncover effects of hair cell MET activity on mitochondria in an intact organism. With acute stimulation, hair cells exhibit increased cytosolic and mitochondrial Ca^{2+} influx with distinct kinetic properties. With chronic changes to hair cell MET activity, we observed corresponding changes in mitoTimer fluorescence, indicative of altered mitochondrial oxidation and turnover. In support of this interpretation, we also observed activity-dependent changes in mitochondrial polarization

as well as hair cell oxidation. Our ability to visualize the chronic impact of hair cell activity on mitochondria allowed us to identify hair cells that are more susceptible to aminoglycoside-induced damage. Our findings show that the cumulative history of MET and mitochondrial activity are predictive of differential hair cell death.

3.4.1 *Mitochondrial metabolism and dynamics during normal cellular activity*

Mitochondria are critical organelles, generating ATP through OXPHOS, while also playing an important role in Ca^{2+} homeostasis and production of ROS. These mitochondrial activities are all interrelated. ROS production within mitochondria occurs as a result of normal metabolic activity at two sites within the electron transport chain, complexes I and III. Electron leakage at these complexes leads to the generation of superoxide, which is converted into membrane-permeable hydrogen peroxide (Loschen et al. 1974; Turrens 2003). Mitochondrial Ca^{2+} signaling influences this process as it can stimulate OXPHOS, and therefore, electron flow (Brookes 2004).

The relationship between Ca^{2+}, metabolic activity, and ROS production is particularly notable for hair cells, where constant stimulation and sensory input leads to Ca^{2+} influx. Increased mitochondrial Ca^{2+} levels were also observed with MET activity, demonstrating that hair cell activity directly affects mitochondria. Compared to cytoplasmic Ca^{2+}, the larger integrated area and rise time of the mitochondrial signal (Figure 3.1F, G) are consistent with the idea that mitochondria may act as Ca^{2+} buffers, mediating Ca^{2+} homeostasis in addition to other means of cellular Ca^{2+} extrusion. This role for hair cell mitochondria has been postulated in mammalian hair cells based, in part, on apical localization of the organelles and through Ca^{2+}-imaging studies during transduction (Weaver and Schweitzer 1994; Rusch et al. 1998; Beurg et al. 2010). Mitochondrial Ca^{2+} buffering could be further investigated through manipulation of Ca^{2+} uptake and release mechanisms during hair cell stimulation.

Constant sensory input and Ca^{2+} flux likely place high demands on mitochondrial activity with potentially long-term consequences. We were able to probe the relationship between mitochondrial history and hair cell activity by monitoring mitoTimer signal in hair cells. mitoTimer fluorescence ratio (red:green) increased as hair cells functionally matured, and after MET was increased by orbital shaking (Figure 3.3, Figure 3.6). When MET activity is significantly reduced or abolished, as with benzamil treatment or in *sputnik* mutants, we observed a dramatic decrease in mitoTimer ratio (Figure 3.5). mitoTimer is a unique but complex indicator, likely reflecting multiple facets of mitochondrial biology. Thus, although there is a significant dependence on hair cell activity, an exact interpretation of mitoTimer fluorescence shifts is less clear. Based on previous studies, we expect that mitoTimer in hair cells reports mitochondrial age, in addition to oxidation, organelle turnover and/or turnover of mitochondrial protein, or a combination of these, as discussed below (Ferree et al. 2013; Hernandez et al. 2013; Laker et al. 2014).

mitoTimer as a reporter of mitochondrial stress and oxidation was first described in a study by Laker *et al.* (2014). mitoTimer red fluorescence shifts were observed in cultured myoblasts and *Drosophila* heart tube after treatment with agents known to increase mitochondrial ROS production, including rotenone, antimycin A, and paraquat. Additionally, the authors observed a significant red shift in aging flies, suggesting that mitoTimer reflects both the age and redox history of the organelles. Later studies also revealed that mitoTimer can be used to assess oxidative stress following ischemia-reperfusion injury in muscle (Wilson et al. 2017). These findings are consistent with studies of the formation of DsRed fluorescent protein, which in itself is mediated by oxidation (Yarbrough et al. 2001; Verkhusha et al. 2004). In lateral line hair cells, we observed shifts in the mitoTimer fluorescence ratio relative to increased or

decreased MET. Given that altered MET is likely to have a substantial metabolic impact on the cells, the change in mitoTimer fluorescence could very well reflect corresponding changes in mitochondrial stress and oxidation over time. This is bolstered by our observation of (1) increased hair cell oxidation with sustained stimulation as reported by CellROX; and (2) reduced JC1 fluorescence in the absence of MET, indicating that MET acutely influences mitochondrial polarization (Figure 3.6, Figure 3.2).

In addition to reporting mitochondrial redox history, mitoTimer has also been used to investigate mitochondrial dynamics and transport (Ferree et al. 2013; Hernandez et al. 2013). The decreased mitoTimer red:green ratio observed in *sputnik* mutants could be interpreted to reflect increased mitochondrial import (with a corresponding increase of "new" green protein relative to red). An important driving factor for mitochondrial import is mitochondrial membrane potential (Wiedemann et al. 2004; Dudek et al. 2013); however we did not observe a correspondence between potential and mitoTimer fluorescence ratio. We observed a decrease in mitochondrial polarity in *sputnik* mutants with JC1 staining, which in isolation would be predicted to result in an increase in the red:green ratio of mitoTimer, rather than the decrease we observed. Decreased red:green ratio might also be interpreted as reflecting increased protein turnover (with degradation of "old" red protein) or increased organelle turnover caused by changes in processes such as mitophagy. We sought to further examine this idea in the context of MET mutants by monitoring changes in red mitoEos fluorescence after photoconversion. A similar strategy has been used previously in mice using the photoconvertible protein Dendra2 (Pham et al. 2012). Although this analysis provides only an estimate of turnover (based on the loss of photoconverted protein), our results suggest that increased mitochondrial turnover or turnover of protein occurs when MET activity is reduced (Figure 3.7), consistent with the

observed changes in mitoTimer. This difference in mitochondrial protein turnover in *sputnik* mutants was unexpected. Previous studies have demonstrated mitochondrial turnover via mitophagy occurs as a quality control process (Zhao et al. 2002; Mizushima et al. 2003; Kim et al. 2007; Nowikovsky et al. 2007; Twig et al. 2008; Campanella et al. 2009). With increased mitochondrial activity in MET active hair cells, we might predict that these cells would incur more damage over time and, as a result, turnover would be higher compared to *sputnik* mutant siblings. One possibility is that mitochondria in wildtype hair cells undergo more fusion and elongation relative to *sputnik* mutants. In other cell types, increased OXPHOS activity has been associated with elongated mitochondrial morphology and, in studies of isolated mitochondria, OXPHOS has been shown to stimulate fusion (reviewed by Mishra and Chan 2016). The fact that mitochondrial activity and dynamics have been shown to reciprocally regulate each other suggests that mitoTimer could also reflect the interrelatedness of the two, as well as mitochondrial turnover via mitophagy. Reduced mitophagy has been observed with increased ROS in neurons (Qi et al. 2011). If similarly true in hair cells, increased or sustained MET activity would predictably lead to red-shifted mitoTimer fluorescence. Studies examining mitochondrial dynamics relative to MET will be important for further elucidating this relationship.

The irreversible nature of mitoTimer conversion afforded us the benefit of examining the cumulative effect on mitochondria over time; however, it does not provide a dynamic picture of mitochondrial activity. It should also be noted that our manipulation of hair cell activity is limited to MET, although other aspects of hair cell function contribute to energy consumption, e.g., neurotransmitter packaging and release. A recent report demonstrates that there is heterogeneity amongst hair cells in their synaptic response to mechanical stimulus (Zhang et al.

2018). Future studies could assess the contribution of basal cellular activity to mitochondrial metabolism and dynamics, as well as a correspondence with hair cell age or susceptibility.

3.4.2 *Selective susceptibility in hair cells*

Early studies of lateral line hair cell susceptibility to aminoglycoside antibiotics demonstrated that hair cell loss is reliably dose-dependent (Harris et al. 2003; Santos et al. 2006), where lower doses of neomycin lead to a smaller percentage of hair cell loss. Upon entering hair cells, neomycin disrupts Ca^{2+} handling and causes increased mitochondrial ROS production prior to hair cell death (Esterberg et al. 2014, 2016). Blocking mitochondrial Ca^{2+} uptake as well as treatment with ROS scavengers that specifically target mitochondria mitigate neomycin-induced damage, highlighting the importance of mitochondrial distress in hair cell susceptibility. The fact that some lateral line hair cells die and others survive has been perplexing. Our data suggest that baseline Ca^{2+} levels or relative levels of mitochondrial membrane polarization just prior to neomycin exposure do not correspond with hair cell susceptibility. Rather, the cumulative impact of mitochondrial activity over a longer period of time serves as better indicator of susceptibility.

Given the impact of MET on mitochondrial activity and the vulnerability of mitochondria to neomycin exposure, we hypothesize that the accumulation of mitochondrial stress underlies differential hair cell susceptibility. Live imaging studies with mitoTimer reveal that cells with a red-shifted fluorescence ratio are more susceptible to low-dose neomycin exposure (Figure 3.9). As older cells, they have been mechanotransducing for a longer period of time (Figure 3.4), but they are not necessarily the most active cells at the time of exposure. We previously showed that maturation of individual hair cells corresponds with neomycin sensitivity: with hair cells in 4dpf fish relatively insensitive to neomycin exposure compared to 5dpf fish (Santos et al. 2006). Here we build on this finding to show an age-dependent difference in cumulative mitochondrial

activity that correlates with neomycin susceptibility. We propose that sustained activity over the life of the hair cell leads to cumulative mitochondrial insult. As a result, older cells are less capable of overcoming acute mitochondrial insult and are more likely to succumb to neomycin-induced damage.

In the cochlea, differential susceptibility and hair cell loss occurs based on hair cell type and location along the tonotopic axis, where outer hair cells are more vulnerable than inner hair cells, and high frequency hair cells more sensitive than low frequency hair cells (Kopke et al. 1999; Forge and Schacht 2000). Our findings are consistent with studies that implicate disparities in metabolic and oxidative stress between cochlear hair cells as an underlying factor of differential susceptibility (Sha et al. 2001a; Jensen-Smith et al. 2012). It is also worth noting that hair cell vulnerability to ROS may also increase with age, as a number of redox-regulating mechanisms display age-related changes. For example, expression of the ROS neutralizing enzyme SOD2 decreases in mammalian hair cells over time (Jiang et al. 2007). Expression of the mitochondrial Sirtuin enzymes, particularly SIRT3, have also been shown to decrease with increasing age in the mammalian cochlea (Takumida et al. 2016). Interestingly, SIRT3 activity has been shown to delay the onset of age-related hearing loss and protect hair cells from both noise and aminoglycoside-induced hair cell damage due to its role in antioxidant defense(Someya et al. 2010; Brown et al. 2014; Quan et al. 2015). Together, these studies suggest that the loss of ROS regulation over time contributes to hair cell susceptibility and hearing loss. This is further supported in work from Someya et al., where overexpression of mitochondria-targeted catalase—another antioxidant enzyme—attenuated hair cell loss and improved hearing thresholds in aging mice (Someya et al. 2009). Although it appears that mitochondrial oxidation may increase over time in lateral line hair cells, changes in the

expression of redox enzymes through maturation have not been examined. Extending analysis of mitoTimer expression to the mammalian cochlea would provide valuable insight into selective susceptibility of mammalian hair cells and a useful comparison to studies focused on the lateral line.

The relationship between mitochondrial dysfunction and hearing loss is of long standing interest. Mitochondrial impairment has been identified in multiple types of cochlear damage and several mutations in mitochondrial genes, as well as nuclear-encoded mitochondrial proteins, are known to cause both syndromic and non-syndromic deafness (Kokotas et al. 2007; Luo et al. 2013; Ding et al. 2013). Moreover, in some cases the mitochondrial mutations appear to synergize with environmental insults, leading to more extensive cochlear damage. For instance, the A1555G mutation in the MTRNR1 gene encoding 12S rRNA has been shown to dramatically predispose patients to hearing loss after exposure to aminoglycoside antibiotics (Prezant et al. 1993; Fischel-Ghodsian et al. 1997). This supports the possibility that as hair cells experience cumulative mitochondrial stress due to normal activity, as indicated in our study, the cellular response to bouts of acute damage may become further compromised over time. This has particular relevance for age-related hearing and hair cell loss. While the exact cause remains unknown, mitochondrial stress has been proposed as a possible mechanism (Seidman et al. 2004). It is also important to consider the complexity of mitochondrial changes that occur over time. In aging and aging-related diseases, mitophagy and mitochondrial dynamics are altered, which can in turn influence OXPHOS and ROS production (Sebastián et al. 2017). Given that the life of a lateral line hair cell is about 10 days, studies of mitochondrial activity, dynamics, and mitophagy in lateral line hair cells could provide valuable insight into age-related hair cell loss and hearing impairment in humans, but with a much shorter time frame. A more thorough

understanding of the stresses incurred during the normal activity of these high-energy cells will inform therapeutic efforts to protect hair cells and hearing function.

3.5 EXPERIMENTAL PROCEDURES

3.5.1 *Transgenesis and mutant fish*

Experiments were conducted on larval zebrafish, ages 5-7 days post-fertilization (unless otherwise noted), prior to sex determination. Larvae were randomly selected for experimental groups. Larvae were raised in E3 embryo medium (14.97 mM NaCl, 500 μM KCL, 42 μM Na_2HPO_4, 150 μM KH_2PO_4, 1 mM $CaCl_2$dehydrate, 1 mM $MgSO_4$, 0.714 mM $NaHCO_3$, pH 7.2) at 28.5°C. All wildtype animals were of the AB strain. Zebrafish experiments and husbandry followed standard protocols in accordance with University of Washington Institutional Animal Care and Use Committee guidelines.

Two genetically-encoded indicators were cloned using the Gateway Tol2 system (Invitrogen) to generate constructs under the hair cell-specific promoter, *myosin6b*(Obholzer et al. 2008), and were maintained as transgenic lines: (1) mitoTimer, a reporter of mitochondrial age, oxidative stress, and turnover; and (2) mitoEos, the photoconvertible fluorophore, Eos, targeted to the mitochondria. Tg[*myo6b:mitoTimer*]^{w208} line was generated using a previously described DsRed mutant, DsREd1-E5, with a cytochrome C oxidase subunit VIII localization sequence(Hernandez et al. 2013; Laker et al. 2014). The Tg[*myo6b:mitoEos*]^{w207} line was generated similarly, with mitochondrial matrix targeting achieved by Eos fusion with the human cytochrome C oxidase subunit VIII localization sequence.

The Tg[*myosin6b:R-GECO1*] ^{vo10Tg} line has been previously described and was provided as gift from Katie Kindt (National Institute of Deafness and Other Communication Disorders, Bethesda, MD, USA) (Maeda et al. 2014). The c*adherin23*^{tj264} mutants (also referred to as

sputnik) have been previously described and were provided as a gift by Teresa Nicolson (Oregon Health and Science University, Portland, OR, USA) (Nicolson et al. 1998). We have shown previously that the Tg[*myosin6b:mitoGCaMP3*]^{w119} line allows reliable detection of mitochondrial Ca^{2+} (Esterberg et al. 2014).

3.5.2 *Spinning disk confocal imaging*

Imaging was performed using an inverted Marianas spinning disk system (Intelligent Imaging Innovations, 3i) with an Evolve 10 MHz EMCCD camera (Photometrics) and a Zeiss C-Apochromat 63x/1.2 numerical aperture water objective. Except where noted, all imaging experiments were conducted with larvae at 5-7 days post-fertilization immersed in E3 media containing 0.2% MESAB (MS-222; ethyl-3-aminobenzoate methanesulfonate). Fish were stabilized using a slice anchor harp (Harvard Instruments) so that neuromasts on immobilized animals had access to the surrounding media. Imaging was performed at ambient temperature, typically 25°C. Fish were oriented in two different positions for *in vivo* imaging studies. For waterjet experiments, fish were placed ventral side up and neuromasts OC1, D1, or D2 were imaged (Raible and Kruse 2000). For all other imaging studies, fish were positioned on their sides against the cover glass to image neuromasts from the posterior lateral line.

3.5.2.1 In vivo waterjet imaging

Waterjet stimulation was used to stimulate lateral line hair cells via directional displacement of the stereocilia. This consisted of a rectified sinusoidal pressure wave applied at 1 or 10 Hz (Trapani and Nicolson 2010). A glass pipette was filled with extracellular solution and placed approximately 100 μm from the hair cells of a given cluster, or neuromast. Pressure output was driven by a pressure clamp (HSPC-1, ALA Scientific) and movement of the kinocilia was used to confirm pressure wave application. GCaMP and RGECO fluorescence values were acquired

with a 1s capture interval using Slidebook software (3i). For waterjet stimulation paired with time-lapse imaging, camera intensification was set to maintain exposure times at approximately 100 ms for GCaMP and RGECO, keeping pixel intensity <25% of saturation. Camera gain was set to 3 to minimize photobleaching. GCaMP3 fluorescence was acquired with a 488 nm laser and 535/30 emission filter. RGECO fluorescence was acquired with a 561 nm laser and 617/73 emission filter.

For analyses of waterjet hair cell responses, fluorescence measurements were exported to MATLAB. As described previously, fluorescence intensity values for the duration of the acquisition period were normalized to the baseline value prior to stimulation (Sebe et al. 2017). MATLAB scripts were used to compute the integrated area of the response, peak of response, and time to reach 75% of the peak (rise time to 75%) (Esterberg et al. 2014; Sebe et al. 2017). The integrated area of the response is the sum of fluorescence intensity values captured during the waterjet stimulus. The 75% rise time is the number of seconds it takes from the start of the stimulus to reach 75% of the peak value.

3.5.2.2 mitoTimer and JC1 imaging and analysis

For static mitoTimer imaging studies, zebrafish were immobilized with a harp and Z-sections were taken at 2 μm through the depth of the neuromast, typically 16 μm. Camera intensification was set at 650 and gain at 3 in order to keep exposure times less than 500 ms and maximum intensities less than 75% of saturation. Settings were held constant across experiments that were directly compared. Green mitoTimer fluorescence was acquired with a 488 nm laser and 535/30 emission filter, while red fluorescence was acquired with a 561 nm laser and 617/73 emission filter.

When mitoTimer imaging was conducted in combination with vital dye staining, live swimming zebrafish were incubated in EM containing Hoechst 33258 (10 mg/ml, ThermoFisher) diluted at 1:5000 for 30 minutes and washed 3 times in E3 media. Larvae were then immobilized for imaging as described above, 24 hours after treatment. Hoechst fluorescence was captured with a 405 nm laser and 445/45 emission filter. 2 second exposures were used to capture dim signals that persisted 24 hours after labeling. Due to the dimness of the Hoechst signal and the high auto-fluorescence of larvae in this wavelength, we considered fluorescence intensity greater than 1 SD over background to be label retaining.

For analyses of mitoTimer, Z-stacks of Tg[*myo6b:mitoTimer*]^{w208} labeled hair cells were opened in 3i Slidebook software. Using the maximum projection of each image, mean intensity values were extracted by drawing masks across entire neuromasts that were exported for analysis. Fluorescence intensities were calculated less the mean background signal (based on a 30 μm x 30 μm background mask that excludes hair cells). For dye labeling studies, masks were generated for individual cells within neuromasts. For single cell analyses, the median ratio for mitoTimer red and green fluorescence was calculated for all distinguishable cells within a given neuromast. Then, each cell's ratio was normalized to the median value of its cluster.

The same imaging and analysis protocol was followed for static imaging of zebrafish labeled with JC1 dye (ThermoFisher). To load the dye, free-swimming larvae were incubated in 1.5 μM JC1 (diluted in E3 media) for 30 minutes and then washed 3 times in E3 media. Imaging was conducted 90 minutes after JC1 incubation.

3.5.2.3 CellROX imaging and analysis

We have shown previously that CellROX green dye allows reliable detection of hair cell oxidation(Esterberg et al. 2016). Free-swimming zebrafish larvae were incubated for 24 hours in

2.5 μM CellROX Green (ThermoFisher) diluted in E3 media. CellROX fluorescence was acquired with a 488 nm laser and 535/30 emission filter. Image acquisition and analysis was conducted as described above for static imaging, but with a notable difference. Because the dye labels both hair cell and support cell nuclei, image analysis was conducted in a single plane. Mean intensity values were extracted by drawing a mask around all cells that were reliably distinguished as hair cells based on nucleus shape and location. Mean intensity was then normalized by the area of the mask to control for differences in the number of distinguishable cells.

3.5.2.4 mitoEos imaging and analysis

Tg[*myo6b:mitoEos*] ^{w207} larvae were exposed to UV illumination with a AUKEY LT-SET1 UV flashlight for 10 minutes with 1-minute rest. This was repeated three times for a total of 30 minutes of UV exposure to maximize photoconversion of Eos protein. Imaging and analysis were conducted as described above for static imaging studies at the time points indicated.

3.5.2.5 Time-lapse imaging

For time-lapse imaging studies, baseline fluorescence readings were taken prior to aminoglycoside exposure**.** Neomycin was then added as a 5x concentrated stock to achieve a final concentration of 50 μM. Fluorescence images were captured in 3-minute intervals for 75 minutes. A motorized stage with set x, y, and z coordinates allowed acquisition from multiple neuromasts per fish during time-lapse recordings. For imaging of all indicators, camera gain and intensification were set to minimize photobleaching and to keep baseline pixel intensity less than 25% of saturation. Z-sections were taken at 2 μm intervals through the depth of the neuromast, typically 16 μm. The same imaging strategy was used for all indicators, however, images were collected at 2-minute intervals with mitoGCaMP3 and cytoRGECO. Time-lapse images were

aligned using 3i Slidebook software. Baseline fluorescence was extracted as noted above for single cells. As described previously, cells were categorized as living or dying based on their fragmentation and clearance from the neuromast following neomycin exposure(Esterberg et al. 2013).

3.5.3 *Statistical analysis*

Statistical parameters, including reporting mean and SD as well as n values, are stated both in the results section and the figure legends for each experiment described. The waterjet and imaging data collected using mitoGCaMP3 and cytoRGECO were analyzed using two-tailed Student's t tests. All other imaging data was analyzed using Mann-Whitney U tests for a comparison of two groups, or Kruskal-Wallis tests with Dunn's post-test to take into account multiple comparisons, as indicated in the text. A p value of less than 0.05 was considered significant. GraphPad Prism 6.0 software was used for all statistical analyses and graphical representations.

3.6 ACKNOWLEDGEMENTS

The authors thank David White and the UW Fish Facility staff for animal care and Max Turner and Jonathan David Ramos for assistance with data analysis. We thank Katie Kindt for the Tg[*myo6b:R-GECO1*] line and Teresa Nicolson for the *sputnik* mutants. This work was supported by the National Institute on Deafness and Other Communication Disorders, grant DC015783, and the National Science Foundation Graduate Research Fellowship, grant DGE-1256082.

3.7 FIGURES

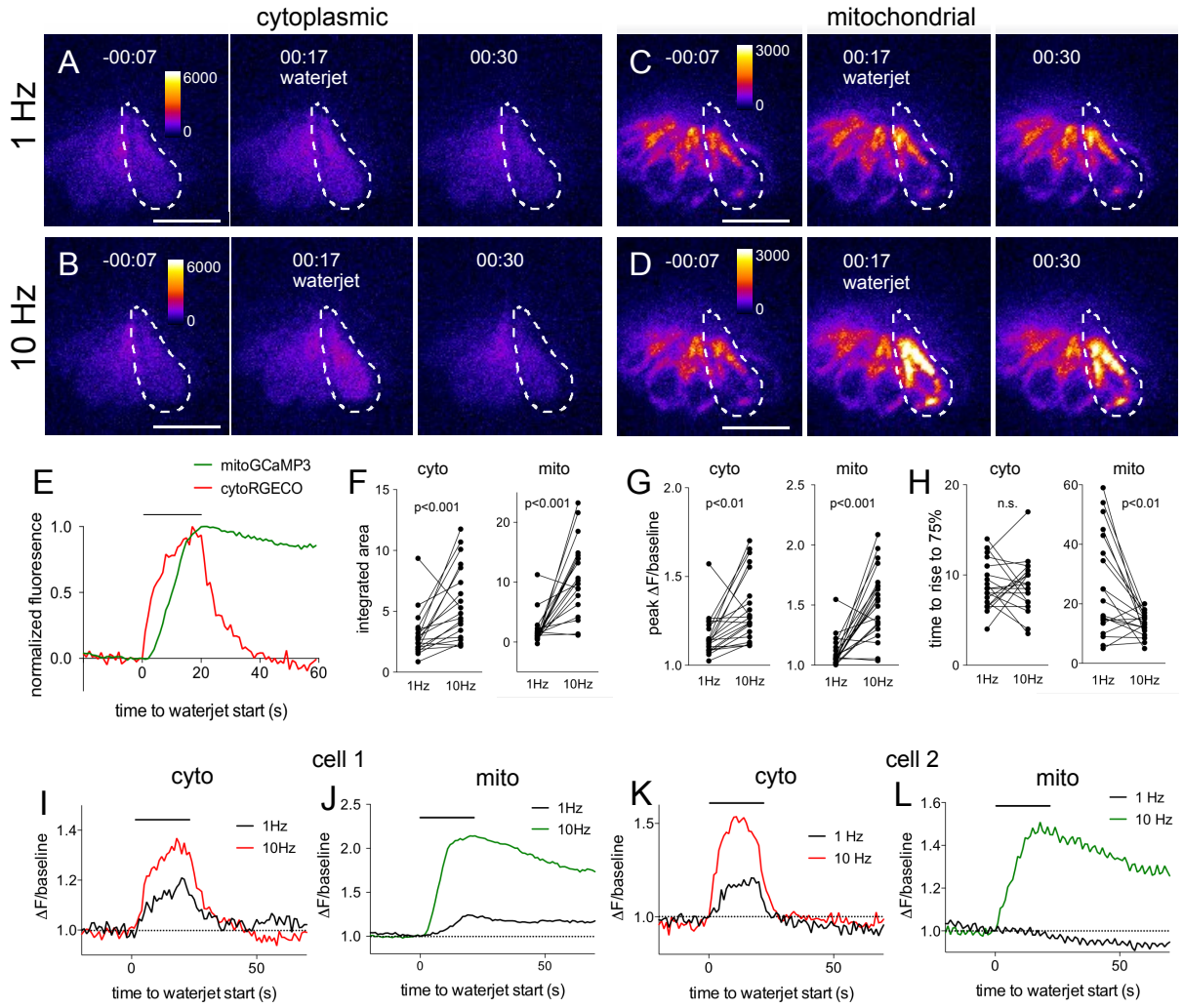

Figure 3.1. Mitochondrial Ca^{2+} increases in response to hair cell stimulation.

Frames from a time-lapse calcium imaging video acquired from Tg*[myo6b:RGECO]*^{vo10Tg} fish **(A,B)** and Tg[*myo6b:mitoGCaMP3*]^{w119} fish **(C,D)** during waterjet stimulation at 1 Hz **(A,C)** and 10Hz **(B,D)**. For each condition, fluorescence is shown before, during, and after stimulation (left, middle, right, respectively). **(E)** Normalized fluorescence of the example cell outlined by the dotted line in A-D. Summary data of the integrated area **(F)**, peak fluorescence **(G)**, and rise time **(H)** for the cytoplasmic and mitochondrial calcium signal at 1Hz and 10Hz stimulation. Values for **(F)**: 1 vs 10 Hz: cyto 3.0 ± 0.4 vs 5.6 ± 0.7; mito 2.0 ± 0.6 vs 11 ± 1.3; mean ± SE; n = 19 cells; **(G)**: 1 vs 10 Hz: cyto 1.2 ± 0.03 vs 1.3 ± 0.04; mito 1.1 ± 0.03 vs 1.5 ± 0.06; mean ± SE; n = 21 cells; (H): 1 vs 10 Hz: cyto 9.1 ± 0.6s vs 8.9 ± 0.7s (p = 0.73); mito 26 ± 3.8s vs 13 ±

0.9s; mean ± SE; n = 21 cells. Cells were analyzed from 10 different fish across three different experiments. **(I,J)** Example cell in which the cytoplasmic calcium increases in response to stimulation at both frequencies, but the mitochondrial calcium signal increases dramatically at 10Hz. **(K,L)** Example cell in which mitochondrial calcium signal decreases at 1Hz stimulation and increases at 10Hz, while cytoplasmic calcium increases at both frequencies. Horizontal line marks the duration of the waterjet stimulus **(E-L)**. Two-tailed paired Student's t test was used to assess significance. Scale bar = 10 μm.

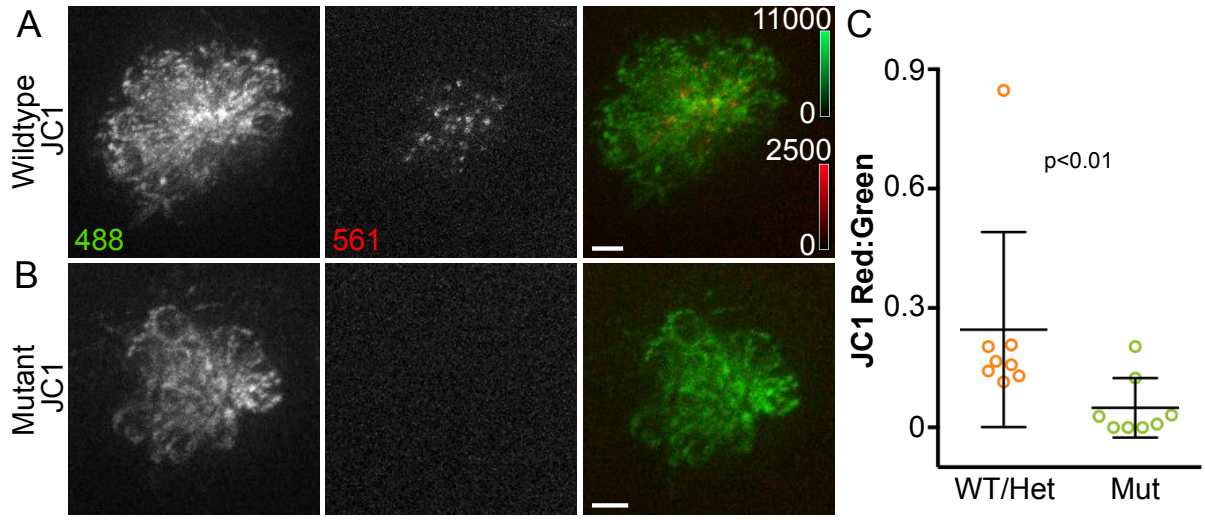

Figure 3.2. Acute mitochondrial activity is reduced in the absence of MET.

(A, B) Maximum projections of hair cells from WT/Het and *sputnik* mutant siblings incubated in JC1 dye. **(C)** Mean JC1 fluorescence plotted as a ratio of red:green. WT/Het: 0.25 ± 0.24 n = 8 fish; Mutant: 0.05 ± 0.07 n = 8 fish; mean ratio ± SD. Mann-Whitney U test was used to assess significance. Value for each fish represents the mean of 3 neuromasts. Scale bar = 5 μm.

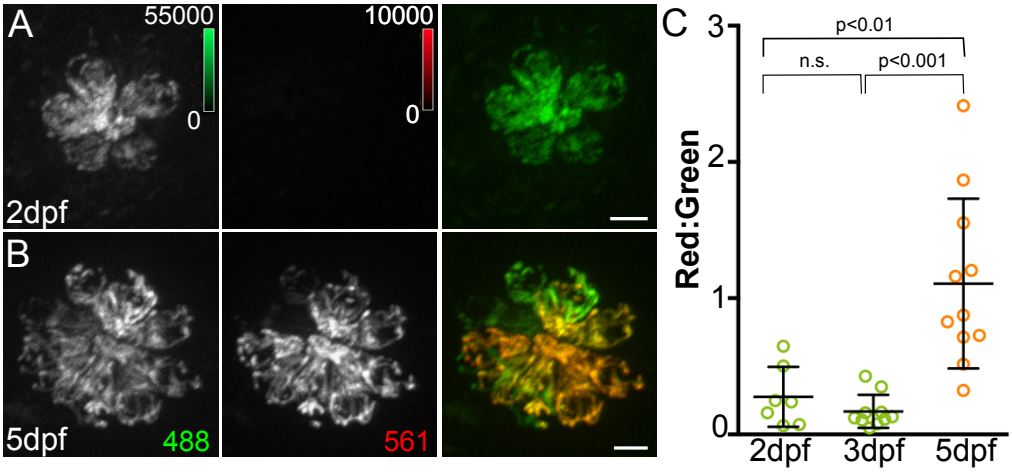

Figure 3.3. MitoTimer fluorescence ratio increases with neuromast maturation.

Maximum projections of hair cells from Tg[*myo6b:mitoTimer*]^{w208} fish at 2dpf **(A)** and 5dpf **(B)**. **(C)** Mean mitoTimer fluorescence plotted as ratio of red:green at 2, 3, and 5dpf. 2dpf: 0.28 ± 0.22, 3dpf: 0.17 ± 0.12, 5dpf: 1.11 ± 0.62; mean ratio ± SD; n = 7-11 fish. Significance was analyzed by Kruskal-Wallis test with Dunn's post-test. Value for each fish represents the mean of 2-4 neuromasts. Scale bar = 5 μm.

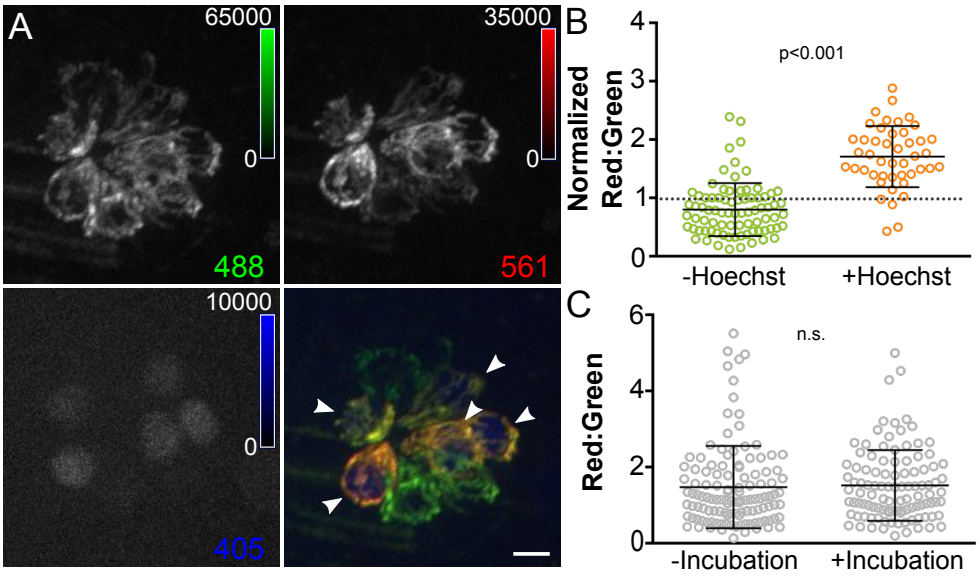

Figure 3.4. Mitochondrial oxidation corresponds with hair cell age and mechanotransduction activity.

(A) Maximum projection of mitoTimer expressing hair cells co-labeled with Hoechst. Hair cells were imaged at 4dpf, 24 hours after Hoechst treatment. Arrowheads mark Hoechst-positive cells. **(B)** mitoTimer fluorescence ratio for cells that are positive for Hoechst staining compared to Hoechst negative cells. mitoTimer ratios are normalized to the median, which is indicated by the dotted line. Hoechst positive: 1.71 ± 0.52, n = 45 cells; Hoechst negative: 0.80 ± 0.45, n = 80 cells; mean ratio (normalized) ± SD; 5 fish, 3 neuromasts per fish. **(C)** Hoechst incubation does not affect mitoTimer ratio compared to control. Incubation: 1.51 ± .093, n = 105 cells; No incubation: 1.48 ± 1.08, n = 119 cells (p = 0.34); mean ratio ± SD; 5 fish, 3 neuromasts per fish. Mann-Whitney U test was used to assess significance. Scale bar = 5 µm.

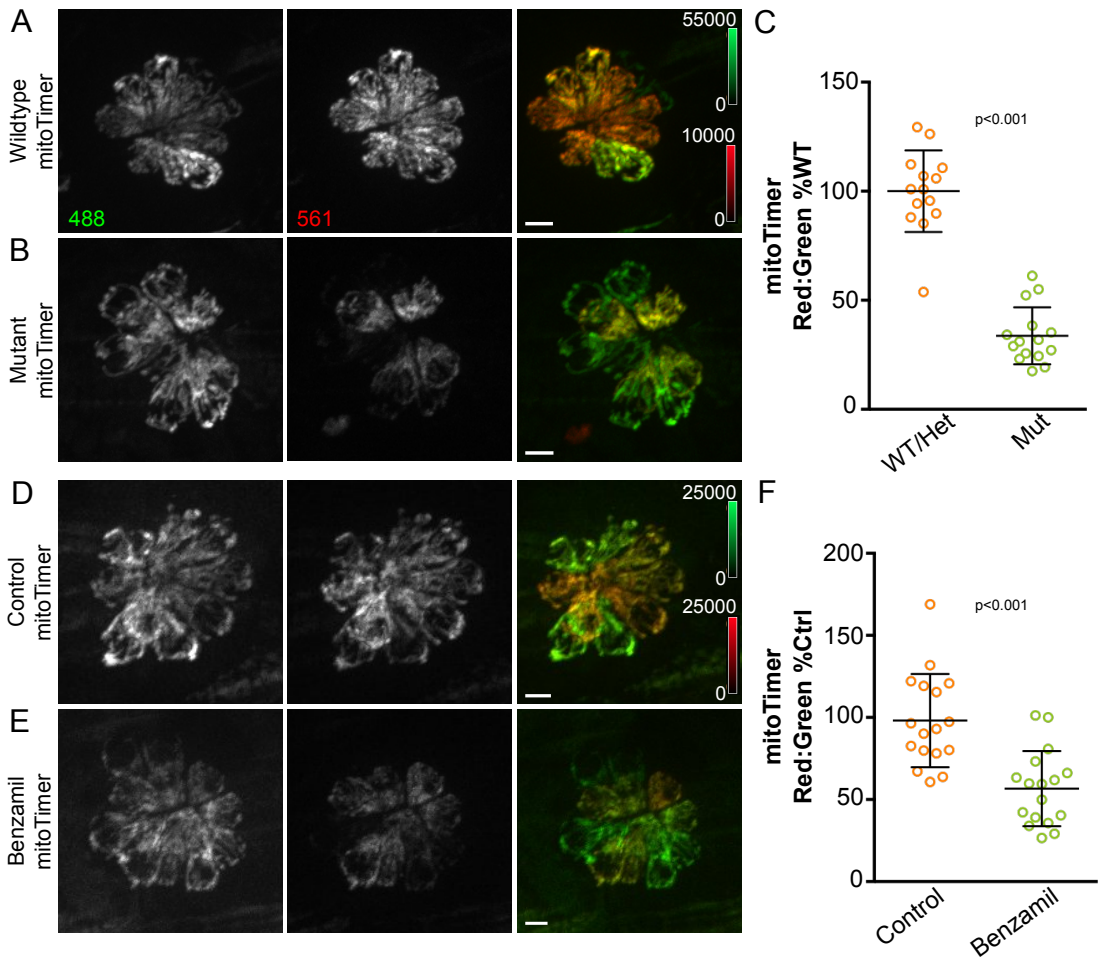

Figure 3.5. Mitochondrial activity depends on hair cell mechanotransduction.

(A, B) Maximum projections of hair cells from WT/Het and *sputnik* mutant siblings crossed to Tg[*myo6b:mitoTimer*]^{w208}. **(C)** mitoTimer mean fluorescence ratio for WT/Het and *sputnik* larvae. WT/Het: 100 ± 18.7, n = 14 fish; Mutant: 34 ± 13.1,15 mutant fish; mean (% WT/Het) ± SD. Value for each fish represents the mean of 2-4 neuromasts. **(D, E)** Maximum projections of mitoTimer-expressing hair cells from control larvae and larvae incubated in 200 µM benzamil. **(F)** mitoTimer mean fluorescence ratio for larvae incubated in benzamil compared to DMSO control. Control: 100 ± 28.7; Treated: 56.6 ± 22.7, n = 17 fish per group; mean (% Control) ± SD. Value for each fish represents the mean of 2-4 neuromasts. Mann-Whitney U test was used to assess significance. All larvae imaged at 5dpf. Scale bar = 5 µm.

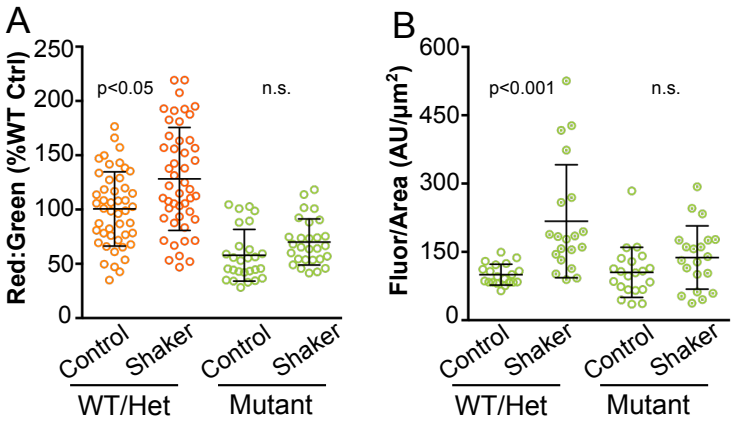

Figure 3.6. Sustained hair cell stimulation through orbital shaking increases hair cell oxidation and mitochondrial activity.

(A) mitoTimer fluorescence ratio and **(B)** CellROX green fluorescence measured from hair cells in WT/Het and *sputnik* mutants following 24 hrs of orbital shaking. For mitoTimer (A): WT/Het Control: 100 ± 34 n = 47 fish, WT/Het Orbital shaker: 128 ± 47 n = 48 fish, Mutant Control: 58 ± 24 n = 27 fish, Mutant Orbital shaker: 70 ± 21 n = 28 fish; mean (%WT/Het Control) WT/Het Control ± SD. For CellROX (B): WT/Het Control: 100 ± 23 n = 20 fish, WT/Het Orbital shaker: 217 ± 124 n = 20 fish, Mutant Control: 105 ± 55 n = 21 fish, Mutant Orbital shaker: 138 ± 58 n = 20 fish; mean (%WT/Het Control) ± SD. Values for each fish represent the mean of 2-3 neuromasts. Significance analyzed by Kruskal-Wallis test with Dunn's post-test. All larvae imaged at 5dpf.

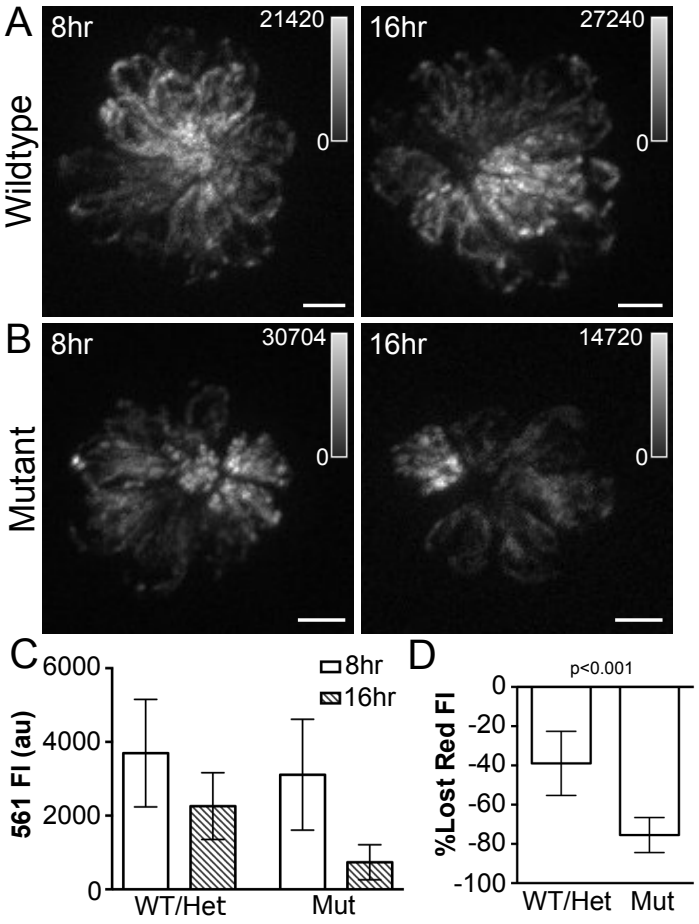

Figure 3.7. Hair cell activity influences mitochondrial turnover.

(A, B) Maximum projections of mitoEos red fluorescence (shown in grayscale) 8 and 16 hours after photoconversion in wildtype and *sputnik* fish crossed to Tg[*myo6b:mitoEos*]^{w207}. **(C)** Mean red fluorescence decreases over time in both wildtype and mutant fish WT/Het: 8hr 3696 ± 1083; 16hr 2257 ± 604; Mutant: 8hr 2942 ± 878; 16hr 721 ± 262, mean ± SD. **(D)** The loss of red fluorescence is significantly greater in mutant animals. WT/Het: 38.9 ± 16.4; Mutant: 75.5 ± 8.9; mean (% lost) ± SD. n = 9 fish per group. Value for each fish represents the mean of 3 neuromasts. Significance analyzed by Mann-Whitney U test. Scale bar = 5 μm.

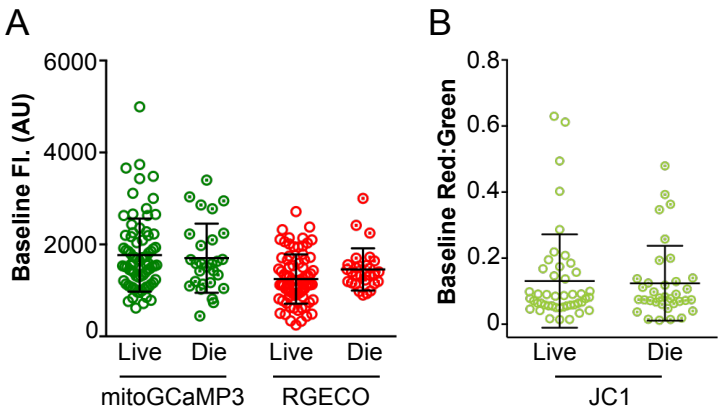

Figure 3.8. Acute hair cell and mitochondrial activity do not correspond with likelihood of hair cell death in response to 50 μM neomycin exposure.

(A) Baseline mean intensity of cytoRGECO and mitoGCaMP3 for living and dying cells. mitoGCaMP3 live: 1769 ± 794, n = 78 cells; mitoGCaMP3 die: 1701 ± 753, n = 28 cells; two-tailed Student's t-test, p = 0.69; RGECO live: 1248 ± 538, n = 46 cells; RGECO die: 1457 ± 459.7, n = 35 cells; two-tailed Student's t-test, p = 0.07; 5 fish, 2-3 neuromasts per fish. **(B)** Baseline mean fluorescence ratio of JC1 for living and dying cells. Living cells: 0.13 ± 0.14, n = 46; dying cells: 0.12 ± 0.11, n = 35; Mann-Whitney U test, p = 0.60; 6 fish, 2-3 neuromasts per fish. Fluorescence measurements were taken just prior to neomycin treatment.

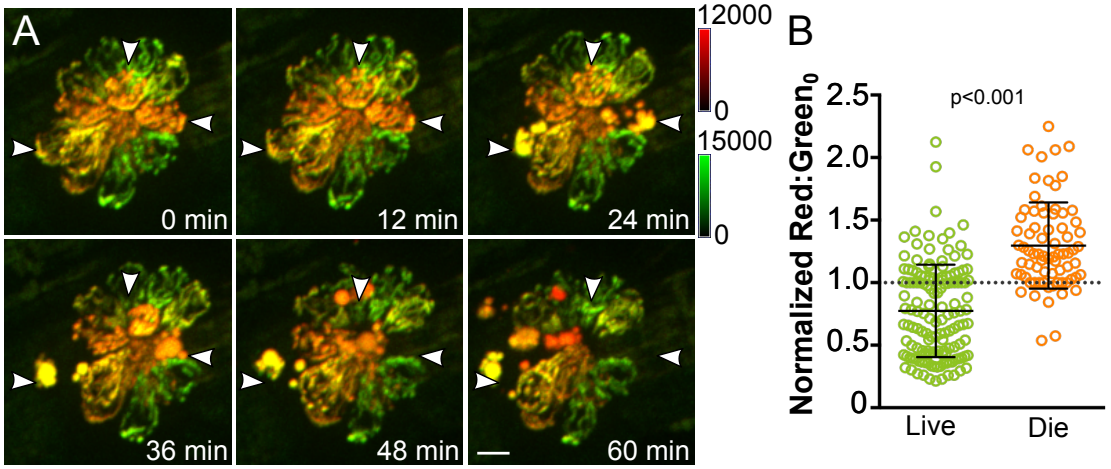

Figure 3.9. Cumulative mitochondrial activity reflects the likelihood of hair cell death following neomycin-induced damage.

(A) Frames from a time-lapse imaging video acquired from Tg[*myo6b:mitoTimer*]^{w208} fish treated with 50 µM neomycin. Images are maximum projections. Arrowheads indicate dying cells. **(B)** Baseline mitoTimer fluorescence ratio for living and dying cells following neomycin exposure. mitoTimer ratios are normalized to the median, which is indicated by the dotted line. Live: 0.77 ± 0.37, n = 142 cells; Die: 1.30 ± 0.34, n = 74 cells; mean ratio (normalized) ± SD; 6 fish, 2-3 neuromasts per fish. Mann-Whitney U test was used to assess significance. Scale bar = 5 µm.

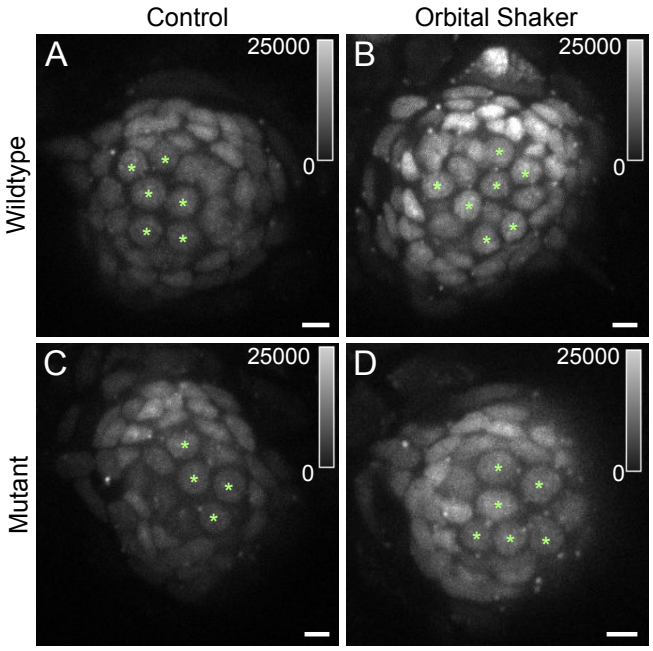

Supplemental Figure 3.10. Hair cell oxidation increases with sustained stimulation via orbital shaking.

(A,C) CellROX green fluorescence labeling in WT/Het and *sputnik* mutants in the no-shaker control condition. **(B,D)** CellROX green fluorescence in WT/Het and *sputnik* mutants after 24 hours of orbital shaking. CellROX green labels hair cell and support cell nuclei. Green asterisks indicate hair cells, identified based on nuclear shape and location. Fluorescence is shown in grayscale. Scale bar = 5 μm

3.8 MOVIES

Movie 3.1. Dynamic changes in hair cell cytoplasmic and mitochondrial Ca^{2+} fluorescence with waterjet stimulation. Time-lapse movie of a lateral line neuromast acquired from Tg*[myo6b:RGECO]*^{vo10Tg} (left) and Tg[*myo6b:mitoGCaMP3*]^{w119} (right) crossed fish. Hair cells were stimulated with a 10 Hz pressure wave, the timing of which is indicated (min:sec). Scale bar = 5 μm.

Movie 3.2. Differential cell death after low-dose neomycin exposure among mitoTimer-expressing hair cells. Time-lapse movie of a lateral line neuromast from a Tg[*myo6b:mitoTimer*]^{w208} fish exposed to 50 μM neomycin. Still frames from this time-lapse movie are shown in Figure 9. Scale bar = 5 μm.

Chapter 4. CONCLUSIONS AND FUTURE DIRECTIONS

4.1 SUMMARY

In this thesis, I explored the use of zebrafish as a model for the auditory system, with particular emphasis on study of the lateral line sensory system. Although the lateral line and auditory systems represent distinct sensory modalities, the sensory receptors of both systems share many structural and functional similarities. As a result, the advantages of using zebrafish can be leveraged for investigations that would be more challenging to conduct with mammalian model organisms.

In Chapter 3, I relied on the zebrafish model to characterize the influence of hair cell activity on mitochondrial biology *in vivo*, addressing two open questions related to hair cell function and death. First, how do mitochondria in hair cells respond to activity? Second, is there a relationship between mitochondrial activity and hair cell selective susceptibility? Using genetically-encoded fluorescent indicators, I observed that mitochondrial calcium flux and oxidation are regulated by mechanotransduction and demonstrated that hair cell activity has both acute and long-term consequences on mitochondrial function. I then examined variation in mitochondrial activity, finding that the cumulative history of hair cell and mitochondrial activity (rather than instantaneous activity levels) correspond with increased vulnerability to aminoglycoside-induced toxicity.

4.2 FUTURE DIRECTIONS

Despite their importance to cell function, there remains a remarkable lack of information about the role and behavior of mitochondria in hair cells. The work so far presented in this thesis suggests several lines of inquiry that could be pursued to uncover potential roles for these

organelles in the development, life, and death of hair cells. In the sections below, I discuss topics for future investigations. In addition to further characterization of mitochondrial activity in lateral line hair cells – including morphology and dynamics – I propose expanding studies of mitochondrial activity to lateral line support cells and mammalian cochlear hair cells. Additionally, I briefly explore possible implications of ROS signaling in support cells following hair cell damage and ROS production.

4.2.1 *Mitochondrial morphology and dynamics in lateral line hair cells*

In Chapter 3, I examined aspects of mitochondrial activity in hair cells, including mitochondrial calcium flux, age and oxidation, and turnover relative to hair cell activity. Further investigation of these and other aspects of mitochondrial behavior remain to be addressed, however, including mitochondrial localization, morphology, and dynamics. Exploration of these topics could provide interesting insights into the relationship between cell metabolism and mitochondrial networks and morphology.

Across cell types, mitochondria are known to localize to sites of intracellular energy demand and calcium signaling (e.g., sperm, muscle, neurons, lymphocytes) (Kuznetsov et al. 2009; Westermann 2012). Hints from mammalian studies suggest that, like other cell types, mitochondrial distribution in hair cells may reflect their functional roles. In gerbil cochlear outer hair cells, mitochondria shift from being homogenously distributed throughout the cell to being localized around the cell perimeter. This shift occurs during cell maturation, perhaps to support the outer hair cell specialization of electromotility (Weaver and Schweitzer 1994). Maturing mouse utricle and rat cochlear hair cells have apically localized mitochondria found just below the cuticular plate (Rusch et al. 1998; Beurg et al. 2010). This localization may reflect the role of mitochondria as calcium buffers, since calcium readily flows through mechanotransduction

channels into the apical region of the cell (Beurg et al. 2010). Moreover, as demonstrated in Chapter 3, mitochondrial calcium increases in response to hair cell stimulation.

Tools to determine the distribution of mitochondria within lateral line hair cells are readily available. Transgenic zebrafish expressing a hair cell-specific, mitochondria-targeted fluorophore (e.g., mitoEos) could be imaged using high-resolution fluorescent microscopy. Quantification of the mitochondrial distribution could be compared in apical or basal regions. Similar experiments could be performed with comparisons to mechanotransduction mutants (e.g., *sputnik* mutants) or synaptic transmission mutants (e.g., *gemini* mutants) (Sidi et al. 2004; Söllner et al. 2004). Disrupting major hair cell activities in different regions of the cell would reveal the extent to which the apical or basal cellular demands influence mitochondrial distribution. In addition to cellular activity, mitochondrial interactions with other organelles, e.g., the endoplasmic reticulum (ER), might also influence their localization. Mitochondrial distribution relative to the ER could be explored and even extended to studies of calcium flow between the two compartments (Rizzuto et al. 1998; Rowland and Voeltz 2012). Identification of ER-mitochondrial contacts within hair cells might be better addressed using scanning electron microscopy and organelle reconstructions.

In addition to distribution of mitochondria within the cell, mitochondrial morphology and dynamics are also important factors in cell function and can vary across cell types and with metabolic demand (Collins et al. 2002; Kuznetsov et al. 2009; Woods 2017). For example, elongated mitochondrial morphology has been observed in cells with higher rates of cellular respiration (Egner et al. 2002; Jakobs et al. 2003; Rossignol et al. 2004; Westermann 2012; Mishra and Chan 2016). Elongated mitochondrial networks have also been shown to correspond with efficient ATP production and mitochondrial content mixing (Amchenkova et al. 1988;

Skulachev 2001; Meeusen et al. 2004; Chen et al. 2005; Malka et al. 2005). Relatedly, mitochondrial fusion depends on mitochondrial membrane potential, which corresponds with mitochondrial activity (Meeusen et al. 2004; Malka et al. 2005). Further investigation of mitochondrial networks would provide additional insight into our findings in Chapter 3, where wildtype hair cells exhibited red-shifted mitoTimer fluorescence and reduced mitochondrial turnover relative to *sputnik* mutants. Based on the connection between mitochondrial elongation and metabolism described above, it might be that mitochondria in wildtype hair cells undergo more fusion and elongation in response to the demands of mechanotransduction activity. To characterize the effect of hair cell activity on mitochondrial dynamics, future studies might rely on high-resolution fluorescent microscopy to measure mitochondrial networks, assessing the length and connectivity of the mitochondria over time.

Mitochondrial dynamics in hair cells could be perturbed through CRISPR-mediated mutagenesis of the genes required for mitochondrial fission and fusion with predictable phenotypic changes. Mitochondrial dynamics are primarily mediated by a handful of GTPases that facilitate the fusion or separation of mitochondrial membranes. Mitochondrial fusion depends on mitofusins (Mfn 1 & 2) for outer membrane fusion and optic-atrophy 1 (Opa1) for inner membrane fusion. Dynamin-related protein 1 (Drp1) is required for mitochondrial fission (reviewed in Otera and Mihara 2011). Mfn1/2 or Opa1 are appropriate initial targets, as mitochondria within wildtype lateral line hair cells appear to form a relatively elongated mitochondrial network and Mfn1/2 or Opa1 gene mutations would be predicted to cause to a more punctate mitochondrial phenotype. Functional consequences of impaired mitochondrial dynamics could be assessed with respect to hair cell stimulation as well as susceptibility to neomycin.

4.2.2 *Extending mitochondrial characterization to lateral line support cells*

Beyond the study of hair cells, the composition of lateral line neuromasts present a unique opportunity to examine mitochondrial morphology and dynamics across cells in varying states of pluripotency. Following hair cell damage, support cells surrounding the hair cells divide symmetrically to give rise to new hair cells (López-Schier and Hudspeth 2006; Wibowo et al. 2011). These support cells constitute a population of unipotent hair cell progenitors. Evidence suggests that there is also a stem cell-like population that serves to replace the unipotent progenitor pool (Cruz et al. 2015; Romero-Carvajal et al. 2015). Exploration of mitochondrial networks in support cells could be an interesting comparison to hair cells. In other systems, progenitor cells have been shown to exhibit punctate, fragmented mitochondrial networks that shift upon cell differentiation to elongated networks, along with shifts in metabolic demand (Zhang et al. 2011; Kasahara et al. 2013). If this is the case in neuromasts, support cell mitochondrial networks might be predictably dissimilar from hair cells and perhaps varying across support cell subpopulations. With CRISPR knock-in techniques, the ability to label different subpopulations of support cells could be harnessed to drive expression of mitochondria-localized fluorescent reporters in those cells (Eric Thomas, *in preparation*).

The lateral line could also be an interesting system with which to study mitochondrial partitioning during progenitor cell proliferation. Although mitochondrial partitioning has been studied in yeast, how mitochondrial partitioning occurs and the functional consequences of asymmetric vs. symmetric partitioning for daughter cells in vertebrates is less well characterized (Mishra and Chan 2014). In a study of human mammary stem-cell like cells, Katajisto et al. (2015) demonstrated that daughter cells inheriting fewer older mitochondria following cell division were more likely to maintain stem-cell like qualities. In this case, mitochondrial

partitioning and cell division were both asymmetric. Given that neuromasts contain both support cell and hair cell progenitors, mitochondrial partitioning could be examined and compared during regeneration, where potentially both symmetric and asymmetric cell divisions occur. Following hair cell ablation with aminoglycoside antibiotics, lateral line regenerative events, including cell proliferation and differentiation, are well described (Ma et al. 2008; Wibowo et al. 2011; Cruz et al. 2015; Romero-Carvajal et al. 2015). As a result, this is a tractable system for live monitoring of mitochondrial movement during regenerative events. Since mitoTimer fluorescence reflects mitochondrial age and activity, expression of this indicator in support cells would not only allow for visualization of the organelles, but also a means for distinguishing whether they are partitioned differently based on these qualities. For example, if similar to the human mammary cells, mitochondrial partitioning during asymmetric support cell divisions might reveal a daughter cell with older and historically more active mitochondria (higher red:green ratio), while the opposite may be true for the other daughter cell. In this case, one might predict that the daughter cell with older and more active mitochondria would be more likely to become a unipotent hair cell progenitor.

4.2.3 *Mitochondrial biogenesis in lateral line hair cell development*

In addition to differences in mitochondrial dynamics and morphology, we might also predict that, as active sensory receptors, hair cells have greater mitochondrial content relative to their progenitors to sustain their energy demands. In yeast and muscle, mitochondrial mass and number increase with metabolic shifts or increased cell activity (Holloszy 1967; Takahashi and Hood 1993; Visser et al. 1995; Hood et al. 2011). Evidence for this idea in the auditory system stems from electron micrographs of cells in the chick basilar papilla, which reveal that hair cells have comparatively more mitochondria than surrounding support cells (Duckert and Rubel

1990). Since support cells serve as hair cell progenitors, they might experience an increase in mitochondrial biogenesis during differentiation.

In addressing this idea, I examined mitochondrial expansion during lateral line hair cell development. I relied on hair cell-specific expression of two fluorescent proteins: (1) mitochondrial matrix-targeted GFP paired with the *myosin6b* promoter (*myo6b:mitoGFP*), to label mitochondria; and (2) cytosolic red fluorescent protein driven by the promoter *ribeye a* [Tg(*ribA:tRFP*)^{w87}] (Figure 4.1). These genes are expressed sequentially during hair cell maturation, such that *ribeye a* is expressed slightly later relative to *myosin6b*. Based on the sequential expression of these genes, the relative age of hair cells within a neuromast can be distinguished. Double-labeled hair cell cells are identified as older and more mature, while single-labeled, mitoGFP-positive cells are slightly younger, and less mature. To quantify mitochondrial content, I measured mitochondrial volume in immature and mature hair cells in transgenic *ribA:tRFP* fish transiently expressing *myo6b:mitoGFP*. Mitochondrial volume was calculated for single cells using the program MitoGraph (Viana et al. 2015). The measurements demonstrate that mitochondrial volume increases as cells transition from being *myosin6b*-postive (immature) to both *myosin6b*- and *ribeye a*-positive (mature) (Figure 4.1). This pattern remained consistent across stages of larval fish development (2, 3, and 5dpf).

To investigate whether mitochondrial increase depends on hair cell activity, I measured mitochondrial volume in *sputnik* mechanotransduction mutants transiently expressing the *myo6b:mitoGFP* construct (Figure 4.1). *Sputnik* mutants exhibited a slight but significant reduction in mitochondrial volume, suggesting that mechanotransduction activity influences mitochondrial volume, but may not be the primary factor driving mitochondrial biogenesis. In this case, mitochondrial expansion might be regulated by factors downstream of genes that

promote hair cell differentiation. Targeted mutagenesis of genes known for their role in mitochondrial biogenesis, e.g., *PGC1α*, could be used to uncover developmentally regulated aspects of mitochondrial growth (Wu et al. 1999; Lehman et al. 2000; Cheng et al. 2012).

4.2.4 *Examining mitochondria in mammalian cochlear hair cells*

A natural extension of the exploration of mitochondria in lateral line hair cells presented in this thesis would be to examine mitochondrial stress relative to activity in mammalian hair cells. This line of inquiry would be particularly intriguing given the characteristic pattern of cell death observed in the cochlea. Whether by toxic chemical exposure, or as a result of aging, hearing loss and cell death occurs from high frequency to low frequency (or basal to apical), and by cell type, where inner hair cells are less susceptible than outer hair cells (Richardson and Russell 1991; Forge and Richardson 1993; Kopke et al. 1999; Forge and Schacht 2000; Alharazneh et al. 2011; Mahendrasingam et al. 2011). Using the reporter mitoTimer, the results reported in Chapter 3 demonstrate that historically more active hair cells are more sensitive to damage due to changes in mitochondrial state. Expression of mitoTimer in the cochlea would provide an opportunity to examine whether similar mechanisms underlie differential susceptibility among auditory hair cells.

mitoTimer fluorescence could be examined in mouse models by injecting animals with a strain of AAV virus developed for efficient cochlear transfection (a more rapid alternative to the generation of a transgenic line) (Landegger et al. 2017). Initial characterization might include determination of mitoTimer fluorescence ratios for hair cells at different points along the tonotopic axis, or between inner and outer hair cells. Based on the increased sensitivity of basal and outer hair cells to damage, these cells might be predicted to have higher mitoTimer red:green fluorescence. Investigations could also parallel zebrafish studies by examining mitoTimer in

murine mechanotransduction mutants. Additionally, mitoTimer fluorescence could be measured following noise exposure within a specific frequency range and at levels known to cause temporary threshold shifts in hearing. Since hair cell frequency tuning along the cochlea is mapped, fluorescence could be compared for hair cells within and outside the known band of noise damage. Results from these or similar experiments would provide insight into mitochondrial changes in mammalian hair cells under normal and damage conditions and could reveal potential differences between hair cells that reflect differential susceptibility. Elucidating underlying mechanisms of differential hair cell damage will inform therapeutic strategies to combat human hearing loss.

4.2.5 *ROS in support cells during hair cell damage: a functional role?*

Esterberg et al. demonstrated that lateral line hair cells produce ROS in response to neomycin-induced damage and that mitochondria serve as a source of ROS (Esterberg et al. 2016). Intriguingly, in investigating this response, we also observed increases in support cell ROS following hair cell damage. Support cell ROS increases were detected using the ROS indicator dye CellROX and were only observed in conditions of hair cell damage following neomycin exposure (Figure 4.2, Movie 4.1). Although the work described in this thesis is entirely hair cell-focused, this observation suggests that examination of support cell activity during damage may be another interesting area of investigation. Support cell behavior following hair cell death has been a long-standing topic of interest, since support cells serve as hair cell progenitors during regeneration (Balak et al. 1990; Ma et al. 2008; Wibowo et al. 2011; Cruz et al. 2015; Romero-Carvajal et al. 2015). Although lateral line regeneration was discovered over 70 years ago (Stone 1937), it is unknown exactly what triggers surrounding support cells to replace dying hair cells.

ROS signaling has been implicated in wound healing and regeneration as well as in the regulation of progenitor cell behavior in other systems. After tail fin resection in zebrafish and tadpoles, ROS signaling was found to serve as a short-range signaling molecule produced by cells at the site of injury (Niethammer et al. 2009; Love et al. 2013). Inhibiting ROS production in the tadpole study impaired fin tissue regeneration. Given that hair cells also produce ROS after insult, ROS could be a signaling molecule allowing support cells to detect nearby damage. ROS signaling as a regulator of progenitor cell proliferation and/or differentiation has been observed across cell types, including intestinal stem cells, hematopoietic progenitor cells, cultured neuronal progenitors, as well as keratinocytes and hair follicles (Owusu-Ansah and Banerjee 2009; Le Belle et al. 2011; Dickinson et al. 2011; Hochmuth et al. 2011; Hamanaka et al. 2013). For example, in *Drosophila* hematopoietic progenitors, ROS was reported to "prime" cells for differentiation. The cells displayed an elevated level of ROS that decreased as they differentiated. While scavenging ROS impaired differentiation, increasing ROS beyond basal levels lead to precocious differentiation (Owusu-Ansah and Banerjee 2009). Since support cells serve as hair cell progenitors, it is tempting to speculate that the regenerative process may be initiated by ROS signaling in support cells in response to hair cell damage.

The ability to express transgenes and manipulate support cell genetics in the lateral line has been much improved with CRISPR gene editing technology. To more easily and dynamically visualize ROS in supporting cells, CRISPR knock-in drivers could be used to express genetically-encoded, fluorescent ROS indicators in support cell populations (e.g., HyPer or roGFP2) (Bilan and Belousov 2016; Lismont et al. 2017). With live imaging of spectrally distinct indicators, fluorescence could be measured simultaneously in hair cells and support cells during neomycin-induced damage. Support cell ROS levels could also be monitored during

regeneration as these cells undergo proliferation and differentiation. To assay potential functional consequences, ROS signaling could be manipulated through the targeted expression of ROS neutralizing enzymes, such as catalase or superoxide dismutase. If ROS is a required regeneration signal, reducing ROS levels in support cells after hair cell damage and death would be predicted to reduce the number of regenerated hair cells.

4.3 FIGURES

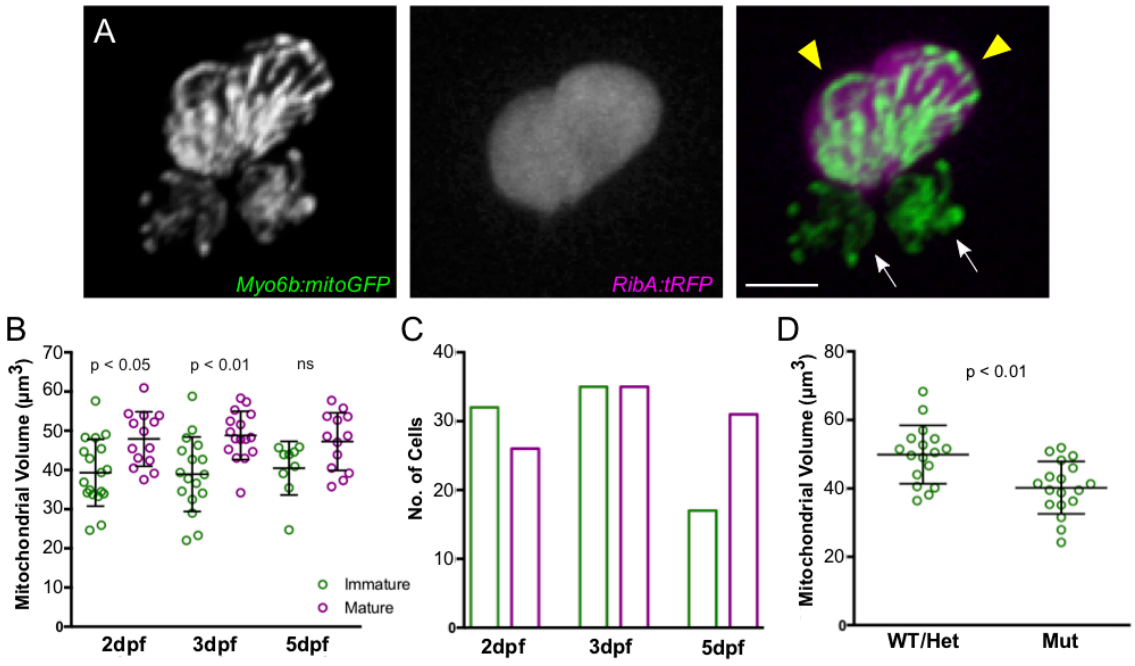

Figure 4.1. Mitochondrial content increases as hair cells mature and is influenced by hair cell mechanotransduction activity.

(A) Maximum projection image of hair cells from a 2dpf larval zebrafish. Expression of mitochondria-targeted GFP is driven by the *myosin6b* promoter (*myo6b:mitoGFP*), while cytosolic tRFP expression is driven by the *ribeye a* promoter (Tg[*ribA:tRFP*] ^{w87}). White arrows indicate immature hair cells and yellow arrow heads indicate the mature hair cells. Scale bar = 5 µm. **(B)** Mean mitochondrial volume for mature vs. immature hair cells in a neuromast during zebrafish maturation. Transient mitoGFP expression was used to label mitochondria in individual cells and mitochondrial volume (µm^3) was measured using the program MitoGraph. 2dpf: 39.3 ± 8.5 (18), 47.9 ± 6.9 (14); 3dpf: 38.9 ± 9.5 (17), 48.8 ± 6.2 (16); 5dpf: 40.5 ± 6.8 (9); 47.3 ± 7.4 (13); immature, mature; mean ± SD (n = neuromasts). Kruskal-Wallis test with Dunn's post-test was used for statistical analysis. **(C)** The number of immature and mature hair cells analyzed in the graph B (green = immature cells; magenta = mature cells). **(D)** Mean mitochondrial volume measured with MitoGraph in wildtype and *cadherin23/sputnik* mutants at 5dpf. WT/Het: 49.91 ± 8.5 (17); Mut: 40.21 ± 7.7 (18); mean ± SD (n = neuromasts). Mann-Whitney test used for statistical analysis.

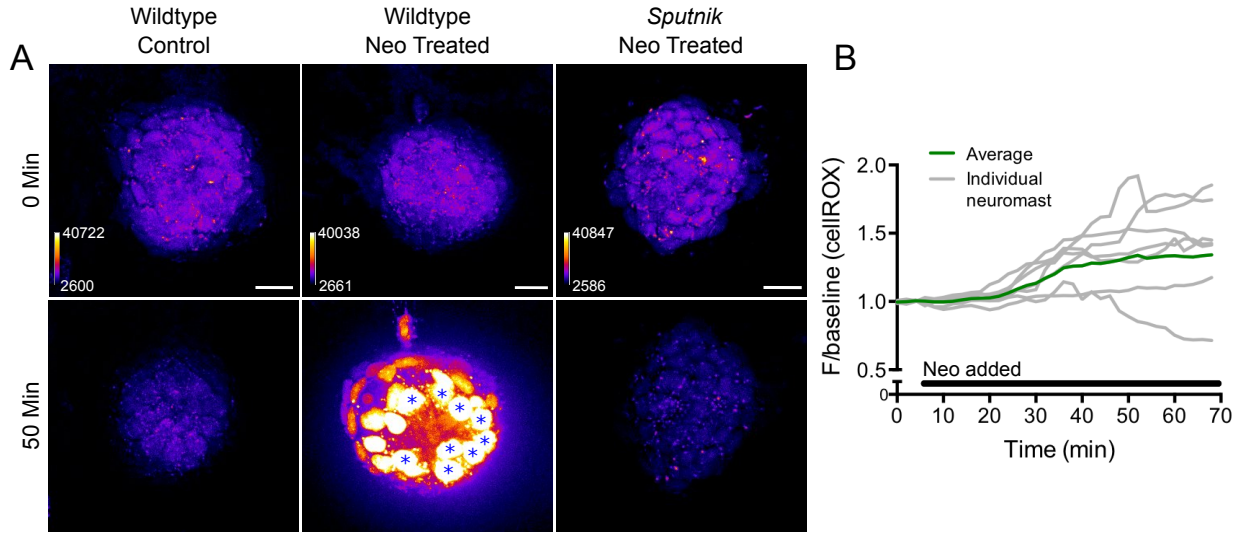

Figure 4.2. ROS increases in lateral line support cells following hair cell death.

(A) Frames from time-lapse imaging videos of neuromasts after 24 hours of CellROX incubation under three conditions: control (wildtype), neomycin treated (wildtype), and neomycin treated *sputnik* mutants. 400 µM neomycin was used for treatments. CellROX fluorescence increased in hair cells and support cells only when hair cell death is induced. *Sputnik* mutants are not susceptible to neomycin induced damage due to lack of mechanotransduction. Asterisks indicate hair cells. Scale bar = 10 µm. **(B)** Normalized CellROX fluorescence in support cells following hair cell damage induced by 400 µM neomycin treatment.

4.4 MOVIES

Movie 4.1. ROS increases in hair cells and support cells following neomycin-induced hair cell damage. Time-lapse movie of a neuromast from a Tg[*ribA:tRFP*] ^{w87} fish incubated for 24hrs in CellROX (green) and exposed to 400 μM neomycin. tRFP expression (magenta) is hair cell specific. Still frames of the CellROX fluorescence from this time-lapse movie are shown in Figure 4.2.

BIBLIOGRAPHY

Ahmed ZM, Goodyear R, Riazuddin S, et al (2006) The Tip-Link Antigen, a Protein Associated with the Transduction Complex of Sensory Hair Cells, Is Protocadherin-15. J Neurosci 26:7022–7034. doi: 10.1523/JNEUROSCI.1163-06.2006

Albert JT, Winter H, Schaechinger TJ, et al (2007) Voltage-sensitive prestin orthologue expressed in zebrafish hair cells. J Physiol 580:451–61. doi: 10.1113/jphysiol.2007.127993

Alexandre D, Ghysen A (1999) Somatotopy of the lateral line projection in larval zebrafish. Proc Natl Acad Sci 96:7558–7562. doi: 10.1073/pnas.96.13.7558

Alharazneh A, Luk L, Huth M, et al (2011) Functional Hair Cell Mechanotransducer Channels Are Required for Aminoglycoside Ototoxicity. PLoS One 6:e22347. doi: 10.1371/journal.pone.0022347

Amchenkova AA, Bakeeva LE, Chentsov YS, et al (1988) Coupling membranes as energy-transmitting cables. I. Filamentous mitochondria in fibroblasts and mitochondrial clusters in cardiomyocytes. J Cell Biol 107:481–95. doi: 10.1083/JCB.107.2.481

Ames A (2000) CNS energy metabolism as related to function. Brain Res Rev 34:42–68. doi: 10.1016/S0165-0173(00)00038-2

Arunachalam M, Raja M, Vijayakumar C, et al (2013) Natural History of Zebrafish (*Danio rerio*) in India. Zebrafish 10:1–14. doi: 10.1089/zeb.2012.0803

Azaiez H, Decker AR, Booth KT, et al (2015) HOMER2, a stereociliary scaffolding protein, is essential for normal hearing in humans and mice. PLoS Genet 11:e1005137. doi: 10.1371/journal.pgen.1005137

Bagger-Sjöbäck D, Wersäll J (1978) Gentamicin-induced mitochondrial damage in inner ear sensory cells of the lizard Calotes versicolor. Acta Otolaryngol 86:35–51

Balak K, Corwin J, Jones J (1990) Regenerated hair cells can originate from supporting cell progeny: evidence from phototoxicity and laser ablation experiments in the lateral line system. J Neurosci 10:2502–2512

Bayaa M, Vulesevic B, Esbaugh A, et al (2009) The involvement of SLC26 anion transporters in chloride uptake in zebrafish (Danio rerio) larvae. J Exp Biol 212:3283–95. doi: 10.1242/jeb.033910

Becker L, Schnee ME, Niwa M, et al (2018) The presynaptic ribbon maintains vesicle populations at the hair cell afferent fiber synapse. Elife 7:. doi: 10.7554/eLife.30241

Beckman KB, Ames BN (1998) The free radical theory of aging matures. Physiol Rev 78:547–81

Belousov V V, Fradkov AF, Lukyanov KA, et al (2006) Genetically encoded fluorescent indicator for intracellular hydrogen peroxide. Nat Methods 3:281–6. doi: 10.1038/nmeth866

Beurg M, Nam J-H, Chen Q, Fettiplace R (2010) Calcium balance and mechanotransduction in rat cochlear hair cells. J Neurophysiol 104:18–34. doi: 10.1152/jn.00019.2010

Bilan DS, Belousov V V. (2016) HyPer Family Probes: State of the Art. Antioxid Redox Signal 24:731–751. doi: 10.1089/ars.2015.6586

Blanco-Sánchez B, Clément A, Fierro J, et al (2014) Complexes of Usher proteins preassemble at the endoplasmic reticulum and are required for trafficking and ER homeostasis. Dis Model Mech 7:547–59. doi: 10.1242/dmm.014068

Bleckmann H (2008) Peripheral and central processing of lateral line information. J Comp Physiol A Neuroethol Sens Neural Behav Physiol 194:145–58. doi: 10.1007/s00359-007-

0282-2
Böttger EC, Schacht J (2013) The mitochondrion: a perpetrator of acquired hearing loss. Hear Res 303:. doi: 10.1016/j.heares.2013.01.006
Bricaud O, Chaar V, Dambly-Chaudière C, Ghysen A (2001) Early efferent innervation of the zebrafish lateral line. J Comp Neurol 434:253–261. doi: 10.1002/cne.1175
Bricaud O, Collazo A (2006) The Transcription Factor six1 Inhibits Neuronal and Promotes Hair Cell Fate in the Developing Zebrafish (Danio rerio) Inner Ear. J Neurosci 26:10438–10451. doi: 10.1523/JNEUROSCI.1025-06.2006
Bricaud O, Collazo A (2011) Balancing cell numbers during organogenesis: Six1a differentially affects neurons and sensory hair cells in the inner ear. Dev Biol 357:191–201. doi: 10.1016/j.ydbio.2011.06.035
Brookes PS (2004) Calcium, ATP, and ROS: a mitochondrial love-hate triangle. AJP Cell Physiol 287:C817–C833. doi: 10.1152/ajpcell.00139.2004
Brown KD, Maqsood S, Huang JY, et al (2014) Activation of SIRT3 by the NAD+precursor nicotinamide riboside protects from noise-induced hearing loss. Cell Metab 20:1059–1068. doi: 10.1016/j.cmet.2014.11.003
Busch-Nentwich E, Söllner C, Roehl H, Nicolson T (2004) The deafness gene dfna5 is crucial for ugdh expression and HA production in the developing ear in zebrafish. Development 131:943–951. doi: 10.1242/dev.00961
Campanella M, Seraphim A, Abeti R, et al (2009) IF1, the endogenous regulator of the F1Fo-ATPsynthase, defines mitochondrial volume fraction in HeLa cells by regulating autophagy. Biochim Biophys Acta - Bioenerg 1787:393–401. doi: 10.1016/j.bbabio.2009.02.023
Chang-Chien J, Yen Y-C, Chien K-H, et al (2014) The connexin 30.3 of zebrafish homologue of human connexin 26 may play similar role in the inner ear. Hear Res 313:55–66. doi: 10.1016/j.heares.2014.04.010
Chatterjee P, Padmanarayana M, Abdullah N, et al (2015) Otoferlin deficiency in zebrafish results in defects in balance and hearing: rescue of the balance and hearing phenotype with full-length and truncated forms of mouse otoferlin. Mol Cell Biol 35:1043–54. doi: 10.1128/MCB.01439-14
Chen F-Q, Zheng H-W, Schacht J, Sha S-H (2013) Mitochondrial Peroxiredoxin 3 Regulates Sensory Cell Survival in the Cochlea. PLoS One 8:e61999. doi: 10.1371/journal.pone.0061999
Chen H, Chomyn A, Chan DC (2005) Disruption of fusion results in mitochondrial heterogeneity and dysfunction. J Biol Chem 280:26185–92. doi: 10.1074/jbc.M503062200
Chen Z, Chou S-W, McDermott BM (2017) Ribeye protein is intrinsically dynamic but is stabilized in the context of the ribbon synapse. J Physiol. doi: 10.1113/JP271215
Cheng A, Wan R, Yang J-L, et al (2012) Involvement of PGC-1α in the formation and maintenance of neuronal dendritic spines. Nat Commun 3:1250. doi: 10.1038/ncomms2238
Cheng AG, Cunningham LL, Rubel EW, et al (2005) Mechanisms of hair cell death and protection. Curr Opin Otolaryngol Head Neck Surg 13:343–8
Chittka L, Brockmann A (2005) Perception space--the final frontier. PLoS Biol 3:e137. doi: 10.1371/journal.pbio.0030137
Chiu LL, Cunningham LL, Raible DW, et al (2008) Using the Zebrafish Lateral Line to Screen for Ototoxicity. J Assoc Res Otolaryngol 9:178–190. doi: 10.1007/s10162-008-0118-y
Chou S-W, Chen Z, Zhu S, et al (2017) A molecular basis for water motion detection by the mechanosensory lateral line of zebrafish. Nat Commun 8:2234. doi: 10.1038/s41467-017-

01604-2
Choung YH, Taura A, Pak K, et al (2009) Generation of highly-reactive oxygen species is closely related to hair cell damage in rat organ of Corti treated with gentamicin. Neuroscience 161:. doi: 10.1016/j.neuroscience.2009.02.085
Chowdhury S, Owens KN, Herr RJ, et al (2018) Phenotypic Optimization of Urea–Thiophene Carboxamides To Yield Potent, Well Tolerated, and Orally Active Protective Agents against Aminoglycoside-Induced Hearing Loss. J Med Chem 61:84–97. doi: 10.1021/acs.jmedchem.7b00932
Clerici WJ, Hensley K, DiMartino DL, Butterfield DA (1996) Direct detection of ototoxicant-induced reactive oxygen species generation in cochlear explants. Hear Res 98:116–24
Coffin AB, Ou H, Owens KN, et al (2010) Chemical Screening for Hair Cell Loss and Protection in the Zebrafish Lateral Line. Zebrafish 7:3–11. doi: 10.1089/zeb.2009.0639
Coffin AB, Reinhart KE, Owens KN, et al (2009) Extracellular divalent cations modulate aminoglycoside-induced hair cell death in the zebrafish lateral line. Hear Res 253:42–51. doi: 10.1016/j.heares.2009.03.004
Coffin AB, Rubel EW, Raible DW (2013a) Bax, Bcl2, and p53 Differentially Regulate Neomycin- and Gentamicin-Induced Hair Cell Death in the Zebrafish Lateral Line. J Assoc Res Otolaryngol 14:645–659. doi: 10.1007/s10162-013-0404-1
Coffin AB, Williamson KL, Mamiya A, et al (2013b) Profiling drug-induced cell death pathways in the zebrafish lateral line. Apoptosis 18:393–408. doi: 10.1007/s10495-013-0816-8
Collins TJ, Berridge MJ, Lipp P, Bootman MD (2002) Mitochondria are morphologically and functionally heterogeneous within cells. EMBO J 21:1616–27. doi: 10.1093/emboj/21.7.1616
Corey DP, Hudspeth AJ (1979) Ionic basis of the receptor potential in a vertebrate hair cell. Nature 281:675–7
Corey DP, Hudspeth AJ (1980) Mechanical stimulation and micromanipulation with piezoelectric bimorph elements. J Neurosci Methods 3:183–202
Cruz IA, Kappedal R, Mackenzie SM, et al (2015) Robust regeneration of adult zebrafish lateral line hair cells reflects continued precursor pool maintenance. Dev Biol 402:229–38. doi: 10.1016/j.ydbio.2015.03.019
Cunningham CL, Wu Z, Jafari A, et al (2017) The murine catecholamine methyltransferase mTOMT is essential for mechanotransduction by cochlear hair cells. Elife 6:e24318. doi: 10.7554/eLife.24318
Dawkins R, Keller SL, Sewell WF (2005) Pharmacology of Acetylcholine-Mediated Cell Signaling in the Lateral Line Organ Following Efferent Stimulation. J Neurophysiol 93:2541–2551. doi: 10.1152/jn.01283.2004
Delmaghani S, Aghaie A, Bouyacoub Y, et al (2016) Mutations in CDC14A, Encoding a Protein Phosphatase Involved in Hair Cell Ciliogenesis, Cause Autosomal-Recessive Severe to Profound Deafness. Am J Hum Genet 98:1266–1270. doi: 10.1016/j.ajhg.2016.04.015
Di Donato V, Auer TO, Duroure K, Del Bene F (2013) Characterization of the Calcium Binding Protein Family in Zebrafish. PLoS One 8:e53299. doi: 10.1371/journal.pone.0053299
Dickinson BC, Peltier J, Stone D, et al (2011) Nox2 redox signaling maintains essential cell populations in the brain. Nat Chem Biol 7:106–12. doi: 10.1038/nchembio.497
Dijkgraaf S (1963) The functioning and significance of the lateral-line organs. Biol Rev Camb Philos Soc 38:51–105
Ding Y, Leng J, Fan F, et al (2013) The Role of Mitochondrial DNA Mutations in Hearing Loss.

Biochem Genet 51:588–602. doi: 10.1007/s10528-013-9589-6
Dow E, Siletti K, Hudspeth AJ (2015) Cellular projections from sensory hair cells form polarity-specific scaffolds during synaptogenesis. Genes Dev 29:1087–94. doi: 10.1101/gad.259838.115
Duckert LG, Rubel EW (1990) Ultrastructural observations on regenerating hair cells in the chick basilar papilla. Hear Res 48:161–182. doi: 10.1016/0378-5955(90)90206-5
Dudek J, Rehling P, van der Laan M (2013) Mitochondrial protein import: Common principles and physiological networks. Biochim Biophys Acta - Mol Cell Res 1833:274–285. doi: 10.1016/J.BBAMCR.2012.05.028
Duvall AJ, Wersäll J (1964) Site of Action of Streptomycin Upon Inner Ear Sensory Cells. Acta Otolaryngol 57:581–598. doi: 10.3109/00016486409137120
Eatock RA, Fay RR, Popper AN (2006) Vertebrate Hair Cells. Springer-Verlag, New York
Ebermann I, Phillips JB, Liebau MC, et al (2010) PDZD7 is a modifier of retinal disease and a contributor to digenic Usher syndrome. J Clin Invest 120:1812–23. doi: 10.1172/JCI39715
Egner A, Jakobs S, Hell SW (2002) Fast 100-nm resolution three-dimensional microscope reveals structural plasticity of mitochondria in live yeast. Proc Natl Acad Sci U S A 99:3370–5. doi: 10.1073/pnas.052545099
Einhorn Z, Trapani JG, Liu Q, Nicolson T (2012) Rabconnectin3α promotes stable activity of the H+ pump on synaptic vesicles in hair cells. J Neurosci 32:11144–56. doi: 10.1523/JNEUROSCI.1705-12.2012
Ekdale EG (2016) Form and function of the mammalian inner ear. J Anat 228:324–337. doi: 10.1111/joa.12308
Engel J, Braig C, Rüttiger L, et al (2006) Two classes of outer hair cells along the tonotopic axis of the cochlea. Neuroscience 143:837–849. doi: 10.1016/j.neuroscience.2006.08.060
Engeszer RE, Patterson LB, Rao AA, Parichy DM (2007) Zebrafish in The Wild: A Review of Natural History And New Notes from The Field. Zebrafish 4:21–40. doi: 10.1089/zeb.2006.9997
Erickson T, Morgan CP, Olt J, et al (2017) Integration of Tmc1/2 into the mechanotransduction complex in zebrafish hair cells is regulated by Transmembrane O-methyltransferase (Tomt). Elife 6:e28474. doi: 10.7554/eLife.28474
Ernest S, Rauch GJ, Haffter P, et al (2000) Mariner is defective in myosin VIIA: a zebrafish model for human hereditary deafness. Hum Mol Genet 9:2189–96
Esterberg R, Hailey DW, Coffin AB, et al (2013) Disruption of intracellular calcium regulation is integral to aminoglycoside-induced hair cell death. J Neurosci 33:7513–25. doi: 10.1523/JNEUROSCI.4559-12.2013
Esterberg R, Hailey DW, Rubel EW, Raible DW (2014) ER-mitochondrial calcium flow underlies vulnerability of mechanosensory hair cells to damage. J Neurosci 34:9703–19. doi: 10.1523/JNEUROSCI.0281-14.2014
Esterberg R, Linbo T, Pickett SB, et al (2016) Mitochondrial calcium uptake underlies ROS generation during aminoglycoside-induced hair cell death. J Clin Invest 126:3556–66. doi: 10.1172/JCI84939
Faucherre A, Baudoin J-P, Pujol-Martí J, López-Schier H (2010) Multispectral four-dimensional imaging reveals that evoked activity modulates peripheral arborization and the selection of plane-polarized targets by sensory neurons. Development 137:1635–43. doi: 10.1242/dev.047316
Faucherre A, Pujol-Martí J, Kawakami K, López-Schier H (2009) Afferent Neurons of the

Zebrafish Lateral Line Are Strict Selectors of Hair-Cell Orientation. PLoS One 4:e4477. doi: 10.1371/journal.pone.0004477

Fay RR, Popper AN (1974) Acoustic stimulation of the ear of the goldfish (Carassius auratus). J Exp Biol 61:243–60

Fermin CD, Igarashi M Aminoglycoside ototoxicity in the chick (Gallus domesticus) inner ear: I. The effects of kanamycin and netilmicin on the basilar papilla. Am J Otolaryngol 4:174–83

Ferree AW, Trudeau K, Zik E, et al (2013) MitoTimer probe reveals the impact of autophagy, fusion, and motility on subcellular distribution of young and old mitochondrial protein and on relative mitochondrial protein age. Autophagy 9:1887–96. doi: 10.4161/auto.26503

Fettiplace R, Hackney CM (2006) The sensory and motor roles of auditory hair cells. Nat Rev Neurosci 7:19–29. doi: 10.1038/nrn1828

Finkel T, Holbrook NJ (2000) Oxidants, oxidative stress and the biology of ageing. Nature 408:239–247. doi: 10.1038/35041687

Fischel-Ghodsian N, Prezant TR, Chaltraw WE, et al (1997) Mitochondrial gene mutation is a significant predisposing factor in aminoglycoside ototoxicity. 18:. doi: 10.1016/S0196-0709(97)90078-8

Flock Å, Russell IJ (1973) The post-synaptic action of efferent fibres in the lateral line organ of the burbot *Lota lota*. J Physiol 235:591–605. doi: 10.1113/jphysiol.1973.sp010406

Forge A, Richardson G (1993) Freeze fracture analysis of apical membranes in cochlear cultures: differences between basal and apical-coil outer hair cells and effects of neomycin. J Neurocytol 22:854–67

Forge A, Schacht J (2000) Aminoglycoside antibiotics. Audiol Neuro-Otology 5:3–22. doi: 10.1159/000013861

Gale JE, Marcotti W, Kennedy HJ, et al (2001) FM1-43 dye behaves as a permeant blocker of the hair-cell mechanotransducer channel. J Neurosci 21:7013–25

Gibson F, Walsh J, Mburu P, et al (1995) A type VII myosin encoded by the mouse deafness gene shaker-1. Nature 374:62–64. doi: 10.1038/374062a0

Gleason MR, Nagiel A, Jamet S, et al (2009) The transmembrane inner ear (Tmie) protein is essential for normal hearing and balance in the zebrafish. Proc Natl Acad Sci U S A 106:21347–52. doi: 10.1073/pnas.0911632106

Glueckert R, Wietzorrek G, Kammen-Jolly K, et al (2003) Role of class D L-type Ca2+ channels for cochlear morphology. Hear Res 178:95–105

Goman AM, Lin FR (2016) Prevalence of Hearing Loss by Severity in the United States. Am J Public Health 106:1820–2. doi: 10.2105/AJPH.2016.303299

Gopal SR, Chen DH-C, Chou S-W, et al (2015) Zebrafish Models for the Mechanosensory Hair Cell Dysfunction in Usher Syndrome 3 Reveal That Clarin-1 Is an Essential Hair Bundle Protein. J Neurosci 35:10188–10201. doi: 10.1523/JNEUROSCI.1096-15.2015

Grati M, Chakchouk I, Ma Q, et al (2015) A missense mutation in DCDC2 causes human recessive deafness DFNB66, likely by interfering with sensory hair cell and supporting cell cilia length regulation. Hum Mol Genet 24:2482–2491. doi: 10.1093/hmg/ddv009

Graydon CW, Manor U, Kindt KS (2017) In Vivo Ribbon Mobility and Turnover of Ribeye at Zebrafish Hair Cell Synapses. Sci Rep 7:7467. doi: 10.1038/s41598-017-07940-z

Haehnel-Taguchi M, Akanyeti O, Liao JC (2014) Afferent and motoneuron activity in response to single neuromast stimulation in the posterior lateral line of larval zebrafish. J Neurophysiol 112:1329–1339. doi: 10.1152/jn.00274.2014

Hailey DW, Esterberg R, Linbo TH, et al (2017) Fluorescent aminoglycosides reveal

intracellular trafficking routes in mechanosensory hair cells. J Clin Invest 127:472–486. doi: 10.1172/JCI85052

Hailey DW, Roberts B, Owens KN, et al (2012) Loss of Slc4a1b Chloride/Bicarbonate Exchanger Function Protects Mechanosensory Hair Cells from Aminoglycoside Damage in the Zebrafish Mutant persephone. PLoS Genet 8:e1002971. doi: 10.1371/journal.pgen.1002971

Hamanaka RB, Glasauer A, Hoover P, et al (2013) Mitochondrial reactive oxygen species promote epidermal differentiation and hair follicle development. Sci Signal 6:ra8. doi: 10.1126/scisignal.2003638

Han Y, Mu Y, Li X, et al (2011) Grhl2 deficiency impairs otic development and hearing ability in a zebrafish model of the progressive dominant hearing loss DFNA28. Hum Mol Genet 20:3213–26. doi: 10.1093/hmg/ddr234

Harman D (1956) Aging: A Theory Based on Free Radical and Radiation Chemistry. J Gerontol 11:298–300. doi: 10.1093/geronj/11.3.298

Harris JA, Cheng AG, Cunningham LL, et al (2003) Neomycin-induced hair cell death and rapid regeneration in the lateral line of zebrafish (Danio rerio). J Assoc Res Otolaryngol 4:219–34. doi: 10.1007/s10162-002-3022-x

Hernandez G, Thornton C, Stotland A, et al (2013) MitoTimer: A novel tool for monitoring mitochondrial turnover. Autophagy 9:1852–1861. doi: 10.4161/auto.26501

Hernández PP, Moreno V, Olivari FA, Allende ML (2006) Sub-lethal concentrations of waterborne copper are toxic to lateral line neuromasts in zebrafish (Danio rerio). Hear Res 213:1–10. doi: 10.1016/j.heares.2005.10.015

Hildebrand JD, Soriano P (2002) Overlapping and unique roles for C-terminal binding protein 1 (CtBP1) and CtBP2 during mouse development. Mol Cell Biol 22:5296–307. doi: 10.1128/MCB.22.15.5296-5307.2002

Hirose K, Westrum LE, Cunningham DE, Rubel EW (2004) Electron microscopy of degenerative changes in the chick basilar papilla after gentamicin exposure. J Comp Neurol 470:164–180. doi: 10.1002/cne.11046

Hirose K, Westrum LE, Stone JS, et al (1999) Dynamic Studies of Ototoxicity in Mature Avian Auditory Epithelium. Ann N Y Acad Sci 884:389–409. doi: 10.1111/j.1749-6632.1999.tb08657.x

Hirose Y, Simon JA, Ou HC (2011) Hair Cell Toxicity in Anti-cancer Drugs: Evaluating an Anti-cancer Drug Library for Independent and Synergistic Toxic Effects on Hair Cells Using the Zebrafish Lateral Line. J Assoc Res Otolaryngol 12:719–728. doi: 10.1007/s10162-011-0278-z

Hochmuth CE, Biteau B, Bohmann D, Jasper H (2011) Redox regulation by Keap1 and Nrf2 controls intestinal stem cell proliferation in Drosophila. Cell Stem Cell 8:188–99. doi: 10.1016/j.stem.2010.12.006

Holloszy JO (1967) Biochemical adaptations in muscle. Effects of exercise on mitochondrial oxygen uptake and respiratory enzyme activity in skeletal muscle. J Biol Chem 242:2278–82

Hood DA, Uguccioni G, Vainshtein A, D'souza D (2011) Mechanisms of Exercise-Induced Mitochondrial Biogenesis in Skeletal Muscle: Implications for Health and Disease. In: Comprehensive Physiology. John Wiley & Sons, Inc., Hoboken, NJ, USA, pp 1119–1134

Hu J, Li B, Apisa L, et al (2016) ER stress inhibitor attenuates hearing loss and hair cell death in Cdh23erl/erl mutant mice. Cell Death Dis 7:e2485. doi: 10.1038/cddis.2016.386

Hu Z, Zhang Q, Qin W, et al (2013) Gene miles-apart is required for formation of otic vesicle and hair cells in zebrafish. Cell Death Dis 4:e900. doi: 10.1038/cddis.2013.432

Hudspeth AJ (1982) Extracellular current flow and the site of transduction by vertebrate hair cells. J Neurosci 2:1–10. doi: 10.1523/JNEUROSCI.02-01-00001.1982

Hudspeth AJ, Corey DP (1977) Sensitivity, polarity, and conductance change in the response of vertebrate hair cells to controlled mechanical stimuli. Proc Natl Acad Sci U S A 74:2407–11. doi: 10.1073/PNAS.74.6.2407

Hudspeth AJ, Jacobs R (1979) Stereocilia mediate transduction in vertebrate hair cells (auditory system/cilium/vestibular system). Proc Natl Acad Sci U S A 76:1506–9

Imtiaz A, Belyantseva IA, Beirl AJ, et al (2018) CDC14A phosphatase is essential for hearing and male fertility in mouse and human. Hum Mol Genet 27:780–798. doi: 10.1093/hmg/ddx440

Jakobs S, Martini N, Schauss AC, et al (2003) Spatial and temporal dynamics of budding yeast mitochondria lacking the division component Fis1p. J Cell Sci 116:2005–2014. doi: 10.1242/jcs.00423

Jean P, Lopez de la Morena D, Michanski S, et al (2018) The synaptic ribbon is critical for sound encoding at high rates and with temporal precision. Elife 7:e29275. doi: 10.7554/eLife.29275

Jensen-Smith HC, Hallworth R, Nichols MG, et al (2012) Gentamicin Rapidly Inhibits Mitochondrial Metabolism in High-Frequency Cochlear Outer Hair Cells. PLoS One 7:e38471. doi: 10.1371/journal.pone.0038471

Ji YR, Warrier S, Jiang T, et al (2018) Directional selectivity of afferent neurons in zebrafish neuromasts is regulated by Emx2 in presynaptic hair cells. Elife 7:e35796. doi: 10.7554/eLife.35796

Jiang H, Sha S-H, Schacht J (2005) NF-?B pathway protects cochlear hair cells from aminoglycoside-induced ototoxicity. J Neurosci Res 79:644–651. doi: 10.1002/jnr.20392

Jiang H, Talaska AE, Schacht J, Sha S-H (2007) Oxidative imbalance in the aging inner ear. 28:. doi: 10.1016/j.neurobiolaging.2006.06.025

Jiang T, Kindt K, Wu DK (2017) Transcription factor Emx2 controls stereociliary bundle orientation of sensory hair cells. Elife 6:. doi: 10.7554/eLife.23661

Johnson SL (2015) Membrane properties specialize mammalian inner hair cells for frequency or intensity encoding. Elife 4:e08177. doi: 10.7554/eLife.08177

Johnson SL, Eckrich T, Kuhn S, et al (2011) Position-dependent patterning of spontaneous action potentials in immature cochlear inner hair cells. Nat Neurosci 14:711–717. doi: 10.1038/nn.2803

Johnson SL, Kuhn S, Franz C, et al (2013) Presynaptic maturation in auditory hair cells requires a critical period of sensory-independent spiking activity. Proc Natl Acad Sci 110:8720–8725. doi: 10.1073/pnas.1219578110

Jové M, Portero-Otín M, Naudí A, et al (2014) Metabolomics of Human Brain Aging and Age-Related Neurodegenerative Diseases. J Neuropathol Exp Neurol 73:640–657. doi: 10.1097/NEN.0000000000000091

Kamimura T, Whitworth CA, Rybak LP (1999) Effect of 4-methylthiobenzoic acid on cisplatin-induced ototoxicity in the rat. Hear Res 131:117–27

Kappler JA, Starr CJ, Chan DK, et al (2004) A nonsense mutation in the gene encoding a zebrafish myosin VI isoform causes defects in hair-cell mechanotransduction. Proc Natl Acad Sci U S A 101:13056–61. doi: 10.1073/pnas.0405224101

Kasahara A, Cipolat S, Chen Y, et al (2013) Mitochondrial fusion directs cardiomyocyte differentiation via calcineurin and Notch signaling. Science (80-) 342:734–737. doi: 10.1126/science.1241359

Katajisto P, Döhla J, Chaffer CL, et al (2015) Stem cells. Asymmetric apportioning of aged mitochondria between daughter cells is required for stemness. Science 348:340–3. doi: 10.1126/science.1260384

Kawamoto K, Sha S-H, Minoda R, et al (2004) Antioxidant Gene Therapy Can Protect Hearing and Hair Cells from Ototoxicity. Mol Ther 9:173–181. doi: 10.1016/j.ymthe.2003.11.020

Kazmierczak P, Sakaguchi H, Tokita J, et al (2007) Cadherin 23 and protocadherin 15 interact to form tip-link filaments in sensory hair cells. Nature 449:87–91. doi: 10.1038/nature06091

Kenyon EJ, Kirkwood NK, Kitcher SR, et al (2017) Identification of ion-channel modulators that protect against aminoglycoside-induced hair cell death. JCI insight 2:. doi: 10.1172/jci.insight.96773

Kim I, Rodriguez-Enriquez S, Lemasters JJ (2007) Selective degradation of mitochondria by mitophagy. Arch Biochem Biophys 462:245–53. doi: 10.1016/j.abb.2007.03.034

Kim WT, Chang S, Daniell L, et al (2002) Delayed reentry of recycling vesicles into the fusion-competent synaptic vesicle pool in synaptojanin 1 knockout mice

Kindt KS, Finch G, Nicolson T (2012) Kinocilia mediate mechanosensitivity in developing zebrafish hair cells. Dev Cell 23:329–41. doi: 10.1016/j.devcel.2012.05.022

Kniss JS, Jiang L, Piotrowski T (2016) Insights into sensory hair cell regeneration from the zebrafish lateral line. Curr Opin Genet Dev 40:32–40. doi: 10.1016/j.gde.2016.05.012

Kokotas H, Petersen M, Willems P (2007) Mitochondrial deafness. Clin Genet 71:379–391. doi: 10.1111/j.1399-0004.2007.00800.x

Kopke R, Allen K a, Henderson D, et al (1999) A radical demise. Toxins and trauma share common pathways in hair cell death. Ann N Y Acad Sci 884:171–191. doi: 10.1111/j.1749-6632.1999.tb08641.x

Kroese, A. B., & Van Netten SM (1989) Sensory transduction in lateral line hair cells. In: The mechanosensory lateral line. pp 265–284

Kruger M, Boney R, Ordoobadi AJ, et al (2016) Natural Bizbenzoquinoline Derivatives Protect Zebrafish Lateral Line Sensory Hair Cells from Aminoglycoside Toxicity. Front Cell Neurosci 10:83. doi: 10.3389/fncel.2016.00083

Kurima K, Ebrahim S, Pan B, et al (2015) TMC1 and TMC2 Localize at the Site of Mechanotransduction in Mammalian Inner Ear Hair Cell Stereocilia. Cell Rep 12:1606–1617. doi: 10.1016/J.CELREP.2015.07.058

Kuznetsov A V., Hermann M, Saks V, et al (2009) The cell-type specificity of mitochondrial dynamics. Int J Biochem Cell Biol 41:1928–1939. doi: 10.1016/j.biocel.2009.03.007

Laker RC, Drake JC, Wilson RJ, et al (2017) Ampk phosphorylation of Ulk1 is required for targeting of mitochondria to lysosomes in exercise-induced mitophagy. Nat Commun 8:548. doi: 10.1038/s41467-017-00520-9

Laker RC, Xu P, Ryall KA, et al (2014) A novel MitoTimer reporter gene for mitochondrial content, structure, stress, and damage in vivo. J Biol Chem 289:12005–15. doi: 10.1074/jbc.M113.530527

Landegger LD, Pan B, Askew C, et al (2017) A synthetic AAV vector enables safe and efficient gene transfer to the mammalian inner ear. Nat Biotechnol 35:280–284. doi: 10.1038/nbt.3781

Lang H, Liu C (1997) Apoptosis and hair cell degeneration in the vestibular sensory epithelia of

the guinea pig following a gentamicin insult. Hear Res 111:177–84
Le Belle JE, Orozco NM, Paucar AA, et al (2011) Proliferative neural stem cells have high endogenous ROS levels that regulate self-renewal and neurogenesis in a PI3K/Akt-dependant manner. Cell Stem Cell 8:59–71. doi: 10.1016/j.stem.2010.11.028
Lehman JJ, Barger PM, Kovacs A, et al (2000) Peroxisome proliferator-activated receptor gamma coactivator-1 promotes cardiac mitochondrial biogenesis. J Clin Invest 106:847–56. doi: 10.1172/JCI10268
Li H, Kloosterman W, Fekete DM (2010) MicroRNA-183 family members regulate sensorineural fates in the inner ear. J Neurosci 30:3254–63. doi: 10.1523/JNEUROSCI.4948-09.2010
Li J, Zhao X, Xin Q, et al (2015) Whole-Exome Sequencing Identifies a Variant in *TMEM132E* Causing Autosomal-Recessive Nonsyndromic Hearing Loss DFNB99. Hum Mutat 36:98–105. doi: 10.1002/humu.22712
Liao JC (2010) Organization and physiology of posterior lateral line afferent neurons in larval zebrafish. Biol Lett 6:402–5. doi: 10.1098/rsbl.2009.0995
Liao JC, Haehnel M (2012) Physiology of afferent neurons in larval zebrafish provides a functional framework for lateral line somatotopy. J Neurophysiol 107:2615–23. doi: 10.1152/jn.01108.2011
Lim DJ, Anniko M (1985) Developmental morphology of the mouse inner ear. A scanning electron microscopic observation. Acta Otolaryngol Suppl 422:1–69
Lin S-Y, Vollrath MA, Mangosing S, et al (2016) The zebrafish pinball wizard gene encodes WRB, a tail-anchored-protein receptor essential for inner-ear hair cells and retinal photoreceptors. J Physiol 594:895–914. doi: 10.1113/JP271437
Linbo TL, Stehr CM, Incardona JP, Scholz NL (2006) Dissolved copper triggers cell death in the peripheral mechanosensory system of larval fish. Environ Toxicol Chem 25:597–603
Lismont C, Walton PA, Fransen M (2017) Quantitative Monitoring of Subcellular Redox Dynamics in Living Mammalian Cells Using RoGFP2-Based Probes. Humana Press, New York, NY, pp 151–164
Longo-Guess CM, Gagnon LH, Cook SA, et al (2005) A missense mutation in the previously undescribed gene Tmhs underlies deafness in hurry-scurry (hscy) mice. Proc Natl Acad Sci U S A 102:7894–9. doi: 10.1073/pnas.0500760102
López-Schier H, Hudspeth AJ (2006) A two-step mechanism underlies the planar polarization of regenerating sensory hair cells. Proc Natl Acad Sci U S A 103:18615–20. doi: 10.1073/pnas.0608536103
López-Schier H, Starr CJ, Kappler JA, et al (2004) Directional Cell Migration Establishes the Axes of Planar Polarity in the Posterior Lateral-Line Organ of the Zebrafish. Dev Cell 7:401–412. doi: 10.1016/j.devcel.2004.07.018
Loschen G, Azzi A, Richter C, Flohé L (1974) Superoxide radicals as precursors of mitochondrial hydrogen peroxide. FEBS Lett 42:68–72. doi: 10.1016/0014-5793(74)80281-4
Love NR, Chen Y, Ishibashi S, et al (2013) Amputation-induced reactive oxygen species are required for successful Xenopus tadpole tail regeneration. Nat Cell Biol 15:222–8. doi: 10.1038/ncb2659
Lundquist PG, Wersäll J (1966) Kanamycin-induced changes in cochlear hair cells of the guinea pig. Z Zellforsch Mikrosk Anat 72:543–61
Luo L-F, Hou C-C, Yang W-X (2013) Nuclear factors: Roles related to mitochondrial deafness.

Gene 520:79–89. doi: 10.1016/j.gene.2013.03.041
Lv C, Stewart WJ, Akanyeti O, et al (2016) Synaptic Ribbons Require Ribeye for Electron Density, Proper Synaptic Localization, and Recruitment of Calcium Channels. Cell Rep 15:2784–2795. doi: 10.1016/j.celrep.2016.05.045
Ma EY, Rubel EW, Raible DW (2008) Notch signaling regulates the extent of hair cell regeneration in the zebrafish lateral line. J Neurosci 28:2261–73. doi: 10.1523/JNEUROSCI.4372-07.2008
Maeda R, Kindt KS, Mo W, et al (2014) Tip-link protein protocadherin 15 interacts with transmembrane channel-like proteins TMC1 and TMC2. Proc Natl Acad Sci U S A 111:12907–12. doi: 10.1073/pnas.1402152111
Maeda R, Pacentine I V., Erickson T, Nicolson T (2017) Functional Analysis of the Transmembrane and Cytoplasmic Domains of Pcdh15a in Zebrafish Hair Cells. J Neurosci 37:3231–3245. doi: 10.1523/JNEUROSCI.2216-16.2017
Mahendrasingam S, MacDonald JA, Furness DN (2011) Relative Time Course of Degeneration of Different Cochlear Structures in the CD/1 Mouse Model of Accelerated Aging. J Assoc Res Otolaryngol 12:437–453. doi: 10.1007/s10162-011-0263-6
Malka F, Guillery O, Cifuentes-Diaz C, et al (2005) Separate fusion of outer and inner mitochondrial membranes. EMBO Rep 6:853–9. doi: 10.1038/sj.embor.7400488
Mangiardi DA, McLaughlin-Williamson K, May KE, et al (2004) Progression of hair cell ejection and molecular markers of apoptosis in the avian cochlea following gentamicin treatment. J Comp Neurol 475:1–18. doi: 10.1002/cne.20129
Manji SSM, Williams LH, Miller KA, et al (2011) A Mutation in Synaptojanin 2 Causes Progressive Hearing Loss in the ENU-Mutagenised Mouse Strain Mozart. PLoS One 6:e17607. doi: 10.1371/journal.pone.0017607
Marcotti W, van Netten SM, Kros CJ (2005) The aminoglycoside antibiotic dihydrostreptomycin rapidly enters mouse outer hair cells through the mechano-electrical transducer channels. J Physiol 567:505–21. doi: 10.1113/jphysiol.2005.085951
Matthews G, Fuchs P (2010) The diverse roles of ribbon synapses in sensory neurotransmission. Nat Rev Neurosci 11:812–822. doi: 10.1038/nrn2924
Maxeiner S, Luo F, Tan A, et al (2016) How to make a synaptic ribbon: RIBEYE deletion abolishes ribbons in retinal synapses and disrupts neurotransmitter release. EMBO J 35:1098–1114. doi: 10.15252/embj.201592701
McFadden SL, Ding D, Salvemini D, Salvi RJ (2003) M40403, a superoxide dismutase mimetic, protects cochlear hair cells from gentamicin, but not cisplatin toxicity. Toxicol Appl Pharmacol 186:46–54
McHenry MJ, Feitl KE, Strother JA, Van Trump WJ (2009) Larval zebrafish rapidly sense the water flow of a predator's strike. Biol Lett 5:477–9. doi: 10.1098/rsbl.2009.0048
Meeusen S, McCaffery JM, Nunnari J (2004) Mitochondrial Fusion Intermediates Revealed in Vitro. Science (80-) 305:1747–1752. doi: 10.1126/science.1100612
Metcalfe WK, Kimmel CB, Schabtach E (1985) Anatomy of the posterior lateral line system in young larvae of the zebrafish. J Comp Neurol 233:377–389. doi: 10.1002/cne.902330307
Mirjany M, Preuss T, Faber DS (2011) Role of the lateral line mechanosensory system in directionality of goldfish auditory evoked escape response. J Exp Biol 214:3358–67. doi: 10.1242/jeb.052894
Mirkovic I, Pylawka S, Hudspeth AJ (2012) Rearrangements between differentiating hair cells coordinate planar polarity and the establishment of mirror symmetry in lateral-line

neuromasts. Biol Open 1:498–505. doi: 10.1242/bio.2012570
Mishra P, Chan DC (2016) Metabolic regulation of mitochondrial dynamics. J Cell Biol 212:379–87. doi: 10.1083/jcb.201511036
Mishra P, Chan DC (2014) Mitochondrial dynamics and inheritance during cell division, development and disease. Nat Rev Mol Cell Biol 15:634–46. doi: 10.1038/nrm3877
Mizushima N, Kuma A, Kobayashi Y, et al (2003) Mouse Apg16L, a novel WD-repeat protein, targets to the autophagic isolation membrane with the Apg12-Apg5 conjugate. J Cell Sci 116:1679–88. doi: 10.1242/jcs.00381
Monesson-Olson BD, Browning-Kamins J, Aziz-Bose R, et al (2014) Optical Stimulation of Zebrafish Hair Cells Expressing Channelrhodopsin-2. PLoS One 9:e96641. doi: 10.1371/journal.pone.0096641
Montcouquiol M, Rachel RA, Lanford PJ, et al (2003) Identification of Vangl2 and Scrb1 as planar polarity genes in mammals. Nature 423:173–177. doi: 10.1038/nature01618
Montgomery JC, Bodznick D (1994) An adaptive filter that cancels self-induced noise in the electrosensory and lateral line mechanosensory systems of fish. Neurosci Lett 174:145–148. doi: 10.1016/0304-3940(94)90007-8
Morton CC, Nance WE (2006) Newborn Hearing Screening — A Silent Revolution. N Engl J Med 354:2151–2164. doi: 10.1056/NEJMra050700
Moser T, Beutner D (2000) Kinetics of exocytosis and endocytosis at the cochlear inner hair cell afferent synapse of the mouse. Proc Natl Acad Sci U S A 97:883–8
Murphy MP (2009) How mitochondria produce reactive oxygen species. Biochem J 417:1–13. doi: 10.1042/BJ20081386
Nagiel A, Andor-Ardó D, Hudspeth AJ (2008) Specificity of afferent synapses onto plane-polarized hair cells in the posterior lateral line of the zebrafish. J Neurosci 28:8442–53. doi: 10.1523/JNEUROSCI.2425-08.2008
Nagiel A, Patel SH, Andor-Ardó D, Hudspeth AJ (2009) Activity-independent specification of synaptic targets in the posterior lateral line of the larval zebrafish. Proc Natl Acad Sci U S A 106:21948–53. doi: 10.1073/pnas.0912082106
Nemzou N. RM, Bulankina AV, Khimich D, et al (2006) Synaptic organization in cochlear inner hair cells deficient for the CaV1.3 (α1D) subunit of L-type Ca2+ channels. Neuroscience 141:1849–1860. doi: 10.1016/j.neuroscience.2006.05.057
Nicolson T (2015) Ribbon synapses in zebrafish hair cells. Hear Res 330:170–7. doi: 10.1016/j.heares.2015.04.003
Nicolson T (2017) The genetics of hair-cell function in zebrafish. J Neurogenet 31:102–112. doi: 10.1080/01677063.2017.1342246
Nicolson T (2005) Fishing for key players in mechanotransduction. Trends Neurosci 28:140–4. doi: 10.1016/j.tins.2004.12.008
Nicolson T, Rüsch A, Friedrich RW, et al (1998) Genetic analysis of vertebrate sensory hair cell mechanosensation: the zebrafish circler mutants. Neuron 20:271–283. doi: 10.1016/S0896-6273(00)80455-9
Niethammer P, Grabher C, Look AT, Mitchison TJ (2009) A tissue-scale gradient of hydrogen peroxide mediates rapid wound detection in zebrafish. Nature 459:996–9. doi: 10.1038/nature08119
Niven JE, Laughlin SB (2008) Energy limitation as a selective pressure on the evolution of sensory systems. J Exp Biol 211:1792–804. doi: 10.1242/jeb.017574
Nowikovsky K, Reipert S, Devenish RJ, Schweyen RJ (2007) Mdm38 protein depletion causes

loss of mitochondrial K+/H+ exchange activity, osmotic swelling and mitophagy. Cell Death Differ 14:1647–1656. doi: 10.1038/sj.cdd.4402167

Obholzer N, Wolfson S, Trapani JG, et al (2008) Vesicular glutamate transporter 3 is required for synaptic transmission in zebrafish hair cells. J Neurosci 28:2110–8. doi: 10.1523/JNEUROSCI.5230-07.2008

Olivari FA, Hernández PP, Allende ML (2008) Acute copper exposure induces oxidative stress and cell death in lateral line hair cells of zebrafish larvae. Brain Res 1244:1–12. doi: 10.1016/j.brainres.2008.09.050

Olszewski J, Haehnel M, Taguchi M, Liao JC (2012) Zebrafish Larvae Exhibit Rheotaxis and Can Escape a Continuous Suction Source Using Their Lateral Line. PLoS One 7:e36661. doi: 10.1371/journal.pone.0036661

Olt J, Allen CE, Marcotti W (2016) In vivo physiological recording from the lateral line of juvenile zebrafish. J Physiol 594:. doi: 10.1113/JP271794

Olt J, Johnson SL, Marcotti W (2014) In vivo and in vitro biophysical properties of hair cells from the lateral line and inner ear of developing and adult zebrafish. J Physiol 592:2041–58. doi: 10.1113/jphysiol.2013.265108

Oteiza P, Odstrcil I, Lauder G, et al (2017) A novel mechanism for mechanosensory-based rheotaxis in larval zebrafish. Nature 547:445–448. doi: 10.1038/nature23014

Otera H, Mihara K (2011) Molecular mechanisms and physiologic functions of mitochondrial dynamics. J Biochem 149:241–251. doi: 10.1093/jb/mvr002

Ou HC, Cunningham LL, Francis SP, et al (2009) Identification of FDA-approved drugs and bioactives that protect hair cells in the zebrafish (Danio rerio) lateral line and mouse (Mus musculus) utricle. J Assoc Res Otolaryngol 10:191–203. doi: 10.1007/s10162-009-0158-y

Ou HC, Raible DW, Rubel EW (2007) Cisplatin-induced hair cell loss in zebrafish (Danio rerio) lateral line. Hear Res 233:46–53. doi: 10.1016/j.heares.2007.07.003

Owens KN, Coffin AB, Hong LS, et al (2009) Response of mechanosensory hair cells of the zebrafish lateral line to aminoglycosides reveals distinct cell death pathways. Hear Res 253:32–41. doi: 10.1016/J.HEARES.2009.03.001

Owens KN, Cunningham DE, Macdonald G, et al (2007) Ultrastructural analysis of aminoglycoside-induced hair cell death in the zebrafish lateral line reveals an early mitochondrial response. J Comp Neurol 502:522–543. doi: 10.1002/cne.21345

Owens KN, Santos F, Roberts B, et al (2008) Identification of Genetic and Chemical Modulators of Zebrafish Mechanosensory Hair Cell Death. PLoS Genet 4:e1000020. doi: 10.1371/journal.pgen.1000020

Owusu-Ansah E, Banerjee U (2009) Reactive oxygen species prime Drosophila haematopoietic progenitors for differentiation. Nature 461:537–41. doi: 10.1038/nature08313

Pan B, Géléoc GS, Asai Y, et al (2013) TMC1 and TMC2 are components of the mechanotransduction channel in hair cells of the mammalian inner ear. Neuron 79:504–15. doi: 10.1016/j.neuron.2013.06.019

Parichy DM (2015) Advancing biology through a deeper understanding of zebrafish ecology and evolution. Elife 4:. doi: 10.7554/eLife.05635

Pataky F, Pironkova R, Hudspeth AJ (2004) Radixin is a constituent of stereocilia in hair cells. Proc Natl Acad Sci U S A 101:2601–6

Pham AH, McCaffery JM, Chan DC (2012) Mouse lines with photo-activatable mitochondria to study mitochondrial dynamics. genesis 50:833–843. doi: 10.1002/dvg.22050

Phillips JB, Blanco-Sanchez B, Lentz JJ, et al (2011) Harmonin (Ush1c) is required in zebrafish

Muller glial cells for photoreceptor synaptic development and function. Dis Model Mech 4:786–800. doi: 10.1242/dmm.006429

Pickles JO (2004) Mutation in mitochondrial DNA as a cause of presbyacusis. Audiol Neurootol 9:23–33. doi: 10.1159/000074184

Popper AN, Fay RR (1993) Sound detection and processing by fish: critical review and major research questions. Brain Behav Evol 41:14–38. doi: 10.1159/000113821

Prezant TR, Agapian J V., Bohlman MC, et al (1993) Mitochondrial ribosomal RNA mutation associated with both antibiotic–induced and non–syndromic deafness. Nat Genet 4:289–294. doi: 10.1038/ng0793-289

Prober DA, Zimmerman S, Myers BR, et al (2008) Zebrafish TRPA1 channels are required for chemosensation but not for thermosensation or mechanosensory hair cell function. J Neurosci 28:10102–10. doi: 10.1523/JNEUROSCI.2740-08.2008

Puel JL, Ruel J, Gervais d'Aldin C, Pujol R (1998) Excitotoxicity and repair of cochlear synapses after noise-trauma induced hearing loss. Neuroreport 9:2109–14

Pujol-Martí J, Faucherre A, Aziz-Bose R, et al (2014) Converging axons collectively initiate and maintain synaptic selectivity in a constantly remodeling sensory organ. Curr Biol 24:2968–74. doi: 10.1016/j.cub.2014.11.012

Pujol-Martí J, Zecca A, Baudoin J-P, et al (2012) Neuronal birth order identifies a dimorphic sensorineural map. J Neurosci 32:2976–87. doi: 10.1523/JNEUROSCI.5157-11.2012

Qi X, Disatnik M-H, Shen N, et al (2011) Aberrant mitochondrial fission in neurons induced by protein kinase C{delta} under oxidative stress conditions in vivo. Mol Biol Cell 22:256–65. doi: 10.1091/mbc.E10-06-0551

Quan Y, Xia L, Shao J, et al (2015) Adjudin protects rodent cochlear hair cells against gentamicin ototoxicity via the SIRT3-ROS pathway. Sci Rep 5:8181. doi: 10.1038/srep08181

Raible DW, Kruse GJ (2000) Organization of the lateral line system in embryonic zebrafish. J Comp Neurol 421:189–198. doi: 10.1002/(SICI)1096-9861(20000529)421:2<189::AID-CNE5>3.0.CO;2-K

Reiners J, Nagel-Wolfrum K, Jürgens K, et al (2006) Molecular basis of human Usher syndrome: Deciphering the meshes of the Usher protein network provides insights into the pathomechanisms of the Usher disease. Exp Eye Res 83:97–119. doi: 10.1016/j.exer.2005.11.010

Riazuddin S, Belyantseva IA, Giese APJ, et al (2012) Alterations of the CIB2 calcium- and integrin-binding protein cause Usher syndrome type 1J and nonsyndromic deafness DFNB48. Nat Genet 44:1265–71. doi: 10.1038/ng.2426

Ricci AJ, Bai J-PJ-P, Song L, et al (2013) Patch-clamp recordings from lateral line neuromast hair cells of the living zebrafish. J Neurosci 33:3131–4. doi: 10.1523/JNEUROSCI.4265-12.2013

Richardson GP, Forge A, Kros CJ, et al (1997) Myosin VIIA is required for aminoglycoside accumulation in cochlear hair cells. J Neurosci 17:9506–19

Richardson GP, Russell IJ (1991) Cochlear cultures as a model system for studying aminoglycoside induced ototoxicity. Hear Res 53:293–311

Rizzuto R, Pinton P, Carrington W, et al (1998) Close contacts with the endoplasmic reticulum as determinants of mitochondrial Ca2+ responses. Science 280:1763–6

Romero-Carvajal A, Navajas Acedo J, Jiang L, et al (2015) Regeneration of Sensory Hair Cells Requires Localized Interactions between the Notch and Wnt Pathways. Dev Cell 34:267–

82. doi: 10.1016/j.devcel.2015.05.025
Rossignol R, Gilkerson R, Aggeler R, et al (2004) Energy substrate modulates mitochondrial structure and oxidative capacity in cancer cells. Cancer Res 64:985–93
Rowland AA, Voeltz GK (2012) Endoplasmic reticulum–mitochondria contacts: function of the junction. Nat Rev Mol Cell Biol 13:607–615. doi: 10.1038/nrm3440
Ruel J, Emery S, Nouvian R, et al (2008) Impairment of SLC17A8 encoding vesicular glutamate transporter-3, VGLUT3, underlies nonsyndromic deafness DFNA25 and inner hair cell dysfunction in null mice. Am J Hum Genet 83:278–92. doi: 10.1016/j.ajhg.2008.07.008
Rusch A, Lysakowski A, Eatock RA (1998) Postnatal Development of Type I and Type II Hair Cells in the Mouse Utricle: Acquisition of Voltage-Gated Conductances and Differentiated Morphology. J Neurosci 18:7487–7501
Sang Q, Zhang J, Feng R, et al (2014) Ildr1b is essential for semicircular canal development, migration of the posterior lateral line primordium and hearing ability in zebrafish: implications for a role in the recessive hearing impairment DFNB42. Hum Mol Genet 23:6201–11. doi: 10.1093/hmg/ddu340
Santos-Cortez RLP, Lee K, Azeem Z, et al (2013) Mutations in KARS, Encoding Lysyl-tRNA Synthetase, Cause Autosomal-Recessive Nonsyndromic Hearing Impairment DFNB89. Am J Hum Genet 93:132–140. doi: 10.1016/j.ajhg.2013.05.018
Santos-Cortez RLP, Lee K, Giese AP, et al (2014) Adenylate cyclase 1 (ADCY1) mutations cause recessive hearing impairment in humans and defects in hair cell function and hearing in zebrafish. Hum Mol Genet 23:3289–98. doi: 10.1093/hmg/ddu042
Santos F, MacDonald G, Rubel EW, Raible DW (2006) Lateral line hair cell maturation is a determinant of aminoglycoside susceptibility in zebrafish (Danio rerio). Hear Res 213:25–33. doi: 10.1016/j.heares.2005.12.009
Saxena S, Caroni P (2011) Selective Neuronal Vulnerability in Neurodegenerative Diseases: from Stressor Thresholds to Degeneration. Neuron 71:35–48
Schaechinger TJ, Oliver D (2007) Nonmammalian orthologs of prestin (SLC26A5) are electrogenic divalent/chloride anion exchangers. Proc Natl Acad Sci 104:7693–7698. doi: 10.1073/pnas.0608583104
Seal RP, Akil O, Yi E, et al (2008) Sensorineural deafness and seizures in mice lacking vesicular glutamate transporter 3. Neuron 57:263–75. doi: 10.1016/j.neuron.2007.11.032
Sebastián D, Palacín M, Zorzano A (2017) Mitochondrial Dynamics: Coupling Mitochondrial Fitness with Healthy Aging. Trends Mol Med 23:201–215. doi: 10.1016/j.molmed.2017.01.003
Sebe JY, Cho S, Sheets L, et al (2017) Ca(2+)-Permeable AMPARs Mediate Glutamatergic Transmission and Excitotoxic Damage at the Hair Cell Ribbon Synapse. J Neurosci 37:6162–6175. doi: 10.1523/JNEUROSCI.3644-16.2017
Seidman MD, Ahmad N, Joshi D, et al (2004) Age-related hearing loss and its association with reactive oxygen species and mitochondrial DNA damage. Acta Otolaryngol Suppl 16–24
Seiler C, Ben-David O, Sidi S, et al (2004) Myosin VI is required for structural integrity of the apical surface of sensory hair cells in zebrafish. Dev Biol 272:328–338. doi: 10.1016/j.ydbio.2004.05.004
Seiler C, Finger-Baier KC, Rinner O, et al (2005) Duplicated genes with split functions: independent roles of protocadherin15 orthologues in zebrafish hearing and vision. Development 132:615–23. doi: 10.1242/dev.01591
Seiler C, Nicolson T (1999) Defective calmodulin-dependent rapid apical endocytosis in

zebrafish sensory hair cell mutants. J Neurobiol 41:424–434. doi: 10.1002/(SICI)1097-4695(19991115)41:3<424::AID-NEU10>3.0.CO;2-G

Self T, Mahony M, Fleming J, et al (1998) Shaker-1 mutations reveal roles for myosin VIIA in both development and function of cochlear hair cells. Development 125:557–66

Sha SH, Schacht J (2000) Antioxidants attenuate gentamicin-induced free radical formation in vitro and ototoxicity in vivo: D-methionine is a potential protectant. Hear Res 142:34–40

Sha SH, Taylor R, Forge A, Schacht J (2001a) Differential vulnerability of basal and apical hair cells is based on intrinsic susceptibility to free radicals. Hear Res 155:1–8. doi: 10.1016/S0378-5955(01)00224-6

Sha SH, Zajic G, Epstein CJ, Schacht J (2001b) Overexpression of copper/zinc-superoxide dismutase protects from kanamycin-induced hearing loss. Audiol Neurootol 6:117–23. doi: 10.1159/000046818

Shearer AE, Hildebrand MS, Smith RJ (2017) Hereditary Hearing Loss and Deafness Overview. University of Washington, Seattle

Sheets L (2017) Excessive activation of ionotropic glutamate receptors induces apoptotic hair-cell death independent of afferent and efferent innervation. Sci Rep 7:41102. doi: 10.1038/srep41102

Sheets L, He XJ, Olt J, et al (2017) Enlargement of Ribbons in Zebrafish Hair Cells Increases Calcium Currents But Disrupts Afferent Spontaneous Activity and Timing of Stimulus Onset. J Neurosci 37:6299–6313. doi: 10.1523/JNEUROSCI.2878-16.2017

Sheets L, Kindt KS, Nicolson T (2012) Presynaptic CaV1.3 Channels Regulate Synaptic Ribbon Size and Are Required for Synaptic Maintenance in Sensory Hair Cells. J Neurosci 32:17273–17286. doi: 10.1523/JNEUROSCI.3005-12.2012

Sheets L, Trapani JG, Mo W, et al (2011) Ribeye is required for presynaptic Ca(V)1.3a channel localization and afferent innervation of sensory hair cells. Development 138:1309–19. doi: 10.1242/dev.059451

Shen X, Liu F, Wang Y, et al (2015) Down-regulation of msrb3 and destruction of normal auditory system development through hair cell apoptosis in zebrafish. Int J Dev Biol 59:195–203. doi: 10.1387/ijdb.140200md

Shen Y-C, Jeyabalan AK, Wu KL, et al (2008) The transmembrane inner ear (tmie) gene contributes to vestibular and lateral line development and function in the zebrafish (Danio rerio). Dev Dyn 237:941–52. doi: 10.1002/dvdy.21486

Sidi S, Busch-Nentwich E, Friedrich R, et al (2004) gemini Encodes a Zebrafish L-Type Calcium Channel That Localizes at Sensory Hair Cell Ribbon Synapses. J Neurosci 24:4213–4223. doi: 10.1523/JNEUROSCI.0223-04.2004

Siemens J, Lillo C, Dumont RA, et al (2004) Cadherin 23 is a component of the tip link in hair-cell stereocilia. Nature 428:950–5. doi: 10.1038/nature02483

Skulachev VP (2001) Mitochondrial filaments and clusters as intracellular power-transmitting cables. Trends Biochem Sci 26:23–29. doi: 10.1016/S0968-0004(00)01735-7

Söllner C, Rauch G-J, Siemens J, et al (2004) Mutations in cadherin 23 affect tip links in zebrafish sensory hair cells. Nature 428:955–9. doi: 10.1038/nature02484

Someya S, Xu J, Kondo K, et al (2009) Age-related hearing loss in C57BL/6J mice is mediated by Bak-dependent mitochondrial apoptosis. Proc Natl Acad Sci U S A 106:19432–7. doi: 10.1073/pnas.0908786106

Someya S, Yu W, Hallows WC, et al (2010) Sirt3 mediates reduction of oxidative damage and prevention of age-related hearing loss under Caloric Restriction. Cell 143:802–812. doi:

10.1016/j.cell.2010.10.002
Stawicki TM, Hernandez L, Esterberg R, et al (2016) Cilia-Associated Genes Play Differing Roles in Aminoglycoside-Induced Hair Cell Death in Zebrafish. G3; Genes|Genomes|Genetics 6:2225–2235. doi: 10.1534/g3.116.030080
Stawicki TM, Owens KN, Linbo T, et al (2014) The zebrafish merovingian mutant reveals a role for pH regulation in hair cell toxicity and function. Dis Model Mech 7:847–856. doi: 10.1242/dmm.016576
Stewart WJ, Cardenas GS, McHenry MJ, et al (2013) Zebrafish larvae evade predators by sensing water flow. J Exp Biol 216:388–398. doi: 10.1242/jeb.072751
Stewart WJ, McHenry MJ (2010) Sensing the strike of a predator fish depends on the specific gravity of a prey fish. J Exp Biol 213:3769–3777. doi: 10.1242/jeb.046946
Stewart WJ, Nair A, Jiang H, McHenry MJ (2014) Prey fish escape by sensing the bow wave of a predator. J Exp Biol 217:4328–4336. doi: 10.1242/jeb.111773
Stone LS (1937) Further experimental studies of the development of lateral-line sense organs in amphibians observed in living preparations. J Comp Neurol 68:83–115. doi: 10.1002/cne.900680105
Stooke-Vaughan GA, Obholzer ND, Baxendale S, et al (2015) Otolith tethering in the zebrafish otic vesicle requires Otogelin and α-Tectorin. Development 142:1137–45. doi: 10.1242/dev.116632
Stotland A, Gottlieb RA (2015) α-MHC MitoTimer mouse: in vivo mitochondrial turnover model reveals remarkable mitochondrial heterogeneity in the heart. J Mol Cell Cardiol 90:53–8. doi: 10.1016/j.yjmcc.2015.11.032
Suli A, Pujol R, Cunningham DE, et al (2016) Innervation regulates synaptic ribbons in lateral line mechanosensory hair cells. J Cell Sci 129:2250–2260. doi: 10.1242/jcs.182592
Suli A, Watson GM, Rubel EW, Raible DW (2012) Rheotaxis in larval zebrafish is mediated by lateral line mechanosensory hair cells. PLoS One 7:e29727. doi: 10.1371/journal.pone.0029727
Takahashi M, Hood DA (1993) Chronic stimulation-induced changes in mitochondria and performance in rat skeletal muscle. J Appl Physiol 74:934–941. doi: 10.1152/jappl.1993.74.2.934
Takumida M, Takumida H, Katagiri Y, Anniko M (2016) Localization of sirtuins (SIRT1-7) in the aged mouse inner ear. Acta Otolaryngol 136:120–131. doi: 10.3109/00016489.2015.1093172
Tan X, Pecka JL, Tang J, et al (2011) From Zebrafish to Mammal: Functional Evolution of Prestin, the Motor Protein of Cochlear Outer Hair Cells. J Neurophysiol 105:36–44. doi: 10.1152/jn.00234.2010
Terskikh A (2000) "Fluorescent Timer": Protein That Changes Color with Time. Science (80-) 290:1585–1588. doi: 10.1126/science.290.5496.1585
Thomas AJ, Hailey DW, Stawicki TM, et al (2013) Functional mechanotransduction is required for cisplatin-induced hair cell death in the zebrafish lateral line. J Neurosci 33:4405–4414. doi: 10.1523/JNEUROSCI.3940-12.2013
Thomas ED, Cruz IA, Hailey DW, Raible DW (2015) There and back again: development and regeneration of the zebrafish lateral line system. Wiley Interdiscip Rev Dev Biol 4:1–16. doi: 10.1002/wdev.160
Ton C, Parng C (2005) The use of zebrafish for assessing ototoxic and otoprotective agents. Hear Res 208:79–88. doi: 10.1016/j.heares.2005.05.005

Toro C, Trapani JG, Pacentine I, et al (2015) Dopamine Modulates the Activity of Sensory Hair Cells. J Neurosci 35:16494–503. doi: 10.1523/JNEUROSCI.1691-15.2015

Trapani JG, Nicolson T (2010) Physiological Recordings from Zebrafish Lateral-Line Hair Cells and Afferent Neurons. Academic Press

Trapani JG, Nicolson T (2011) Mechanism of spontaneous activity in afferent neurons of the zebrafish lateral-line organ. J Neurosci 31:1614–23. doi: 10.1523/JNEUROSCI.3369-10.2011

Trapani JG, Obholzer N, Mo W, et al (2009) synaptojanin1 Is Required for Temporal Fidelity of Synaptic Transmission in Hair Cells. PLoS Genet 5:e1000480. doi: 10.1371/journal.pgen.1000480

Turrens JF (2003) Mitochondrial formation of reactive oxygen species. J Physiol 552:335–44. doi: 10.1113/jphysiol.2003.049478

Twig G, Elorza A, Molina AJA, et al (2008) Fission and selective fusion govern mitochondrial segregation and elimination by autophagy. EMBO J 27:433–46. doi: 10.1038/sj.emboj.7601963

Van Trump WJ, Coombs S, Duncan K, McHenry MJ (2010) Gentamicin is ototoxic to all hair cells in the fish lateral line system. Hear Res 261:42–50. doi: 10.1016/j.heares.2010.01.001

Vargo JW, Walker SN, Gopal SR, et al (2017) Inhibition of Mitochondrial Division Attenuates Cisplatin-Induced Toxicity in the Neuromast Hair Cells. Front Cell Neurosci 11:393. doi: 10.3389/fncel.2017.00393

Verkhusha V V, Chudakov DM, Gurskaya NG, et al (2004) Common Pathway for the Red Chromophore Formation in Fluorescent Proteins and Chromoproteins. Chem Biol 11:845–854. doi: 10.1016/j.chembiol.2004.04.007

Viana MP, Lim S, Rafelski SM (2015) Quantifying mitochondrial content in living cells. In: Methods in cell biology. pp 77–93

Visser W, van Spronsen EA, Nanninga N, et al (1995) Effects of growth conditions on mitochondrial morphology inSaccharomyces cerevisiae. Antonie Van Leeuwenhoek 67:243–253. doi: 10.1007/BF00873688

Vogl C, Panou I, Yamanbaeva G, et al (2016) Tryptophan-rich basic protein (WRB) mediates insertion of the tail-anchored protein otoferlin and is required for hair cell exocytosis and hearing. EMBO J 35:2536–2552. doi: 10.15252/embj.201593565

Vu AA, Nadaraja GS, Huth ME, et al (2013) Integrity and regeneration of mechanotransduction machinery regulate aminoglycoside entry and sensory cell death. PLoS One 8:e54794. doi: 10.1371/journal.pone.0054794

Waguespack J, Salles FT, Kachar B, Ricci AJ (2007) Stepwise Morphological and Functional Maturation of Mechanotransduction in Rat Outer Hair Cells. J Neurosci 27:13890–13902. doi: 10.1523/JNEUROSCI.2159-07.2007

Wallace DC (2005) A Mitochondrial Paradigm of Metabolic and Degenerative Diseases, Aging, and Cancer: A Dawn for Evolutionary Medicine. Annu Rev Genet 39:359–407. doi: 10.1146/annurev.genet.39.110304.095751

Wan L, Almers W, Chen W (2005) Two ribeye Genes in Teleosts: The Role of Ribeye in Ribbon Formation and Bipolar Cell Development. J Neurosci 25:941–949. doi: 10.1523/JNEUROSCI.4657-04.2005

Wang HC, Bergles DE (2015) Spontaneous activity in the developing auditory system. Cell Tissue Res 361:65–75. doi: 10.1007/s00441-014-2007-5

Wang J, Mark S, Zhang X, et al (2005) Regulation of polarized extension and planar cell polarity

in the cochlea by the vertebrate PCP pathway. Nat Genet 37:980–985. doi: 10.1038/ng1622
Wang L, Sewell WF, Kim SD, et al (2008) Eya4 regulation of Na+/K+-ATPase is required for sensory system development in zebrafish. Development 135:3425–34. doi: 10.1242/dev.012237
Wang Y, Guo N, Nathans J (2006) The Role of Frizzled3 and Frizzled6 in Neural Tube Closure and in the Planar Polarity of Inner-Ear Sensory Hair Cells. J Neurosci 26:2147–2156. doi: 10.1523/JNEUROSCI.4698-05.2005
Weaver SP, Schweitzer L (1994) Development of gerbil outer hair cells after the onset of cochlear function: An ultrastructural study. Hear Res 72:44–52. doi: 10.1016/0378-5955(94)90204-6
Webb JF (2013) Morphological Diversity, Development, and Evolution of the Mechanosensory Lateral Line System. In: Coombs S, Bleckman H, Fay RR, Popper AN (eds) The Lateral Line System. New York, NY, pp 17–72
Weber T, Gopfert MC, Winter H, et al (2003) Expression of prestin-homologous solute carrier (SLC26) in auditory organs of nonmammalian vertebrates and insects. Proc Natl Acad Sci U S A 100:7690–5. doi: 10.1073/pnas.1330557100
Westermann B (2012) Bioenergetic role of mitochondrial fusion and fission. Biochim Biophys Acta - Bioenerg 1817:1833–1838. doi: 10.1016/J.BBABIO.2012.02.033
Whitfield TT (2002) Zebrafish as a model for hearing and deafness. J Neurobiol 53:157–171. doi: 10.1002/neu.10123
Wibowo I, Pinto-Teixeira F, Satou C, et al (2011) Compartmentalized Notch signaling sustains epithelial mirror symmetry. Development 138:1143–52. doi: 10.1242/dev.060566
Wiedemann N, Frazier AE, Pfanner N (2004) The protein import machinery of mitochondria. J Biol Chem 279:14473–6. doi: 10.1074/jbc.R400003200
Wilson RJ, Drake JC, Cui D, et al (2017) Conditional MitoTimer reporter mice for assessment of mitochondrial structure, oxidative stress, and mitophagy. Mitochondrion. doi: 10.1016/j.mito.2017.12.008
Wong ACY, Ryan AF (2015) Mechanisms of sensorineural cell damage, death and survival in the cochlea. Front Aging Neurosci 7:58. doi: 10.3389/fnagi.2015.00058
Woods DC (2017) Mitochondrial Heterogeneity: Evaluating Mitochondrial Subpopulation Dynamics in Stem Cells. Stem Cells Int 2017:7068567. doi: 10.1155/2017/7068567
Wu C, Sharma K, Laster K, et al (2014) Kcnq1-5 (Kv7.1-5) potassium channel expression in the adult zebrafish. BMC Physiol 14:1. doi: 10.1186/1472-6793-14-1
Wu Z, Puigserver P, Andersson U, et al (1999) Mechanisms Controlling Mitochondrial Biogenesis and Respiration through the Thermogenic Coactivator PGC-1. Cell 98:115–124. doi: 10.1016/S0092-8674(00)80611-X
Yang C-H, Schrepfer T, Schacht J (2015) Age-related hearing impairment and the triad of acquired hearing loss. Front Cell Neurosci 9:276. doi: 10.3389/fncel.2015.00276
Yarbrough D, Wachter RM, Kallio K, et al (2001) Refined crystal structure of DsRed, a red fluorescent protein from coral, at 2.0-A resolution. Proc Natl Acad Sci 98:462–467. doi: 10.1073/pnas.98.2.462
Yariz KO, Duman D, Zazo Seco C, et al (2012) Mutations in OTOGL , Encoding the Inner Ear Protein Otogelin-like, Cause Moderate Sensorineural Hearing Loss. Am J Hum Genet 91:872–882. doi: 10.1016/j.ajhg.2012.09.011
Zhang J, Khvorostov I, Hong JS, et al (2011) UCP2 regulates energy metabolism and differentiation potential of human pluripotent stem cells. EMBO J 30:4860–73. doi:

10.1038/emboj.2011.401
Zhang Q, Li S, Wong H-TC, et al (2018) Synaptically silent sensory hair cells in zebrafish are recruited after damage. Nat Commun 9:1388. doi: 10.1038/s41467-018-03806-8
Zhao B, Wu Z, Grillet N, et al (2014) TMIE is an essential component of the mechanotransduction machinery of cochlear hair cells. Neuron 84:954–67. doi: 10.1016/j.neuron.2014.10.041
Zhao Q, Wang J, Levichkin I V, et al (2002) A mitochondrial specific stress response in mammalian cells. EMBO J 21:4411–4419. doi: 10.1093/emboj/cdf445
(2015) About Sound | Hearing Loss. https://www.cdc.gov/ncbddd/hearingloss/sound.html. Accessed 3 Jun 2018